Superconducting Single Charge Transistor in a Dissipative Environment: The JQP - Process

by

Konstanze Jähne

Diploma Thesis

Lehrstuhl für Theoretische Festkörperphysik
CeNS und Department für Physik
Ludwig-Maximilians-Universität München

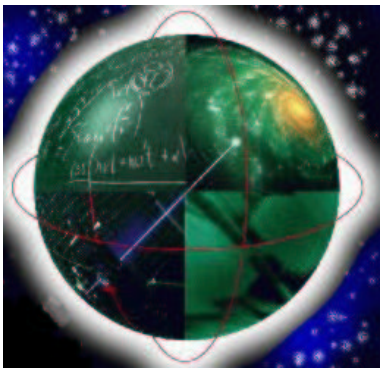

June 1, 2004

Abstract

We investigate the Josephson - quasi-particle (JQP) process in a superconducting single charge (SCT) transistor which is coupled to a tunable electro-magnetic environment. We consider a particular environment, a tunable ohmic resistor implemented as a two-dimensional electron gas (2DEG), that couples only capacitively to the SCT. For this circuit we calculate the correlation function and $P(E)$ for both Cooper pairs and quasi-particles. We derive the modification to the master equation by Averin and Aleshkin [1] to include an environment. Solving these equation for the stationary case and in a voltage range, where the JQP process is the only charge carrying process, we obtain an equation for the current. For the semi-classical limit of the environment we obtain an analytical solution. From this equation we can systematically study the dependence of the current on the strength of the dimensionless Josephson coupling (i.e. the Josephson energy with respect to the charging energy) and on the influence of the environment. As a function of the transport voltage, the current is approximately a Lorentzian for low Josephson energies compared to charging energies. Its width is determined by both the effective impedance and the dimensionless Josephson coupling. Increasing the effective impedance of the environment leads to decoherence broadening of the current peak, as the environment introduces dissipation. The relative effect of the environment on the peak width depends on the ratio of Josephson to charging energy, as this introduces an additional life-time broadening. It it is reduced, as the Josephson coupling is increased.

Contents

Abstract **iii**

1 Introduction **1**

2 Physical Background **5**
2.1 Superconductivity 5
2.1.1 The Josephson Effect 5
2.1.2 Quasi-particle Tunnelling 6
2.2 Theory of the Single Charge Transistor (SCT) 8
2.2.1 Basic Concepts of Coulomb Blockade 8
2.2.2 Conditions for the Observation of Charging Effects 11
2.2.3 Charging Effects for Normal Conducting SCT with Finite Bias Voltage 12
2.2.4 Parity Effect 13

3 Experimental Motivation **19**
3.1 Experimental Set-up 19
3.2 Experimental Observations 20
3.3 The Josephson - Quasi-particle (JQP) - Process 20

4 Hamiltonian for the System **23**
4.1 Model Circuit 23
4.2 Derivation of the Effective Hamiltonian I: Quasi-particles 23
4.3 Derivation of the Effective Hamiltonian II: Josephson Coupling 27
4.4 Full Effective Hamiltonian 28

5 Introduction to the Formalism **29**
5.1 Tunneling Rates across a Single Tunnel Junction and $P(E)$-Theory 29
5.1.1 Tunneling Rate for Quasi-particles across a Single Tunnel Junction . . 29
5.1.2 Tunneling Rates for Cooper Pairs 31
5.2 Charging Energy 32

6 Calculation of the Function $P(E)$ for the SCT **37**
6.1 Calculation of the Effective Impedance $Z_{\text{eff}}(\omega)$ 37
6.2 $P(E)$ in Semi-classical Approximation 39

7 Master Equation **43**
7.1 Master Equation of Averin and Aleshkin [1] 43
7.2 Relevant States for the Master Equation 44
7.3 Charging Energy around the Resonance 49

7.4 Modification of the Master Equations 50
7.4.1 Cooper Pairs 50
7.4.2 Quasi-particles 55
7.5 Master Equation for the JQP-Process 56
7.6 Current for the JQP-Process 57

8 Results **59**
8.1 Semi-classical Approximation for the Complex $P(E)$ for Cooper Pairs 59
8.2 Explicit Calculation of the Current for the JQP Process 60
8.2.1 Quasi-particle Tunnelling Rates 60
8.2.2 Generalised $\tilde{P}'(E)$ for Cooper Pairs 63
8.3 JQP Current 66

9 Concluding Remarks **81**

A Explicit Calculations and Further Details **83**
A.1 Effective Impedance $\mathrm{Re}\{Z_{\mathrm{eff}}(\omega)\}$ 83
A.1.1 Choice of the Parameters 83
A.1.2 Calculation of the Effective Impedance $Z_{\mathrm{eff}}(\omega)$ 83
A.2 Consistency Check for the Semi-Classical Approximation of $P(E)$ 86
A.2.1 Calculation of the Correlation Function 86
A.2.2 Calculation of $P(E)$ 89
A.2.3 Emergence of the Semi-classical Approximation 96
A.3 Integral for the Quasi-particle Tunneling Rate 99

B Interaction Picture **101**

C Bath Correlation Functions **103**

Acknowledgements **109**

Chapter 1

Introduction

What happens to a quantum system, if it is coupled to an environment? This is a question of very general interest as it is connected to the emergence of the classical world out of quantum physics. There exist already various practical implementations and theoretical suggestions for qubits [2], which are the basic components of a quantum computer, which crucially depend on maintaining quantum coherence.

We study a superconducting single charge transistor (SCT) that is coupled to a controllable electro-magnetic environment, which will introduce dissipation to the system. The SCT is a quantum system, it involves transition rates between discrete quantum states and competing energy scales. Because the SCT is superconducting and it is also quite small, we have the competition of Josephson coupling, (superconducting) gap and charging energy, and depending on the chosen energy scales, either charge or phase, which are canonical conjugate, will be good quantum numbers. In this report we want to consider such energy regimes that the Josephson quasi-particle process becomes the dominant process. This is a composite process involving coherent as well as incoherent transitions. The tunnelling rates for this process without an additional environment are already known. In this thesis we want to calculate, how these rates change if we couple the system to an environment. This can be described with a very general technique, the so-called $P(E)$-theory. This theory is introduced in chapter 5.1.

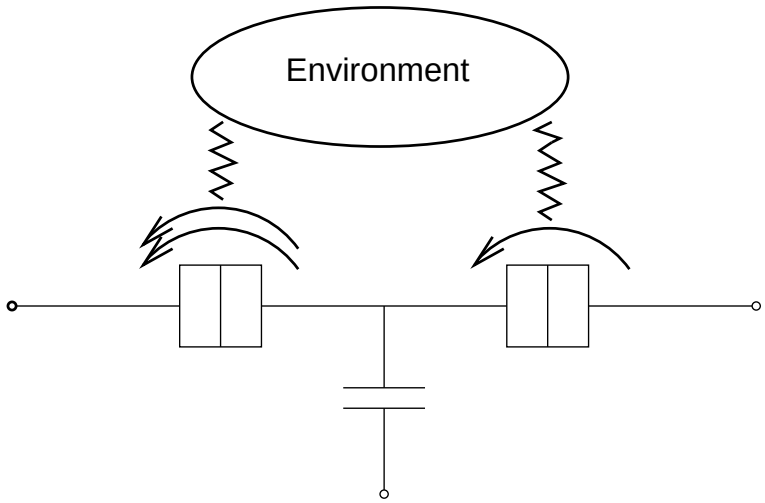

Figure 1.1: Schematic model for the tunnelling in a single charge transistor influenced by a dissipative environment.

For ultra-sensitive detection of charge the tunnelling of single charges is a favoured mechanism. Additionally, the JQP cycle is a process occurring far from equilibrium showing a sharply increasing response curve, where the steep part is well controllable and there is basically no background current. This makes it an ideal detection process. In particular, the JQP process has an important application in the read-out of charge quantum bits [3].

In chapter 2 we will introduce the basic features of superconductivity that are necessary to understand the JQP-resonance and the principles of single charge transistors. Notably, these are the density of states for quasi-particle excitations and tunnelling phenomena at superconducting junctions.

The study of single charge transistors (SCT) is closely related to charging effects. In normal conducting metals the conduction electrons are usually treated as noninteracting particles. But if there is a small island that is weakly connected to external leads, as is the case in an SCT, the electron interaction by Coulomb repulsion becomes important. First experiments on small tunnel junctions, i.e. metal-isolator-metal-contacts, clearly showed that deviations from the Ohmic current-voltage characteristic and charging effects were possible, as the fabrication technology was advanced enough to fabricate junctions of very small capacitances [4]. Soon it was realized that charging effects are easily visible, if there is a large impedance in series with the tunnel junction [5], actually the increase of Coulomb blockade by increasing the series resistance is called dynamical Coulomb blockade. Therefore instead of single tunnel junctions a combination of two tunnel junctions, the single charge transistor, is used to study charging effects. One possible charging process in a superconducting SCT is the JQP process, which has been observed in experiments [6] and is theoretically well explained for ideal SCTs [7], [1]. But, if there is an electro-magnetic environment coupled to the SCT, there exist only few theoretical approaches that deal with it, treating the environment as a small perturbation [8]. Therefore we want to go further and deal with the full dependence of the tunnelling rates on the environment.

In chapter 3 we will consider a particular experiment in a superconducting single charge transistor that was conducted by the group of A. Rimberg at Rice University [9]. This experiment is one of the first experiments, where it is possible to tune the coupling to the electro-magnetic environment in-situ, which allows controlled studies of the dependence of the JQP cycle on the environment and allows detailed comparison with theory.

In 4 we will introduce the circuit model for the SCT and derive the Hamiltonian.

In chapter 5 we will introduce the tunnelling rates for our system in the presence of the electro-magnetic environment. The properties of a mesoscopic device in the quantum limit are strongly influenced by its electro-magnetic environment, which destroys quantum coherence and induces energy relaxation. This is in principle known for a long time and many theoretical descriptions have been developed starting from the early 1990s [10], using the so-called $P(E)$-formalism [11], [12] based on the Caldeira-Leggett model of dissipative quantum mechanics [13]. This formalism outlines the modification of tunnelling rates due to an external impedance.

In chapter 6 we will explicitly calculate the function $P(E)$ for the system under consideration and study its semi-classical approximation.

In chapter 7 we actually consider the JQP process. Pioneering theoretical study of the JQP process for an ideal SET was done by Averin and Aleshkin [1]. We modify their set of master equations such, that it includes the influence of the environment as a generalised $P(E)$ function. Considering only lowest order perturbation theory in the tunnel coupling we calculate the stationary current for a regime of high bias voltages, where the JQP cycle is allowed.

The results are presented in chapter 8. We consider a semi-classical regime of the environment, for which a analytic calculation of the current is possible. We observe that the current depends on the effective impedance of the environment as well as on the Josephson energy compared to the charging energy. Its maximum value is decreased, if the environment becomes larger, but its contribution is extended with respect to the applied voltage. Also, this becomes more prominent when the Josephson coupling is reduced.

We observe a decreasing current, which is broadened as the effective impedance of the environment is increased. This is due to decoherence broadening, because increasing the effective impedance, i.e. enlarging the influence of the environment onto the system, induces more dissipation. For quite small values of the dimensionless Josephson coupling the shape of the current is described by a Lorentzian. For this regime the current is to very good agreement approximated by the function $\tilde{P}'(\delta)$ which describes the impact of the environment on the Cooper pair tunnelling in the JQP process. As one increases the Josephson coupling, the current is broadened due to life-time broadening of the quasi-particles. It is more likely for the quasi-particles to tunnel of the island for an increased Josephson coupling, which decreases the life-time of the double charged state on the island, which results in a broadening of the current peak. For regimes of large Josephson coupling the additionally decoherence broadening of the peak leads to a small contribution only. Furthermore for large values of the Josephson coupling the shape of the current is not fully determined by the shape of $\tilde{P}'(\delta)$ anymore.

Chapter 2

Physical Background

2.1 Superconductivity

As we want to consider superconducting single charge transistors, this section introduces some basic features of superconductivity. Superconductivity is a phenomenon that is well understood (at least for low temperatures). Since its discovery in 1911 by Kamerlingh Onnes [14] it has been apprehended in quite exquisite detail. London and London explained its electro-dynamical effects in the phenomenological London theory in 1935 [15]. Ginzburg and Landau introduced the macroscopic wave function for the superconducting condensate close to the critical temperature [16]. And finally Bardeen, Cooper and Schrieffer [17] introduced a microscopic theory, the BCS-theory, that explains the formation of the condensate by a collapse of the conduction band electrons into a Cooper pair condensate. In the following, we want to discuss the Josephson effect that occurs in superconducting tunnel junctions, so-called Josephson-junctions, and is responsible for the dynamics of Cooper pairs. Second we want to discuss the tunnelling of the other charge carriers in superconductors, the quasi-particles. These topics are covered in standard textbooks, see e.g. [18], [19].

2.1.1 The Josephson Effect

One important effect is the Josephson effect which occurs in a weak link between superconductors. A typical Josephson tunnel junction consists of two superconducting electrodes that are separated by a thin insulating barrier, as can be seen in figure 2.1.

In 1962 Josephson [20], [21] predicted that there will be a current flow through the junction even without voltage-biasing the junction. This current is given by the first Josephson equation

$$I_S = I_C \sin(\Delta\phi). \tag{2.1}$$

$\Delta\phi$ denotes the difference of the phase of the macroscopic Cooper pair wave function. As we have two separated superconductors, a phase difference can be established between them. This macroscopic wave function also explains why the current is dissipation-less (therefore called supercurrent): the phase coherence of the Cooper pairs is retained while they tunnel through the junction and give rise to the current. The amplitude of the supercurrent in a tunnel junction is given by the Ambegaokar-Baratoff-formula [22], [23],

$$I_C R_n = \frac{\pi\Delta}{2e} \tanh\left(\frac{\Delta}{2kT}\right), \tag{2.2}$$

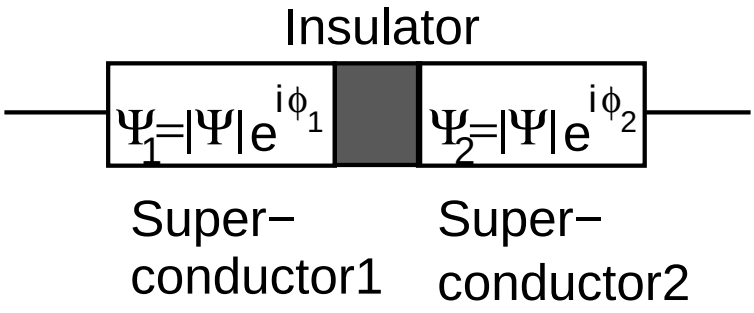

Figure 2.1: Schematic model of a Josephson junction. It consists of two superconductors that are separated by a thin insulating barrier. The macroscopic wave function Ψ , that describes a superconductor, depends on the square root of the density n of Cooper pairs $|\Psi| = \sqrt{n}$ and on the phase ϕ, thus $\Psi = |\Psi|e^{i\phi}$. This is obvious in the Ginzburg - Landau theory [16], but also holds for general conditions ,e.g. for temperatures far from the critical temperature.)

where R_n denote the resistance in the normal state, T the temperature and Δ the (temperature-dependent) superconducting gap energy.

In addition to this so-called DC Josephson effect, there is the AC-Josephson effect. As one applies a finite bias voltage across the Jopsephson junction the phase evolves proportional to the applied voltage, which leads to the second Josephson equation

$$\frac{d(\Delta\phi)}{dt} = \frac{2eV}{\hbar}, \tag{2.3}$$

which by insertion into the first Josephson equation results in an alternating supercurrent

$$I_S = I_C \sin\left(\frac{2eV}{\hbar}t\right), \tag{2.4}$$

This effect is actually used in metrology to define voltage standards.

By calculating the electrical work for the Josephson effect (by inserting equations (2.3), (2.4)) $W = \int I_S V dt = \text{const.} - \frac{\hbar I_C}{2e}\cos(\Delta\phi)$ one can introduce the energy scale that governs the coupling of the two superconductors in the Josephson junction, the Josephson energy, as

$$E_J = \frac{\hbar I_C}{2e}. \tag{2.5}$$

One can view a tunnel junction as two metal plates that are connected by an insulator, which is a dielectric. So the junction contains a geometric capacitance. Therefore the junction can be described by an ideal junction, which shows the just described effects, having a capacitance in parallel. There may be another resistance shunted in parallel, which accounts for the tunnelling of quasi-particles or for external shunts. This so-called resistively and capacitively shunted junction (RCSJ) model is shown in figure 2.2.

2.1.2 Quasi-particle Tunnelling

In addition to the Josephson current there can be a second contribution to the current in the superconductor which is due to the fundamental excitation, the quasi-particles. So if we consider a junction in which the Josephson current is suppressed, one can observe the effect

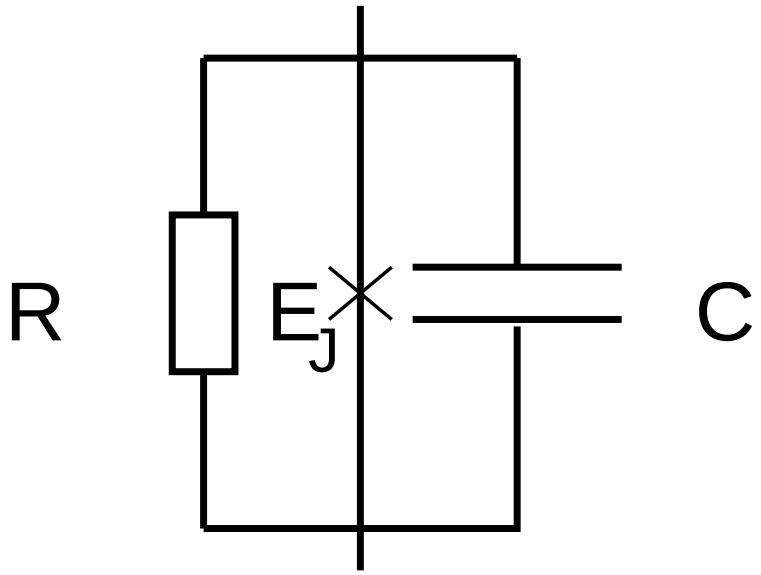

Figure 2.2: Equivalent circuit diagram for a Josephson junction. The cross marks the ideal junction which has a capacitance C and a resistance R in parallel.

of quasi-particles alone. In a superconductor at $T = 0$ without any bias voltage applied, only Cooper pairs exist. A Cooper pair is a bound state that consists of two electrons that have opposite spin and momentum (to overcome the Pauli exclusion principle) with a binding energy of 2Δ. Cooper pairs form a collective condensate whose mean energy defines the chemical potential. One can only break a Cooper pair if one applies an energy of at least Δ per electron. This is expressed in the density of states of quasi-particles, which has a gap for energies below Δ. The energy dependence of the density of states for quasi-particles $N_S(E)$ with respect to the (constant) density of states in the normal state $N_N(0)$ is described by the equation

$$\frac{N_S(E)}{N_N(0)} = \frac{|E|}{\sqrt{E^2 - \Delta^2}}\theta(|E| - \Delta), \tag{2.6}$$

and shown in figure 2.3.

There are now two mechanisms that can allow a quasi-particle current to flow. For temperature $T = 0$ one has to apply a bias voltage that exceeds $2\Delta/e$. This can be understood as we have to break the Cooper pairs. At finite T (but still well below the critical temperature) quasi-particles will be thermally excited and therefore give rise to a small but finite current at voltages below the threshold $2\Delta/e$. A model for describing this is the so-called semiconductor model of superconductor - superconductor tunnelling of quasi-particles which is shown in figures 2.4 a) and 2.4 b).

The current - voltage - plot in figure 2.5 shows a jump at a voltage of $2\Delta/e$ which can be understood, because there the singularities in the densities of states line up. For higher biases the current becomes Ohmic. Measuring the current-voltage characteristics allows to determine the gap energy of a superconductor.

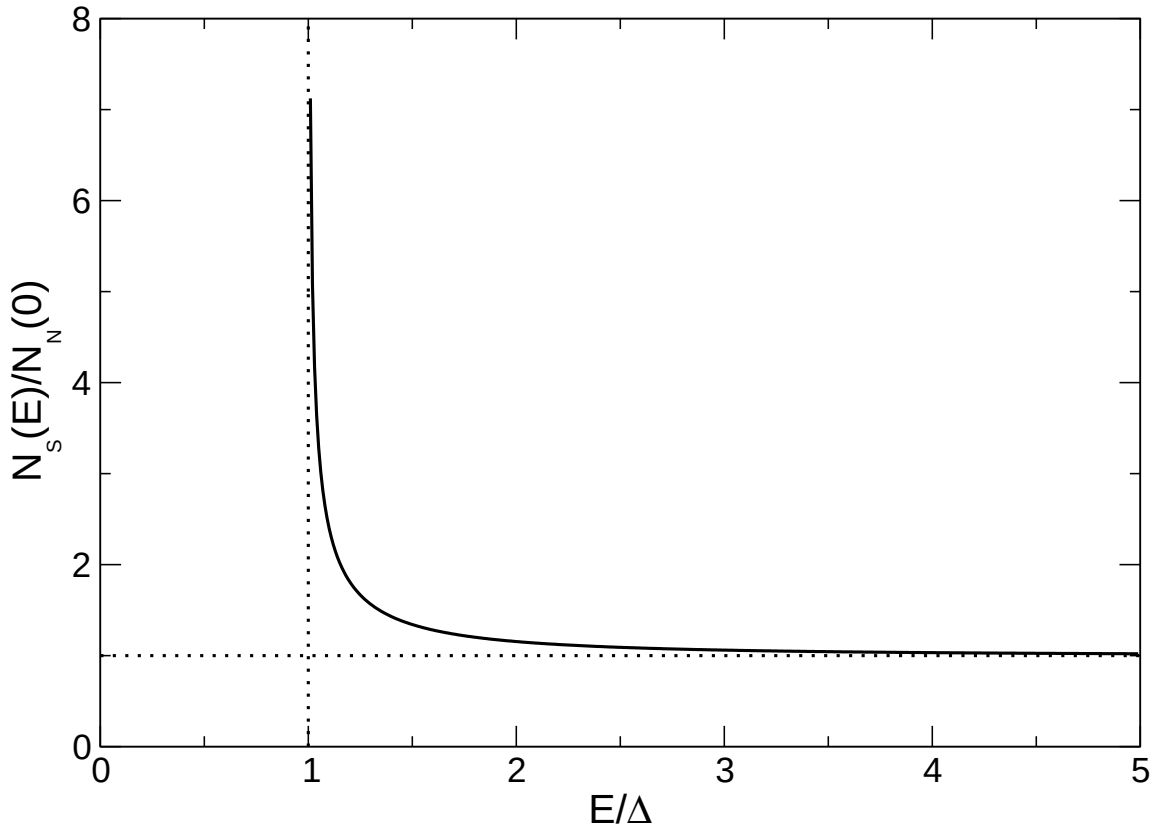

Figure 2.3: Density of states for quasi-particles in a superconductor N_S compared to the density of states in a normal conductor N_N. The energy is plotted in units of the energy of the superconducting gap Δ and the zero of energy corresponds to chemical potential, which is defined by the mean energy of the Cooper pairs.

2.2 Theory of the Single Charge Transistor (SCT)

A single charge transistor consists of two ultra-small tunnel junctions (which are regular tunnel junctions in the normal conducting case and Josephson junctions in the superconducting case). These are connected by a piece of metal that forms an island. There can be a bias voltage V applied to the junctions and the island is connected to an electrostatic gate. The circuit is shown in figure 2.6.

2.2.1 Basic Concepts of Coulomb Blockade

To understand how an SCT works in principle, we consider the simplest possible case, namely a normal conducting SCT without any bias voltage. Now we study how much energy it costs to bring the charge Q onto the island. A single capacitor has a charging energy of $\frac{Q^2}{2C}$ where C is its capacitance. For multiple capacitances the charging energy is described in terms of a capacitance-matrix C as $E_C = \frac{1}{2}Q^T C Q$, where Q is a vector containing the charges on each capacitor. In the case of an SCT the capacitance is given by the sum of all capacitances surrounding the island $C = C_L + C_R + C_G$. The charge is given by the discrete charge ne of n extra electrons that tunnelled onto the island and by a continuous polarisation charge $Q_G = V_G C_G$ that is induced by the gate voltage V_G, therefore $Q = Q_G - ne$. Note that $e = |e|$

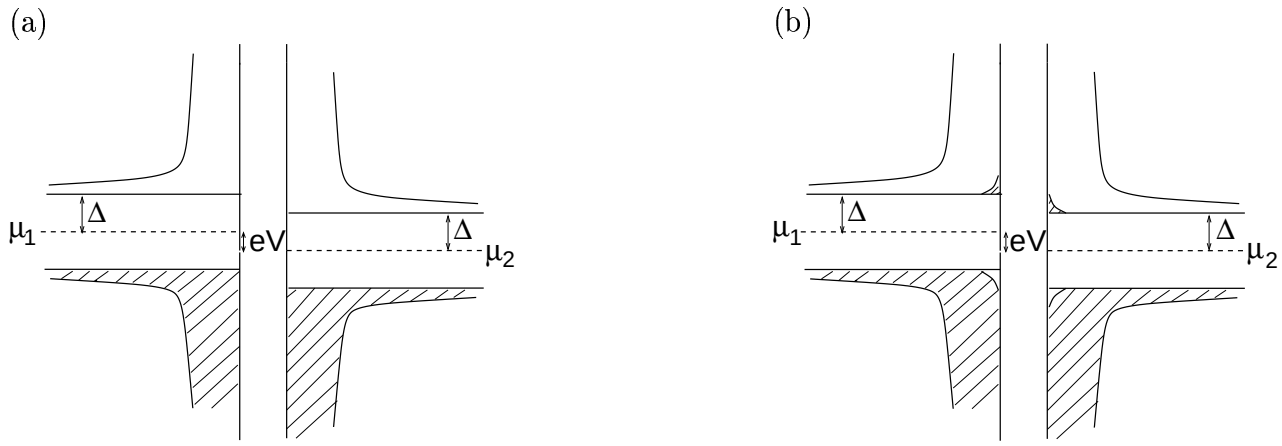

Figure 2.4: "Semiconductor" model of superconductor - superconductor tunneling of quasi-particles for $T = 0$ (a) and $T > 0$ (b). This shows the superconductors on the left and right with their chemical potentials μ and quasi-particle states below (occupied for $T = 0$) and above (empty for $T = 0$) the chemical potential (the density of states is plotted schematically). Applying a bias voltage shifts the respective Fermi levels. Quasi-particle tunneling is only possible, if the voltage shifts the energy levels, such that occupied states line up with empty states at the same energy to allow tunneling. For $T = 0$ this is only possible for $eV > 2\Delta$. There are always occupied states above the Fermi energy for $T > 0$, thus allowing a current flow.

denotes the absolute value of the electron charge. So the charging energy becomes

$$U(n, Q_G) = \frac{(ne - Q_G)^2}{2C} = E_C \left(n - \frac{Q_G}{e} \right)^2 , \tag{2.7}$$

where we introduced the energy scale $E_C = \frac{e^2}{2C}$, which is the charging energy for adding a single electron to the island.

The gate is used to continuously tune the number of electron charges n on the island. This can be seen in figure 2.7. If there are no extra electrons on the island in the beginning and we increase the gate charge, at the degeneracy points of the charging energy ($Q_G = \pm\frac{e}{2}, \pm\frac{3e}{2}$,...) the ground state switches from $n = 0$ to $n = 1$ and so on, so this means single electrons tunnel subsequently onto the island as the gate charge increases, thus the so-called Coulomb staircase shows up in the current - bias voltage characteristics. If one tunes the gate charge to a degeneracy point of the charging energy, this gives rise to a current flow, shown in figure 2.8.

There is, of course, a small bias voltage applied, to favour tunneling in one direction (otherwise the tunneling in both directions results in an averaged current that is zero). The life-time broadening causes a finite width of the peaks. The region where there is no current, which corresponds to the minima in the charging energy, is called Coulomb blockade, because the tunneling of an electron is then forbidden due to Coulomb repulsion.

To understand the Coulomb blockade, we have to derive when it is possible for an electron to tunnel on or off the island. For zero temperature and having initially $n = 0$ electrons on the island, this is energetically allowed, if the difference in electrostatic energy

$$U(\pm 1, Q_G) - U(0, Q_G) = \frac{(Q_G \mp e)^2}{2C} - \frac{Q_G^2}{2C} = \frac{e}{C}(\mp Q_G + \frac{e}{2}) \tag{2.8}$$

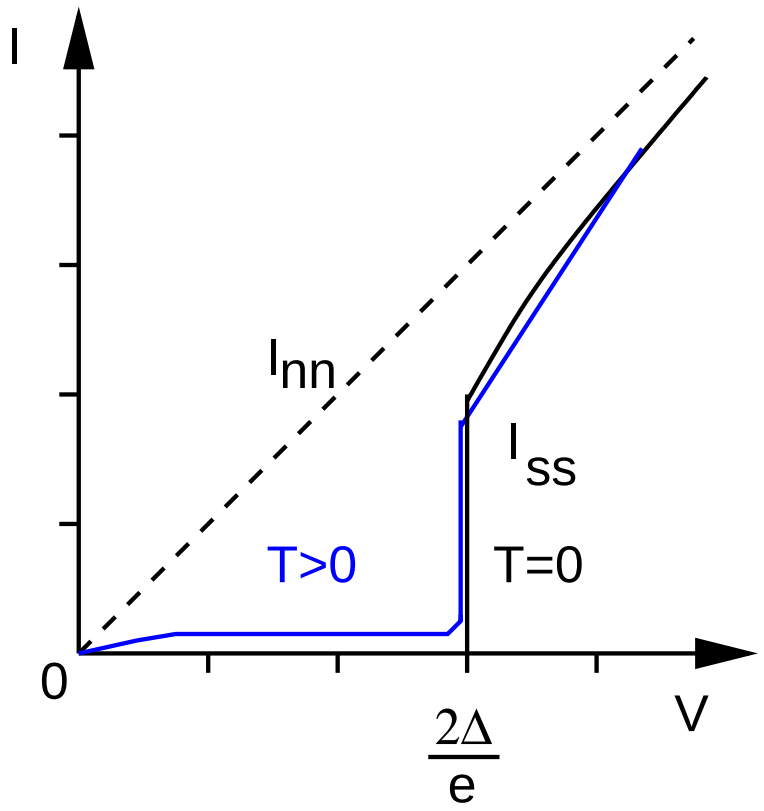

Figure 2.5: Current - Voltage - Characteristics for the quasi-particle current I_{SS} in a superconducting tunnel junction for $T = 0$ and $T > 0$ compared to the current in a normal conducting junction I_{nn}.

is negative. This is fulfilled for $|Q_G| > \frac{e}{2}$, which defines a crucial initial charge $Q_C = \frac{e}{2}$. This critical charge is also the charge where the energy parabolas for charges differing by one electron charge are degenerate. As one can see in the energy diagram figure 2.7, for $|Q_G| > Q_C$ the charging energy for having no extra electrons on the island is larger then the energy to add an extra electron. Therefore tunneling occurs. As the charging energy for n electrons sitting on the island is the same as the energy for having $n = 0$ electrons on the island with a gate charge that is shifted by ne, we can explain the energy differences that occur by tunneling in a reduced charge diagram that shows only the parabola for n=0, which is shown in figure 2.9.

The phenomenon is manifest in the current-voltage-characteristics of a single tunnel junction: there will be no current for

$$|V| = \frac{|Q|}{C} < \frac{Q_C}{C} = \frac{e}{2C} \tag{2.9}$$

This region for $-\frac{e}{2C} < V < \frac{e}{2C}$ is called Coulomb blockade region due to the Coulomb repulsion between the tunneling electron and the influence charges. See figure 2.10

In the normal conducting case the SCT it is also referred to as a SET (single electron transistor) because the charge is carried by single electrons across the island.

One application of SCTs stems from the tunneling of single electrons. One can define current standards by pulsing the gate such that one electron tunnels per cycle.

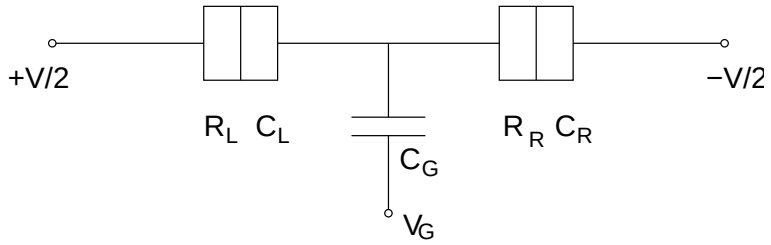

Figure 2.6: Single Charge Transistor with symmetrically applied bias voltage V. The left and right junctions have capacitances C_L/R and resistances R_L/R. The electrostatic gate with voltage V_G and capacitance C_G is connected to the island.

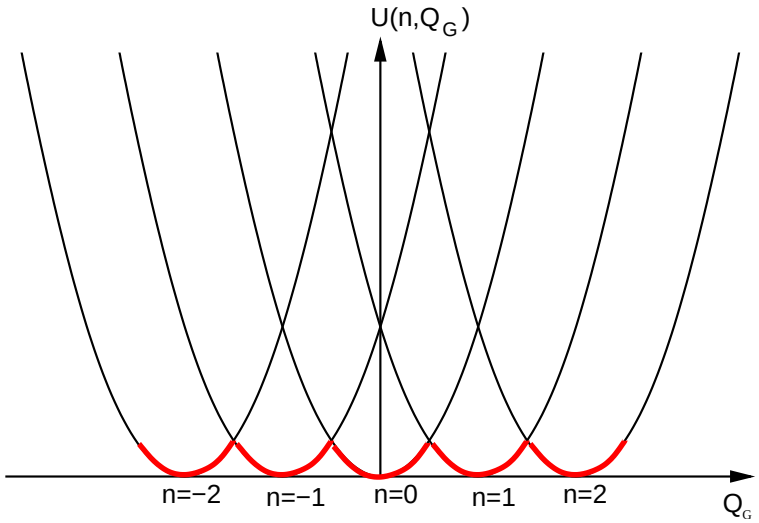

Figure 2.7: Charging energy for a normal conducting SCT without bias voltage. The gate (with gate charge Q_G) is used to continuously tune the number of electron charges n on the island. If there are no extra electrons on the island in the beginning and we increase the gate charge, at the degeneracy points of the charging energy ($Q_G = \pm\frac{e}{2}, \pm\frac{3e}{2}$,...) the ground state (red) switches from $n = 0$ to $n = 1$ and so on. This means single electrons tunnel subsequently onto the island as the gate charge increases.

2.2.2 Conditions for the Observation of Charging Effects

In the SET for low enough temperature both classical and quantum effects play a role. After having introduced the concept of the charging energy, we can explain, why the charging energy is important in the discussion of SETs. It is important, because one uses very small SETs, and as the capacitance scales with the area of the capacitor, the corresponding capacitance is also small, so the charging energy, even for single electrons, is large. A capacitance of $C \approx 1$fF has been experimentally realized for more than ten years. Today it is even possible to achieve capacitances in the order of magnitude of $C \approx 100$aF [25] down to $C \approx 1$aF [26]. If compared to thermal energies, the charging energy of a capacitance of 1fF corresponds to a thermal energy of a temperature of 1K, which is already quite large considering the low temperatures at which experiments on charging effects are usually carried out. For the observation of charging effects the charging energy for a single electron $E_C = \frac{e^2}{2C}$ has to be smaller than the thermal energy $E_{\text{therm}} = k_B T$. Therefore the capacitance has to be $C \ll \frac{e^2}{2k_B T} \approx \frac{10^{-15} FK}{T}$

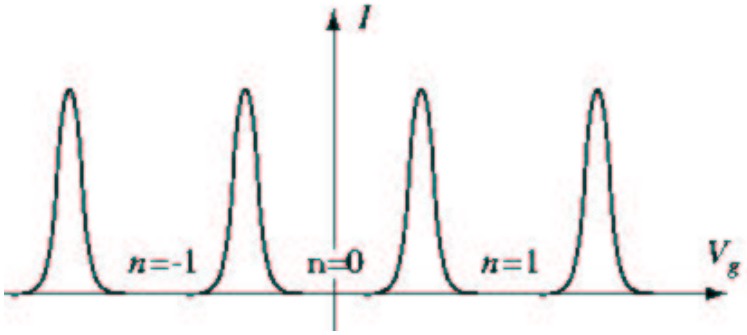

Figure 2.8: Current - gate-voltage characteristics for an SCT showing current peaks that are due to the tunneling of single electrons and the Coulomb blockade as valleys in between. From [24].

and, because the capacitance scales with the dimensions of the capacitor, this explains why we need ultra-small tunnel junctions and low temperatures (in the milli-Kelvin range) for its observation. It is much easier to see charging effects, when one uses SETs instead of a single Josephson junction. For a single junction with capacitance C one also has to take into account its environment (for instance the cables) with resistance R in series. Then the charging time of the capacitor is RC therefore the uncertainty in energy is $\Delta E \approx \frac{h}{2RC}$. This has to be much smaller then the charging energy E_C. Therefore a very high resistance $R \gg \frac{h}{e^2} \approx 25.8k\Omega$ is needed for the observation of charging effects. And this high resistance environment is of course easily achieved by combining two Josephson junctions as a SET, where one junction serves as the high resistance environment for the other one.

In the following, we are mainly interested in discussing tunneling events of single electrons. Tunneling is a purely quantum mechanical effect. It induces quantum fluctuations of the charge. In addition, the charge states are well defined, this means the charge is a good quantum number, which holds for Josephson energies being smaller than charging energies. This is fulfilled, as $\frac{E_J}{E_C}$ scales with the size of the sample, and is thus quite small for a small SCT.

2.2.3 Charging Effects for Normal Conducting SCT with Finite Bias Voltage

The effect of a finite bias voltage can be formally absorbed in a generalised gate charge $Q_{\tilde{G}} = C_G V_G + V_L C_L + V_R C_R$, where $V = V_L - V_R$ denotes the bias voltage and C_L (C_R) the capacitance of the left (right) junction. In the case of a symmetrically applied bias voltage ($V_L = -V_R = \frac{V}{2}$) this reads $Q_{\tilde{G}} = C_G V_G + \frac{V}{2}(C_L - C_R)$. I.e. for equal capacitances of the tunnel junctions the bias voltage does not induce a polarisation charge on the island.

Quantitative discussions of the charging energy for finite voltage are given in [18] and will be applied to the SCT in 5.2.

Figure 2.11 shows the addition energies that have to be paid to change the number of electrons on the island with respect to the applied bias voltage. As long as the addition energy is in the window provided by the voltage, an electron can tunnel, giving rise to a current flow. The larger the voltage the more likely this is. The addition energy can be tuned by the gate voltage.

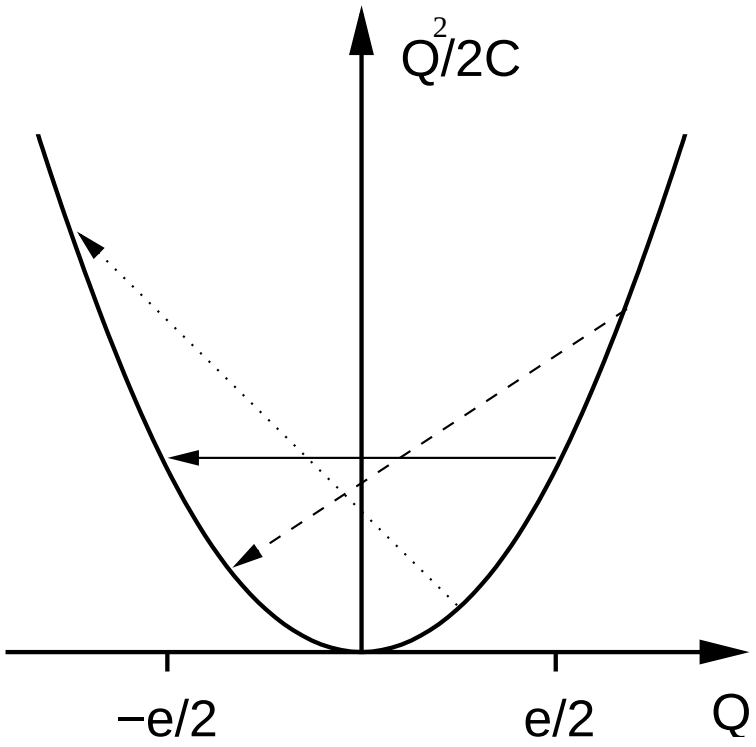

Figure 2.9: Charging energy versus charge on the capacitor and tunnel events. For an initial charge larger $e/2$ tunneling across the junction is allowed(dashed arrow). For an initial charge equal to $e/2$ the change in charging energy would be zero (solid arrow) and for an initial charge less then $e/2$ tunneling is not allowed (dotted arrow).

In figure 2.12 the dependence of the current on the gate charge ($Q_G = C_G V_G$) and on the bias voltage is shown. Increasing the bias voltage reduces the region of Coulomb blockade. For high enough biases the Coulomb blockade is overcome for all gate charges and the current shows linear behaviour.

2.2.4 Parity Effect

So far we have only considered the SET in normal state. Now we tune to the case of an all superconducting SCT. Note that the tunnel junctions now also provide Josephson coupling. There can be two possible charge carriers: Cooper pairs, which transfer two electron charges across the island, and quasi-particles, which transfer a single electron charge. As outlined in section 2.1 the electrons on the island and on the junctions condense into Coopers pairs, thereby their energy is decreased by the superconducting energy gap Δ compared to the normal state. To allow tunneling of a quasi-particle, a Cooper pair has to be broken, which means that the extra gap energy Δ per quasi-particle has to be paid. Therefore the energy parabolas for an odd extra number of electrons on the island differ by Δ from the even parabolas. From this we can understand the charging energy as is plotted in figures 2.13 and 2.14 for zero bias voltage. There are two regimes. If $E_C > \Delta$ it is still more favourable for quasi-particles to tunnel (2.13) but for $E_C < \Delta$ quasi-particle tunneling is suppressed and only the tunneling of Cooper-pairs is allowed, if the gate voltage sits at a degeneracy point of the charging energy (2.14). But by applying a finite voltage one can again reach regimes were the tunneling of quasi-particles is allowed. This can be seen in figure 2.15 where the Tinkham group in Harvard [27] observed

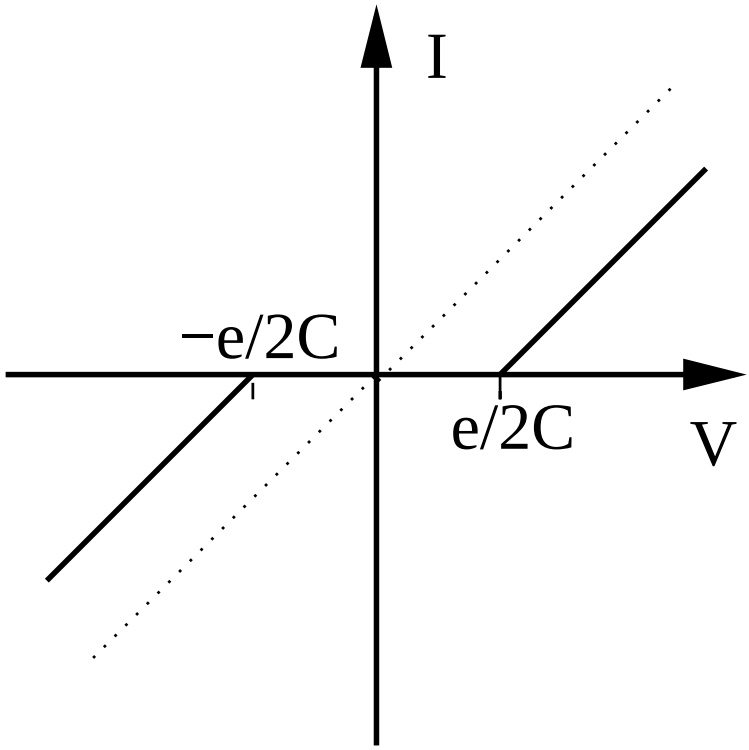

Figure 2.10: Occurrence of the Coulomb blockade in the current-voltage-behaviour for $T = 0K$ for a tunnel element. For a voltage range $-e/2C < V < e/2C$ corresponding to $|Q| < e/2$ electrons are not allowed to tunnel resulting in zero current.

the transition of 2e-periodicity in the current, which is a signature of Cooper pair tunneling to e-periodicity, which is a signature of quasi-particle tunneling.

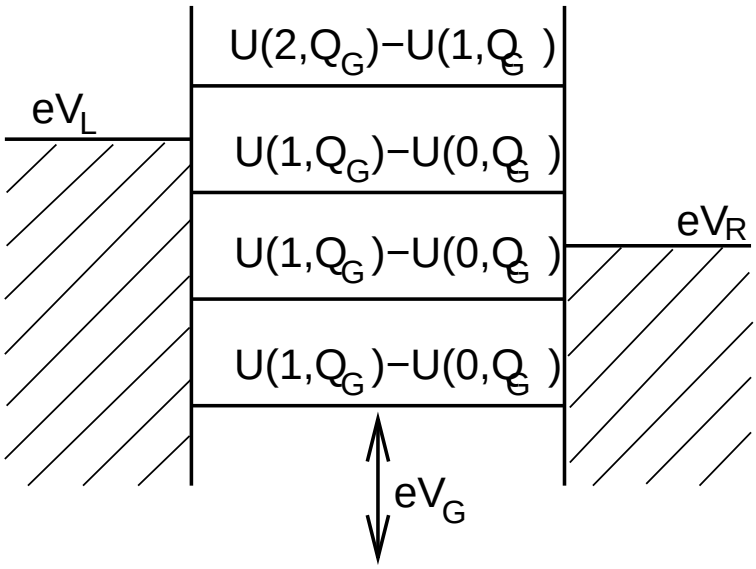

Figure 2.11: Energy levels of the island with respect to the chemical potentials of the leads for finite bias voltage $V = V_L - V_R$. This shows the addition energies for a SCT that have to be paid to change the number of electrons on the island. As long as the addition energy is in the window provided by the voltage, an electron can tunnel through the island, giving rise to a current flow. The larger the voltage the more likely this is. The addition energy can be tuned by the gate voltage. For this particular example, the only process that contributes to a current, is one electron can tunnel from the left lead onto the island, number of electrons on the island from $n = 0$ to $n = 1$ and then from the island to the right lead, changing $n = 1$ to $n = 0$.

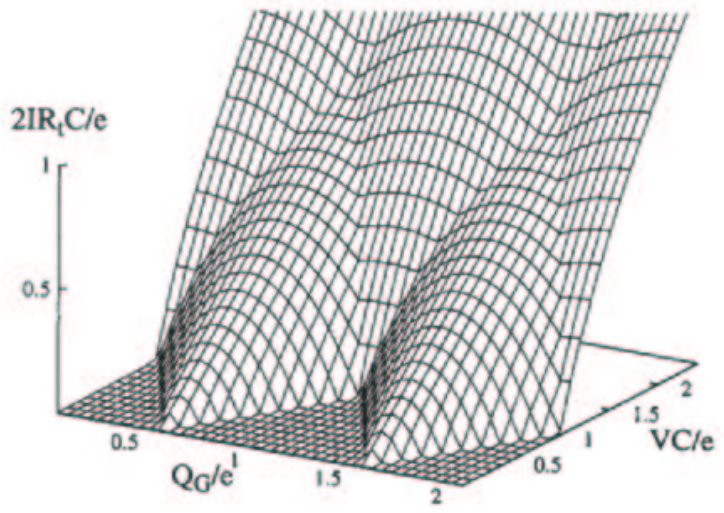

Figure 2.12: Current - Gate Voltage - Voltage Characteristics for a SCT showing the reduction of Coulomb blockade as the bias voltage is increased. From [11]

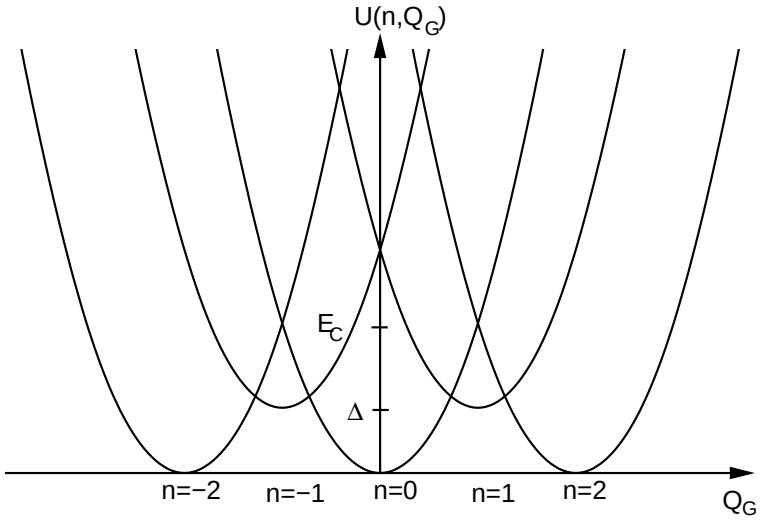

Figure 2.13: Charging energy for all superconducting SCT with $E_C > \Delta$ without bias voltage.

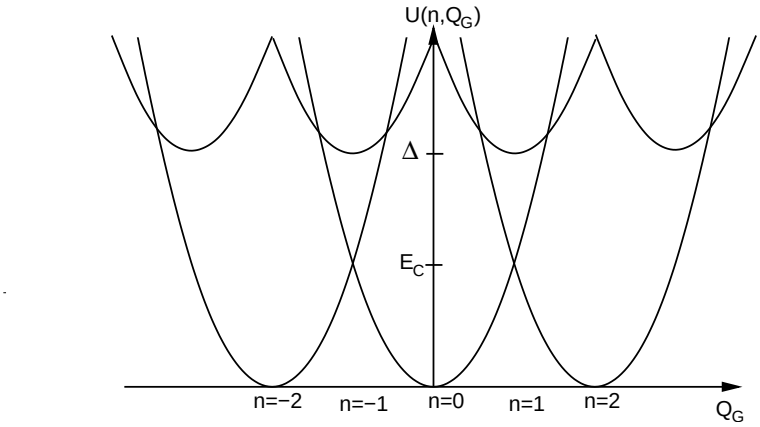

Figure 2.14: Charging energy for all superconducting SCT with $E_C < \Delta$ without bias voltage.

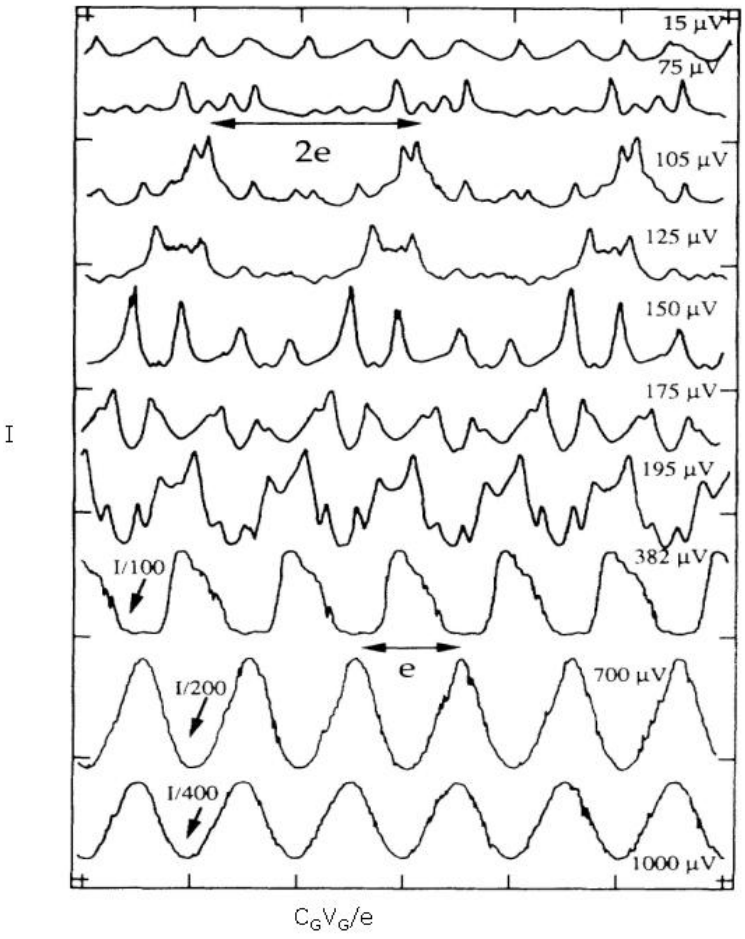

Figure 2.15: Current versus gate charge for different bias voltages in a superconducting SCT. As the bias voltage is increased one observes a crossover from 2e periodicity to e-periodicity. From [27]

Chapter 3

Experimental Motivation

Next to the theoretical interest in studying the tunneling phenomena in a SCT, there was also an experiment [9] done by the Rimberg group at Rice University were they observed the Josephson - quasi-particle process in an SCT that was coupled to an environment.

3.1 Experimental Set-up

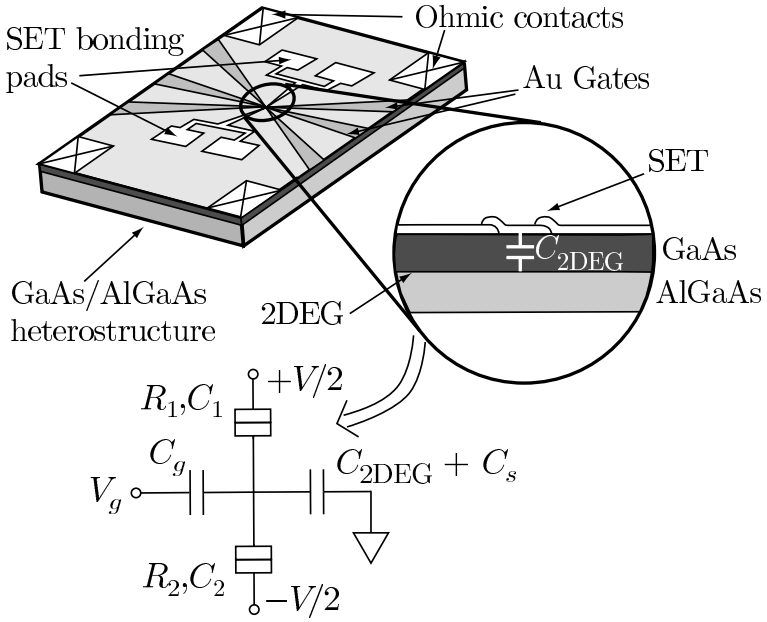

Figure 3.1: Set-up of the experiment by Rimberg et al. [9].The SCT is on top of a semiconductor heterostructure beneath which the 2DEG resides. The 2DEG serves as electro-magnetic environment and has a resistance which is tunable by a back-gate.

The set-up of the experiment can be seen in figure 3.1. There an SCT on top of a semiconductor heterostructure was fabricated. The substrate consists of GaAs and AlGaAs. At the interface of the two materials, a two dimensional electron gas (2DEG) due to the difference in band gap energies of the semiconductors is formed. So the 2DEG resides inside the substrate well underneath the surface and the SCT. The resistance of the 2DEG can be tuned by changing its carrier density through a back gate. As any resistor, the 2DEG causes voltage noise

and therefore serves as an electro-magnetic environment. Because there is no metallic contact between the SCT and the 2DEG the coupling can be modelled as purely capacitive. This is actually the only experimental set-up so far, where it is possible to tune the resistance of the environment in-situ. Previously, for changing the impedance of the environment one had to fabricate a totally new sample [28]. Of course this is not desired, because then one changes the parameters of the SCT at least slightly which makes the results more difficult to compare. So with this experiment the SCT is always the same, but the environment can change. The dimensions and materials of the sample lead to the following energy scales (compared to the charging energy for one electron $E_C \approx 100\mu eV$). The Josephson coupling is weak $E_J < E_C$, which means that the charge states are well defined. The superconducting gap energy is larger than the charging energy $\Delta > E_C$, therefore the parity effect leads to a 2e-periodicity in the current as the voltage is small. The temperature is in the milli-Kelvin range, therefore the thermal energy is small $kT < E_C$, which is a requirement for allowing the observation of charging effects of single electrons and Cooper pairs.

3.2 Experimental Observations

Figure 3.2 shows the contour plot of the measured current versus the gate charge and bias voltage. The different features in the plot are due to a variety of tunneling processes, that can occur in an SCT. These are for instance the tunneling of quasi-particles, Cooper pairs, photon-assisted tunneling of quasi-particles or Cooper pairs and combinations of them. If the voltage is in a certain range, only some of them are allowed, as can be inferred from the former discussion of Coulomb blockade.

For small voltages there is no current due to Coulomb blockade effects. The current starts at finite voltage and is due to the incoherent tunneling of Cooper pairs for voltages below approximately $800\mu V$. For voltages larger $800\mu V$ one observes the onset of quasi-particle tunneling. In between there is one striking feature for voltages between 500 to $800\mu V$. This is the Josephson - quasi-particle (JQP) peak.

3.3 The Josephson - Quasi-particle (JQP) - Process

The Josephson-quasi-particle process is a process occurring far from equilibrium at high bias voltages. It consists of the resonant incoherent tunneling of a Cooper pair onto the island across the left junction followed by the successive tunneling of two quasi-particles across the right junction (the left and right notation refers to a negative bias voltage at the left junction and a positive bias voltage at the right junction). So the whole process brings the charge on the island back to the initial state. A schematic picture of the JQP-cycle is shown in figure 3.3. There can only be a Cooper pair current, if energy is conserved. So the energy gained by the applied bias voltage is to be conserved by the difference in charging energies. The condition of resonant Cooper-pair tunneling leads to a straight line of JQP peaks in the $Q_G - V$-plane. By incoherent tunneling of Cooper pairs one describes a Cooper pair that loses phase coherence with respect to the Cooper pair that tunnelled across the junction before, but still remains a Cooper pair. The transition of a second Cooper pair that would tunnel across the right junction off the island is forbidden by this energy constraint, because then the difference in charging energy is not compensated by the bias voltage anymore. Therefore a current can only flow if quasi-particles tunnel off the island across the right junction. This is allowed for voltages $V > \frac{E_C+2\Delta}{e}$ and gives the onset of the JQP-peak. It stops at the transition at $V = 4\Delta$

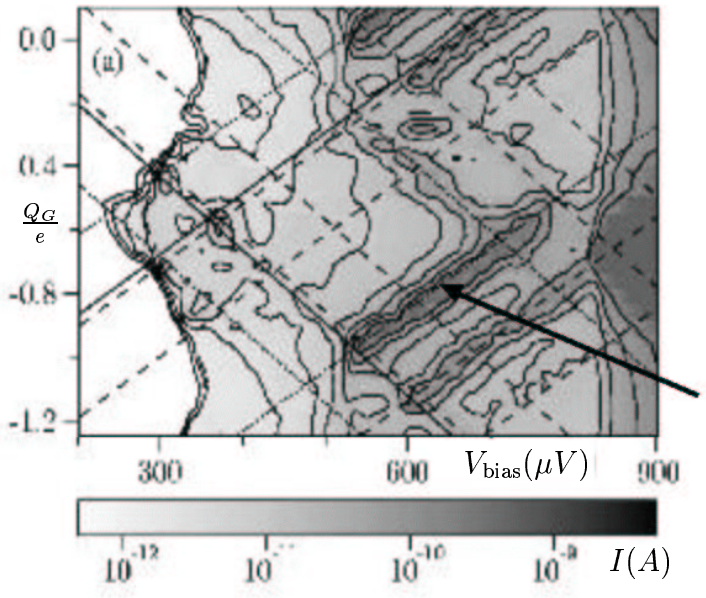

Figure 3.2: Contour plot of the current with respect to gate charge Q_G and bias voltage from the Experiment by Rimberg et al. [9]. The straight solid lines indicate thresholds for allowed quasi-particle transition and the dotted lines for Cooper pair transitions. These lines are parallel for tunneling events through the same junction. In particular we are interested in the large peak structure (indicated by the arrow) for $\approx 500\mu V < V < 800\mu V$ which sits on a Cooper pair transition for the left junction. This is the JQP - peak (see section 3.3).

because then pure quasi-particle tunneling is allowed. This can be understood, because we have already seen in the discussion of quasi-particle tunneling that one has to apply a voltage of 2Δ to allow a quasi-particle current in a single Josephson junction. In an SET there are two Josephson-junctions in series leading to a minimal bias voltage of 4Δ.

Although there exist already several approaches to describe the JQP-process in a single charge transistor [29], [30] there is only one approach that includes an environment [8], [7]. It is still not known how this JQP-current changes, if we include an electro-magnetic environment to the single charge transistor and vary its effective impedance. So this should be calculated in this thesis using the $P(E)$-theory and a master equation approach as outlined in the next sections. There are at least two reasons why one should study the impact of the environment on the JQP process using the $P(E)$-theory. Firstly the JQP cycle can be used as a detection process for charge quantum bits with high sensitivity. Because this is a process that occurs far from equilibrium, showing a sharply increasing, well controllable response curve on top of basically no background current. The environment limits its performance as a detector. As we will see in chapter 8, the current peak is decreased and broadened as the effective impedance of the environment is increased, i.e. if the environment becomes larger. This reduces the sensitivity for the JQP process. Secondly, the JQP cycle is a good systematic test for the $P(E)$-theory. This tests both the concepts underlying $P(E)$-theory and our way of modelling the environment [31]. This is important, as $P(E)$-theory is used for all kinds of single electron logic, e.g. for current standards.

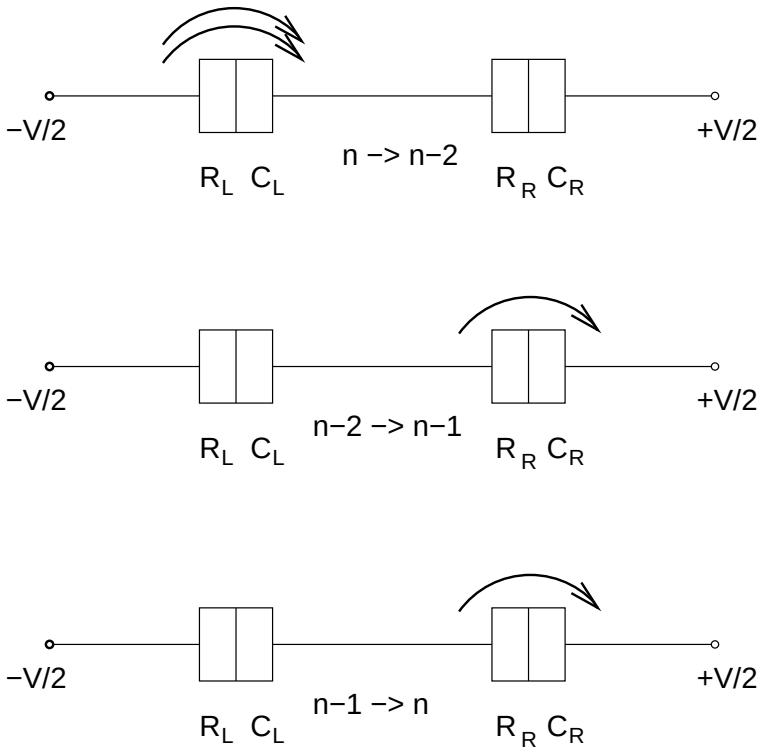

Figure 3.3: Schematics of the Josephson - Quasi-particle (JQP) - process showing the resonant incoherent transition of a Cooper pair across the left junction followed by the successively tunneling of two quasi-particles across the right junction and the changes of the charge on the island, initially given by ne. The voltage range, where this process is allowed, depends crucially on the bias and gate voltage, as the Cooper pair transition has to be resonant, and the voltage must be large enough to allow the quasi-particle tunneling after the tunneling of a Cooper pair, but prevent pure tunneling of quasi-particles (see section 3.3 for the conditions on the voltages).

Chapter 4

Hamiltonian for the System

4.1 Model Circuit

The model circuit for the SCT coupled to a 2DEG is shown in figure 4.1. The SCT was already introduced in section 2.2 and in figure 2.6. The 2DEG is modelled by two resistances R^1_{2DEG} and R^2_{2DEG} that couple capacitively to the leads with capacitance C_{Lead} and to the island with capacitance C_0.

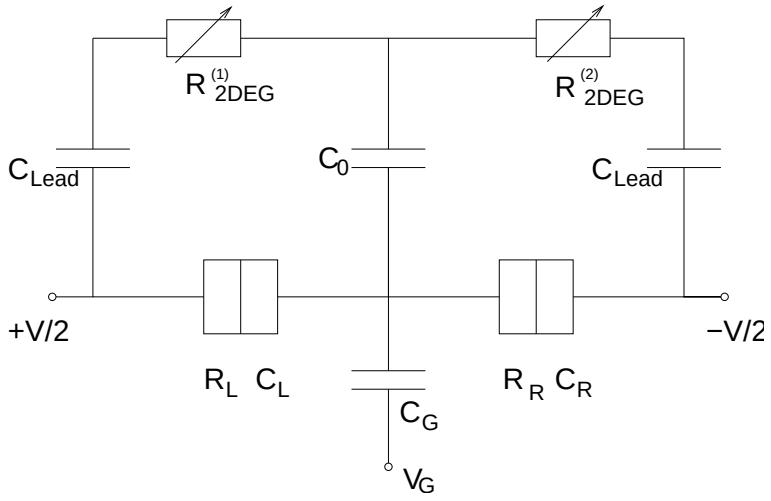

Figure 4.1: Model circuit for the coupling of the single charge transistor (SCT) to the two dimensional electron gas (2DEG) that serves as an environment. The 2DEG is modelled by two tunable resistances R^1_{2DEG} and R^2_{2DEG} that couple capacitively to the leads with capacitance C_{Lead} and to the island with capacitance C_0.

4.2 Derivation of the Effective Hamiltonian I: Quasi-particles

The Hamiltonian that describes the tunneling of quasi-particles in an SET coupled to an electro-magnetic environment can be derived by the generalisation of the quasi-particle Hamiltonian for a single tunnel element in a dissipative environment, as described in [11].

Consider a SET with bias voltage $V = V_L - V_R$ and a dissipative environment which can be parametrised to an impedance $Z(\omega)$. This impedance causes noise, the Johnson-Nyquist noise, which causes voltage fluctuations $\delta V(t)$, therefore the effective voltage across the SET becomes $\tilde{V}(t) = V + \delta V(t)$. These fluctuations can be split into fluctuations for the right and left electrode:

$$\begin{aligned} \tilde{V}(t) &= V + \delta V(t) = V_L - V_R + \delta V_l(t) - \delta V_R(t) \\ &= V_L + \delta V_L(t) - (V_R + \delta V_R(t)) = \tilde{V}_L(t) - \tilde{V}_R(t) \ , \end{aligned} \tag{4.1}$$

which results in $\tilde{V}_L(t) = V_L + \delta V_L(t)$ and $\tilde{V}_R(t) = V_R + \delta V_R(t)$, where we defined $\delta V(t) = \delta V_L(t) - \delta V_R(t)$ in analogy to the definition of $\tilde{V}$.

One can apply a gauge transformation to introduce a phase that is equivalent to the voltage

$$\phi_{L/R}(t) = \frac{1}{\hbar}\int^t dt' e\tilde{V}_{L/R}(t') = \frac{eV_{L/R}t}{\hbar} + \delta\phi_{L/R}(t) \tag{4.2}$$

$$\delta\phi_{L/R}(t) = \frac{1}{\hbar}\int^t dt' e\delta V_{L/R}(t') \text{ and} \tag{4.3}$$

$$\tag{4.4}$$

The Hamiltonian for the system then becomes

$$H^{QP} = H_L + H_I + H_R + H^{QP}_{T,L} + H^{QP}_{T,R} + H_{\text{Ch}} + H_{\text{Bath}}. \tag{4.5}$$

We assume for the following, that the left lead, right lead and the island have electron reservoirs that are distinct. We need this assumption later, e.g. for the commuting of creation or annihilation operators that act on different leads.

The first three terms in the Hamiltonian denote the free quasi-particles on leads and island and take as well the voltage bias into account.

For the left and right lead and the island we will denote the wave vector of the electrons by k, k' and q respectively and the spin by σ. Then we get

$$H_L = \sum_{k,\sigma}(\epsilon_k + e\tilde{V}_L(t))c^\dagger_{k,\sigma}c_{k,\sigma} \tag{4.6}$$

$$H_R = \sum_{k',\sigma}(\epsilon_{k'} - e\tilde{V}_R(t))c^\dagger_{k',\sigma}c_{k',\sigma} \tag{4.7}$$

$$H_I = \sum_{q,\sigma}\epsilon_q b^\dagger_{q,\sigma}b_{q,\sigma} \ , \tag{4.8}$$

where $c^\dagger_{k^{(\prime)},\sigma}$, $c_{k^{(\prime)},\sigma}$ denote the creation and annihilation operators in the left (right) lead and $b^\dagger_{q,\sigma}$, $b_{q,\sigma}$ in the island and $\epsilon_{k^{(\prime)}}$, ϵ_q denotes the kinetic energy of the electrons.

The next two terms describe the tunneling of electrons onto or off the island for the left and right junction

$$H^{QP}_{T,L} = \sum_{k,\sigma}(T_{k,q}c^\dagger_{k,\sigma}b_{q,\sigma} + T^*_{k,q}b^\dagger_{q,\sigma}c_{k,\sigma}) \tag{4.9}$$

$$H^{QP}_{T,R} = \sum_{k',\sigma}(T_{k',q}c^\dagger_{k',\sigma}b_{q,\sigma} + T^*_{k',q}b^\dagger_{q,\sigma}c_{k',\sigma}), \tag{4.10}$$

where $T_{k(')q}$ denotes the tunneling matrix element. E.g. the first term of the tunneling Hamiltonian for the left junction describes the annihilation of quasi-particles in the island and the creation at the left lead.

The charging energy depends on both the gate voltage and the number of additional electrons on the island. This again consists of the number of electrons that were brought onto the island via tunneling and an offset charge N_+ which stems from positively charged ions on the island. The charging Hamiltonian becomes

$$H_{Ch} = \frac{(ne - Q_G)^2}{2C} \,, \tag{4.11}$$

with the total capacitance $C = C_L + C_R + C_G$ and the gate charge $Q_G = C_G V_G + C_L V_L + C_R V_R$ and the number of excess charges on the island $n = \sum_{q,\sigma} b^\dagger_{q,\sigma} b_{q,\sigma} - N_+$.

The environment consists of linear circuit elements, which cause Gaussian noise, so it can be modelled by a bath of harmonic oscillators. The general Hamiltonian will be displayed here. The bath Hamiltonian

$$H_{\text{Bath}} = \sum_j \left(\frac{p_j^2}{2m_j} + \frac{m_j}{2} \Omega_j^2 x_j^2 \right) \tag{4.12}$$

corresponds to our fluctuating phase via

$$\hbar \delta\phi(t) = \sum_j c_j x_j(t).$$

The frequencies Ω_j and the coefficients c_j are determined from the corresponding Johnson-Nyquist noise. Thus the model is fully parametrised by an impedance as shown in chapter 5.1.

So far, we have a model Hamiltonian for our system. But, as one wants to perform perturbation theory in the tunneling terms and treat the lead and island energies as the unperturbed Hamiltonian, one has to transfer the time dependent voltage terms, that are now still in the reservoir terms, to the tunneling terms. Therefore one performs the time-dependent unitary transformation

$$\begin{aligned} H &= U^\dagger H' U - i\hbar U^\dagger \frac{\partial U}{\partial t} \\ \text{therefore } H' &= U H U^\dagger + i\hbar \frac{\partial U}{\partial t} U^\dagger \text{ with} \qquad (4.13) \\ U &= \exp\left[\frac{i}{\hbar} \int^t dt' (e\tilde{V}_L(t') \sum_{k,q} c^\dagger_{k,\sigma} c_{k,\sigma} - e\tilde{V}_R(t') \sum_{k',q} c^\dagger_{k',\sigma} c_{k',\sigma}) \right]. \qquad (4.14) \end{aligned}$$

We constructed a transformation matrix such that the part that contains the phase of the left lead only acts on the left terms and vice versa. One can rewrite equation (4.14) to make this obvious

$$\begin{aligned} U &= \exp\left[\frac{i}{\hbar}\int^t dt' e\tilde{V}_L(t')\sum_{k,q} c^\dagger_{k,\sigma}c_{k,\sigma}\right]\exp\left[-\frac{i}{\hbar}\int^t dt' e\tilde{V}_R(t')\sum_{k',q} c^\dagger_{k',\sigma}c_{k',\sigma}\right] \\ &= \exp\left[i\phi_L(t)\sum_{k,q} c^\dagger_{k,\sigma}c_{k,\sigma}\right]\exp\left[-i\phi_R(t)\sum_{k',q} c^\dagger_{k',\sigma}c_{k',\sigma}\right] \\ &= U_L U_R. \end{aligned} \tag{4.15}$$

By applying the transformation the $i\hbar\frac{\partial U}{\partial t}U^\dagger$-term cancels the voltage dependence in the electrodes

$$i\hbar\frac{\partial U}{\partial t}U^\dagger = -e\tilde{V}_L(t)\sum_{k,q} c^\dagger_{k,q}c_{k,q} + e\tilde{V}_R(t)\sum_{k',q} c^\dagger_{k',q}c_{k',q}. \tag{4.16}$$

There is no account from the $UHU^\dagger$ part onto the leads or the island, because the unitary transform commutes with lead and island Hamiltonian, therefore

$$H'_L = \sum_{k,\sigma}\epsilon_k c^\dagger_{k,\sigma}c_{k,\sigma} \qquad \text{for the left lead} \tag{4.17}$$

$$H'_R = \sum_{k',\sigma}\epsilon_{k'} c^\dagger_{k',\sigma}c_{k',\sigma} \qquad \text{for the right lead} \tag{4.18}$$

$$H'_I = \sum_{q,\sigma}\epsilon_q b^\dagger_{q,\sigma}b_{q,\sigma} = H_I \quad \text{for the island} \tag{4.19}$$

where the island term is left unchanged and as intended with this transformation, the voltage difference between the electrodes disappeared. For the tunneling Hamiltonians the effect of the $UHU^\dagger$ term is to add the voltage (or phase) dependency to the tunneling terms. As we chose the transform such that

$$\left[H^{QP}_{T,L}, U^{(\dagger)}_R\right] = \left[H^{QP}_{T,R}, U^{(\dagger)}_L\right] = 0\ , \tag{4.20}$$

on each tunneling Hamiltonian acts only the transformation matrix for this junction. E.g. for the tunneling across the left junction

$$H'^{QP}_{T,L} = UH^{QP}_{T,L}U^\dagger = U_L U_R H^{QP}_{T,L}U^\dagger_R U^\dagger_L = U_L U_R U^+_R H^{QP}_{T,L}U^\dagger_L = U_L H^{QP}_{T,L}U^\dagger_L. \tag{4.21}$$

In analogy to the calculation in chapter 3.4 of [11] one gets for the new tunneling terms

$$H'^{QP}_{T,L} = \sum_{k,q,\sigma}(T_{k,q}e^{i\phi_L(t)}c^\dagger_{k,\sigma}b_{q,\sigma} + T^*_{k,q}e^{-i\phi_L(t)}b^\dagger_{q,\sigma}c_{k,\sigma}) \tag{4.22}$$

$$H'^{QP}_{T,R} = \sum_{k',q,\sigma}(T_{k',q}e^{-i\phi_R(t)}c^\dagger_{k',\sigma}b_{q,\sigma} + T^*_{k',q}e^{i\phi_R(t)}b^\dagger_{q,\sigma}c_{k',\sigma}). \tag{4.23}$$

As already explained above, the opposite sign of the phase in the right junction takes into account that tunneling occurs in an opposite direction with respect to the bias voltage compared to the left junction.

The unitary transform does not change the bath Hamiltonian or the Hamiltonian for the charging energy because the relevant variables commute.

Finally, the transformed Hamiltonian is

$$H'^{QP} = H'_L + H'_R + H_I + H'^{QP}_{T,L} + H'^{QP}_{T,R} + H_{Ch} + H_{\text{Bath}}. \tag{4.24}$$

4.3 Derivation of the Effective Hamiltonian II: Josephson Coupling

The Hamiltonian that describes tunneling of Cooper pairs differs from the Hamiltonian for the tunneling of quasi-particles only in the structure of the tunneling terms. These are

$$H_{J,L} = -E_J \cos\phi^{CP}_L(t) = -\frac{E_J}{2}(e^{i\phi^{CP}_L(t)} + e^{-i\phi^{CP}_L(t)}) \tag{4.25}$$

$$H_{J,R} = -E_J \cos\phi^{CP}_R(t) = -\frac{E_J}{2}(e^{i\phi^{CP}_R(t)} + e^{-i\phi^{CP}_R(t)}). \tag{4.26}$$

The first terms describe the creation of a Cooper pair in the lead and a destruction on the island, therefore tunneling from island to lead, and the second term describes the opposite. The phase of the Cooper pairs $\phi^{CP}_{L/R}$ can be related to the bias voltage and therefore to the left and right phases $\phi_{L/R}$, which were already introduced in equations (4.2), (4.3), by

$$\phi^{CP}_{L/R}(t) = \frac{1}{\hbar}\int^t dt' 2e\tilde{V}_{L/R}(t') = 2\frac{1}{\hbar}\int^t dt' e\tilde{V}_{L/R}(t') = 2\phi_L(t) \tag{4.27}$$

$$\phi^{CP}_R(t) = \frac{1}{\hbar}\int^t dt' 2e\tilde{V}_R(t') = 2\frac{1}{\hbar}\int^t dt' e\tilde{V}_R(t') = 2\phi_R(t). \tag{4.28}$$

Therefore the Josephson Hamiltonian becomes in terms of left and right phase difference

$$H_{J,L} = -E_J \cos 2\phi_L(t) = -\frac{E_J}{2}(e^{2i\phi_L(t)} + e^{-2i\phi_L(t)}) \tag{4.29}$$

$$H_{J,R} = -E_J \cos 2\phi_R(t) = -\frac{E_J}{2}(e^{2i\phi_R(t)} + e^{-2i\phi_R(t)}). \tag{4.30}$$

The derivation is analogous to the case of the quasi-particle Hamiltonian. One starts with a Hamiltonian that accounts for the voltage in the electrode terms which is the same as in equation (4.5), but with the tunneling terms exchanged by the here defined Hamiltonians for tunneling of Cooper pairs

$$H^{CP} = H_L + H_R + H_I + H_{J,L} + H_{J,R} + H_{Ch} + H_{\text{Bath}}. \tag{4.31}$$

Again, the time-dependent unitary transform equation (4.14) is performed on the Hamiltonian and cancels the voltage dependence in the electrodes. This is, unlike in the quasi-particle

Hamiltonian, the only effect, as the Josephson phase accounts for the voltage. So the resulting transformed Hamiltonian is

$$H'^{CP} = H'_L + H'_R + H_I + H_{J,L} + H_{J,R} + H_{Ch} + H_{\text{Bath}}. \tag{4.32}$$

4.4 Full Effective Hamiltonian

By combining the results of the last two chapters, we arrive at the following Hamiltonian, which describes the tunneling of both quasi-particles and Cooper pairs in a SCT coupled to an electro-magnetic environment,

$$H' = H'_L + H'_R + H_I + H'^{QP}_{T,L} + H'^{QP}_{T,R} + H_{J,L} + H_{J,R} + H_{Ch} + H_{\text{Bath}} \ , \tag{4.33}$$

where the terms were already defined in the last two sections.

Chapter 5

Introduction to the Formalism

5.1 Tunneling Rates across a Single Tunnel Junction and $P(E)$-Theory

The physical regime we are interested in can actually have strong coupling to the environment, but still weak coupling to the junctions. Therefore it is not consistent to apply perturbation theory in the environment, instead one is interested in the full dependence of the system on it. The requirements are met in the systematic approximations leading to $P(E)$-theory. We already derived a Hamiltonian for the system that contains the influence of the environment as phase factors in the off-diagonal tunneling terms. As the tunneling terms are assumed to be much smaller than the diagonal terms, one can apply perturbation theory in the tunnel coupling. This directly leads us to the calculation of tunneling rates. This chapter only sketches the derivation and highlights the important steps. For the full derivation see [12] or [11].

5.1.1 Tunneling Rate for Quasi-particles across a Single Tunnel Junction

Tunneling rates for quasi-particles in first order perturbation theory in the tunneling can be calculated with Fermi's golden rule

$$\Gamma_{i\to f} = \frac{2\pi}{\hbar}|\langle f|H_T|i\rangle|^2\delta(\epsilon_i - \epsilon_f) \tag{5.1}$$

which describes the transition probability of the tunneling for an electron in the initial state $|i\rangle$ with energy ϵ_i to the final state $|f\rangle$ with energy ϵ_f. It is proportional to the matrix element and only allowed if the energy is conserved. See figure 5.1.

By separating the states into the system part $|E\rangle$ and environmental part $|R\rangle$ as $|i\rangle = |E\rangle \otimes |R\rangle$ and $|f\rangle = |E'\rangle \otimes |R'\rangle$, the forward tunneling rate is given as the trace over all possible initial and final states

$$\Gamma(V) = \frac{2\pi}{\hbar}\int_{-\infty}^{\infty} dE\, dE' \sum_{R,R'} |\langle E'|H_T|E\rangle|^2 |\langle R'|e^{-i\phi}|R\rangle|^2 P_\beta(E,E')P_\beta(R)\delta(E + eV + E_R - E' - E_{R'}) \tag{5.2}$$

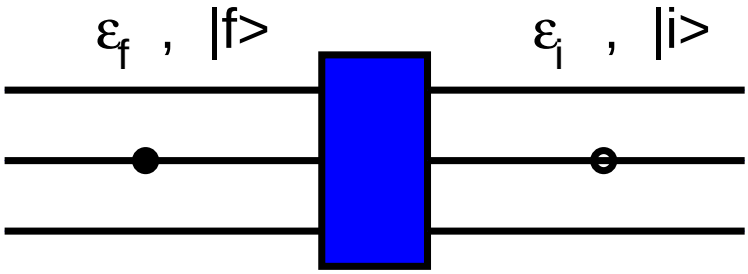

Figure 5.1: Schematic model for the tunneling of an electron from the initial state $|i\rangle$ with energy ϵ_i into the final state $|f\rangle$ with energy ϵ_f.

where $P_\beta(E, E')$ is the thermal energy distribution, which can be expressed for our system as a product of Fermi distributions $f(E) = \frac{1}{1+\exp(\beta E)}$ at temperature T (describing the occupied state with energy E and empty state with energy E') and the superconducting densities of states $N_S(E)$, therefore

$$P_\beta(E, E') = f(E)[1 - f(E')]N_S(E)N_S(E') \ . \tag{5.3}$$

The probabilities for the corresponding environmental degrees of freedom are given as equilibrium matrix elements

$$P_\beta(R) = \frac{\langle R| \exp(-\beta H_{\rm bath})|R\rangle}{\mathrm{tr}\{\exp(-\beta H_{\rm bath})\}} \ . \tag{5.4}$$

By assuming the matrix element of the system to be constant $T = \langle E'|H_T|E\rangle$ and rewriting the delta-function in its Fourier representation one can simplify the expression 5.2 to

$$\begin{aligned}\vec{\Gamma}(V) = \frac{2\pi}{\hbar}|T|^2 \int_{-\infty}^{\infty} \quad & dE\, dE'\, f(E)[1 - f(E')]N_S(E)N_S(E') \times \\ & \times \int_{-\infty}^{\infty} \frac{dt}{2\pi\hbar} \exp\left[\frac{i}{\hbar}(E - E' + eV)t\right] \langle e^{i\phi(t)} e^{-i\phi(0)}\rangle_\beta \end{aligned} \tag{5.5}$$

Here the equilibrium correlation function

$$\langle e^{i\phi(t)} e^{-i\phi(0)}\rangle_\beta = \frac{1}{\mathrm{tr}\{\exp(-\beta H_{\rm bath})\}} \sum_R \langle R| e^{i\phi(t)} e^{-i\phi(0)} e^{-\beta H_{\rm bath}} |R\rangle \tag{5.6}$$

contains the dependence on the environment. In general, this function is very clumsy to deal with. But, as we have a bath of harmonic oscillators, that cause only Gaussian noise, one can simplify this expression by applying Wick's theorem to a two-point correlation function

$$\langle e^{i\phi(t)} e^{-i\phi(0)}\rangle_\beta = \exp\left[\langle(\phi(t) - \phi(0))\phi(0)\rangle_\beta\right] \ . \tag{5.7}$$

For further reference we introduce the correlation function

$$K(t) = \langle(\phi(t) - \phi(0))\phi(0)\rangle_\beta \ . \tag{5.8}$$

Now we can express the tunneling rates in terms of this simpler correlation function as

$$\vec{\Gamma}(V) = \frac{2\pi}{\hbar}|T|^2 \int_{-\infty}^{\infty} dE\, dE'\, f(E)[1-f(E')]N_S(E)N_S(E')P(E-E'+eV)\ , \tag{5.9}$$

where we defined $P(E)$ as

$$P(E) = \frac{1}{2\pi\hbar}\int_{-\infty}^{\infty} dt \exp\left[K(t) + \frac{iEt}{\hbar}\right]\ . \tag{5.10}$$

$P(E)$ contains all effects of the environment in the correlation function $K(t)$, basically this $P(E)$ is the Fourier transform of this correlation function.

The function $P(E)$ replaces the typical energy conservation term of the tunneling system alone in the tunneling theory. It reduces to a delta-function in the case of $K(t) = 0$, which means no coupling of the system to an electro-magnetic environment.

For a particular system that contains only linear circuit elements, one can express the expression of the correlation function in terms of the effective impedance $Z_{\text{eff}}(\omega)$ of the environment [11]. The calculation uses the fluctuation-dissipation theorem [32], with the result

$$K(t) = \frac{1}{R_K}\int_{-\infty}^{\infty}\frac{d\omega}{\omega}\text{Re}\left\{Z_{\text{eff}}(\omega)\right\}\left[\coth\left(\frac{\hbar\omega}{2kT}\right)[\cos(\omega t)-1] - i\sin(\omega t)\right]\ , \tag{5.11}$$

where $R_K = \frac{h}{e^2}$ is the quantum resistance, k the Boltzmann constant and T the temperature.

5.1.2 Tunneling Rates for Cooper Pairs

For the incoherent tunneling of Cooper pairs one can do a similar derivation. The result is simpler, because the Cooper pair tunneling does not involve the annihilation and creation of quasi-particles. Therefore the tunneling rate does not contain Fermi factors or density of state functions, and is given by

$$\vec{\Gamma}(V) = \frac{\pi E_J^2}{2\hbar}P'(2eV) \tag{5.12}$$

where the function $P(E)$ is substituted by the function

$$P'(E) = \frac{1}{2\pi\hbar}\int_{-\infty}^{\infty} dt \exp\left[4K(t) + \frac{iEt}{\hbar}\right]\ , \tag{5.13}$$

which differs from $P(E)$ by a factor of 4 in the correlation functions. This stems from taking twice the charge by considering Cooper pairs instead of electrons, which means doubling the phase, that was inserted into the correlation function and and doubling both phases in the correlation function. This result is a special case for the calculation of $P(E)$ for Cooper pairs for real energy arguments. It will be generalised to complex arguments in chapter 7.

5.2 Charging Energy

We shall follow the derivation of the electro-static energy in [18]. Note the convention $e = -|e|$, n being the number of electrons on the island and $C = \sum_i C_i$. In [18] the charging energy is given by

$$U = \frac{1}{2C} \sum_i \sum_{j>i} C_i C_j (V_i - V_j)^2 + \frac{(ne)^2}{2C}, \tag{5.14}$$

for an island surrounded by an arbitrary number of tunnel junctions with capacitance C_i and biased with voltage V_i. This is exactly the same as in classical electrodynamics. For the set-up used in this thesis, where the bias voltage is applied symmetrically ($V_R = -V/2$, $V_L = V/2$), the charging energy energy becomes

$$U = \frac{1}{2C} \left[C_R C_L V^2 + C_R C_G \left(\frac{V}{2} + V_G \right)^2 + C_L C_G \left(\frac{V}{2} - V_G \right)^2 \right] + \frac{(ne)^2}{2C}. \tag{5.15}$$

If one calculates the change in the charging energy by the tunneling of an electron onto or off the island, it does not matter via which junction the tunneling occurs, the only quantity that affects the change in energy is the change in the number of the electrons on the island. For tunneling of an electron onto the island it changes from n to $n+1$, therefore

$$\Delta U = U(n+1) - U(n) = \frac{e^2}{C} \left(n + \frac{1}{2} \right) \tag{5.16}$$

and for the tunneling of an electron off the island the change in charging energy is

$$\Delta U = U(n-1) - U(n) = \frac{e^2}{C} \left(-n + \frac{1}{2} \right). \tag{5.17}$$

But as we supply a voltage to the SET, one additionally has to take into account the work done by the voltage source. In [18] the work done by the voltage source for the tunneling of an electron across the i-th junction onto the island is given by

$$W_j = e \sum_i (V_j - V_i) \frac{C_i}{C}. \tag{5.18}$$

For a tunneling process onto the island across the right junction

$$W_R = -\frac{e}{C} \left(V \left(C_L + \frac{C_G}{2} \right) + V_G C_G \right) \tag{5.19}$$

and for the tunneling of an electron across the left junction onto the island

$$W_L = \frac{e}{C} \left(V \left(C_R + \frac{C_G}{2} \right) - V_G C_G \right). \tag{5.20}$$

For a tunneling process off the island the work terms get the opposite sign.

To calculate the change in electrostatic energy one has to add the change in charging energy and the work done by the voltage source. So for the different processes the changes in charging energy are:

- for tunneling of an electron onto the island across the right junction

$$\Delta E_R^{\leftarrow} = U(n+1) - U(n) - W_R = \frac{e}{C}\left[\left(n+\frac{1}{2}\right)e + \left(C_L + \frac{C_G}{2}\right)V + C_G V_G\right] \quad (5.21)$$

- for tunneling of an electron onto the island across the left junction

$$\Delta E_L^{\rightarrow} = U(n+1) - U(n) - W_L = \frac{e}{C}\left[\left(n+\frac{1}{2}\right)e - \left(C_R + \frac{C_G}{2}\right)V + C_G V_G\right] \quad (5.22)$$

- for tunneling of an electron off the island across the right junction

$$\Delta E_R^{\rightarrow} = U(n-1) - U(n) + W_R = \frac{e}{C}\left[\left(-n+\frac{1}{2}\right)e - \left(C_L + \frac{C_G}{2}\right)V - C_G V_G\right] \quad (5.23)$$

- for tunneling of an electron off the island across the left junction

$$\Delta E_L^{\leftarrow} = U(n-1) - U(n) + W_L = \frac{e}{C}\left[\left(-n+\frac{1}{2}\right)e + \left(C_R + \frac{C_G}{2}\right)V - C_G V_G\right] . \quad (5.24)$$

From there one can easily calculate, which processes are allowed (processes that retain or gain energy, therefore $\Delta E \leq 0$) and which are forbidden (processes that cost energy, therefore $\Delta E > 0$).

To show that these energy differences are reasonable, we consider three simple examples. The energy diagrams, showing the Fermi energy for the electrons and the allowed tunneling processes can be seen in figures 5.2, 5.3 and 5.4.

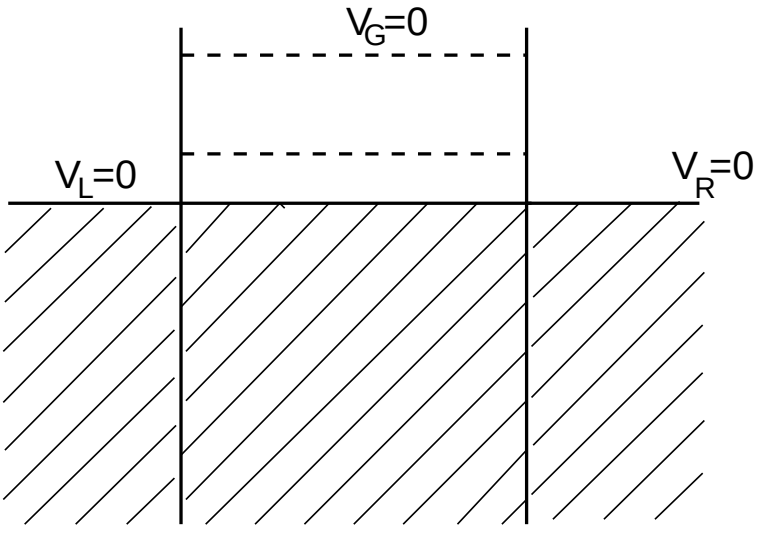

Figure 5.2: There are no allowed tunneling processes in a SCT for $n = 0$, $V = 0$, $V_G = 0$. The diagram shows the Fermi level, up to which the states are occupied, in the left and right junction and on the island. The dotted lines show the charging levels on the island.

For $n = 0$, $V = 0$ and $V_G = 0$ the energy difference is $\Delta E > 0$ for all four possible processes, which is expected as we are in the regime of Coulomb blockade.

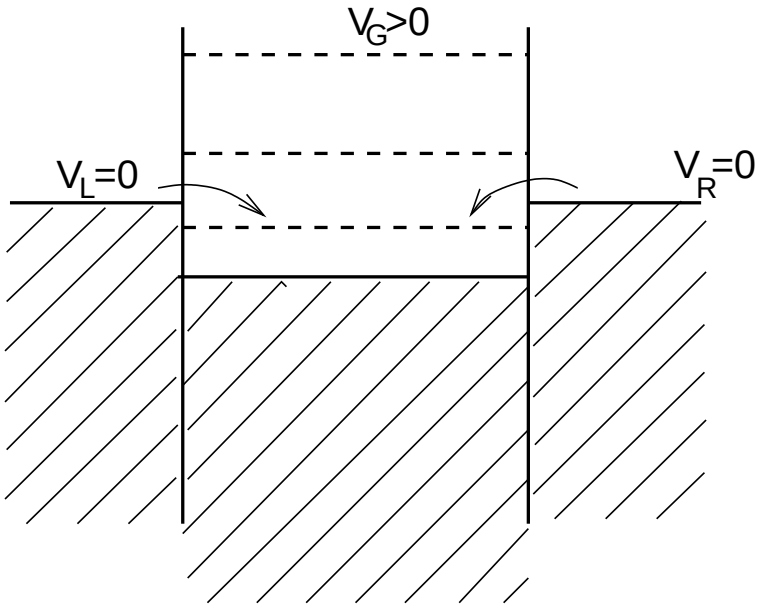

Figure 5.3: A positive gate voltage shifts the Fermi energy to the island downwards with respect to the leads. Therefore there are only tunneling transitions allowed that occur from the leads to the island in a SCT for $n = 0$, $V = 0$, $V_G > 0$.

For $n = 0$, $V = 0$ and $V_G > 0$ the Fermi level on the island is lower than the Fermi level on the right and left leads, therefore one expects only tunneling processes onto the island. Which is fulfilled, as $\Delta E_R^{\rightarrow} > 0$ $\Delta E_L^{\leftarrow} > 0$ and $\Delta E_R^{\leftarrow} < 0$ $\Delta E_L^{\rightarrow} < 0$ for large enough gate voltages ($V_G > \frac{CE_C}{C_G|e|}$) only.

For $n = 0$, $V > 0$ and $V_G = 0$ the Fermi level on the left lead is higher than the Fermi level of the island and the Fermi level on the left lead is lower and the Fermi level on the right lead is lower than the Fermi level on the island therefore one expects that tunneling processes from left to right are forbidden and right to left are allowed (for high enough biases). This is fulfilled, as $\Delta E_R^{\rightarrow} > 0$ $\Delta E_L^{\rightarrow} > 0$ and $\Delta E_R^{\leftarrow} < 0$ $\Delta E_L^{\leftarrow} < 0$ for large enough gate voltages $\left(V > \frac{E_C C}{|e|\left(C_{L/R} + \frac{C_G}{2}\right)}\right)$ only.

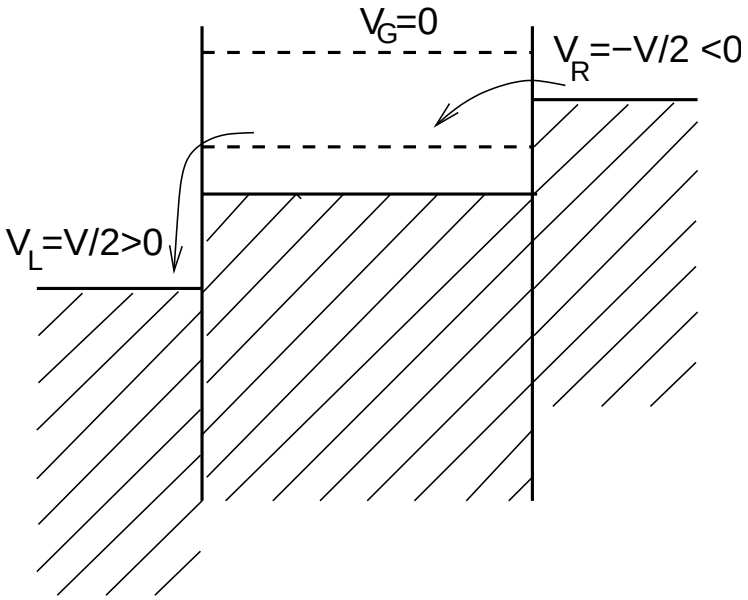

Figure 5.4: The symmetrical bias voltage shifts the Fermi levels of the right and left leads up and down with respect to the Fermi level of the island. Therefore there are only tunneling transitions allowed that go from right to left in a SCT for $n = 0$, $V = 0$, $V_G > 0$.

Chapter 6

Calculation of the Function $P(E)$ for the SCT

As introduced in section 5.1, the effect of the environment on the tunnelling rates of a single charge transistor is described by the function $P(E)$. In this chapter this function will be calculated for the particular circuit model (see figure 4.1) considered in this thesis in the semi-classical limit, which is reached for small energies of the system compared to thermal energies. The function $P(E)$ (defined in equation (5.10)) is the Fourier transform of the exponential of the correlation function $K(t)$ (defined in equation (5.11)), which in turn depends on the effective impedance of the environment seen by the junction through which the tunnelling occurs. Therefore the calculation can be divided into parts. First we will derive the effective impedance seen by one tunnel junction. Afterwards we will calculate the correlation function and $P(E)$. The essentially general calculation of $P(E)$ is shown in appendix A.2 for comparison.

6.1 Calculation of the Effective Impedance $Z_{\text{eff}}(\omega)$

The calculation of the effective impedance of the system seen by one tunnel junction is provided in appendix A.1.2. Here we only quote the result for the limit of the capacitance C_0, which connects the environment to the island, being much smaller than the capacitance, which connects the environment to the leads. We also assume symmetric junctions. These assumptions correspond to the experimental data of the set-up by Rimberg (see appendix A.1.1). The real part of the effective impedance is

$$\mathrm{Re}\{Z_{\text{eff}}(\omega)\} = R_{\text{2DEG}} \frac{1 + 2(C_t R_{\text{2DEG}})^2 \omega^2}{1 + 2\frac{C_t}{C_0} + 18\frac{C_t}{C_0}(R_{\text{2DEG}} C_t)^2 \omega^2 + (C_t R_{\text{2DEG}})^4 \omega^4}, \tag{6.1}$$

where R_{2DEG} denotes the resistance of the 2DEG underneath the junction and C_t the tunneling capacitance of the other junction. For low frequencies this approaches a value that is proportional to the restance of the 2DEG and for high frequencies it has a smooth cut-off at frequencies around $\frac{1}{R_{\text{2DEG}} C_t}$. For simplification of further calculations, we expand $\mathrm{Re}\{Z_{\text{eff}}(\omega)\}$ into partial fractions

$$\mathrm{Re}\{Z_{\text{eff}}(\omega)\} = \sum_j \frac{A_j}{\omega^2 - z_j}\ , \tag{6.2}$$

where the coefficients A_j are given in equation (A.18) and the quadratic roots of the denominator z_j in equation (A.16).

Using this equation we can introduce the dimensionless conductance as

$$\frac{1}{g} = \frac{R_K}{\mathrm{Re}\{Z_{\mathrm{eff}}(\omega = 0)\}} = \sum_j \frac{A_j}{R_K |z_j|} \tag{6.3}$$

which is characteristic for the environment.

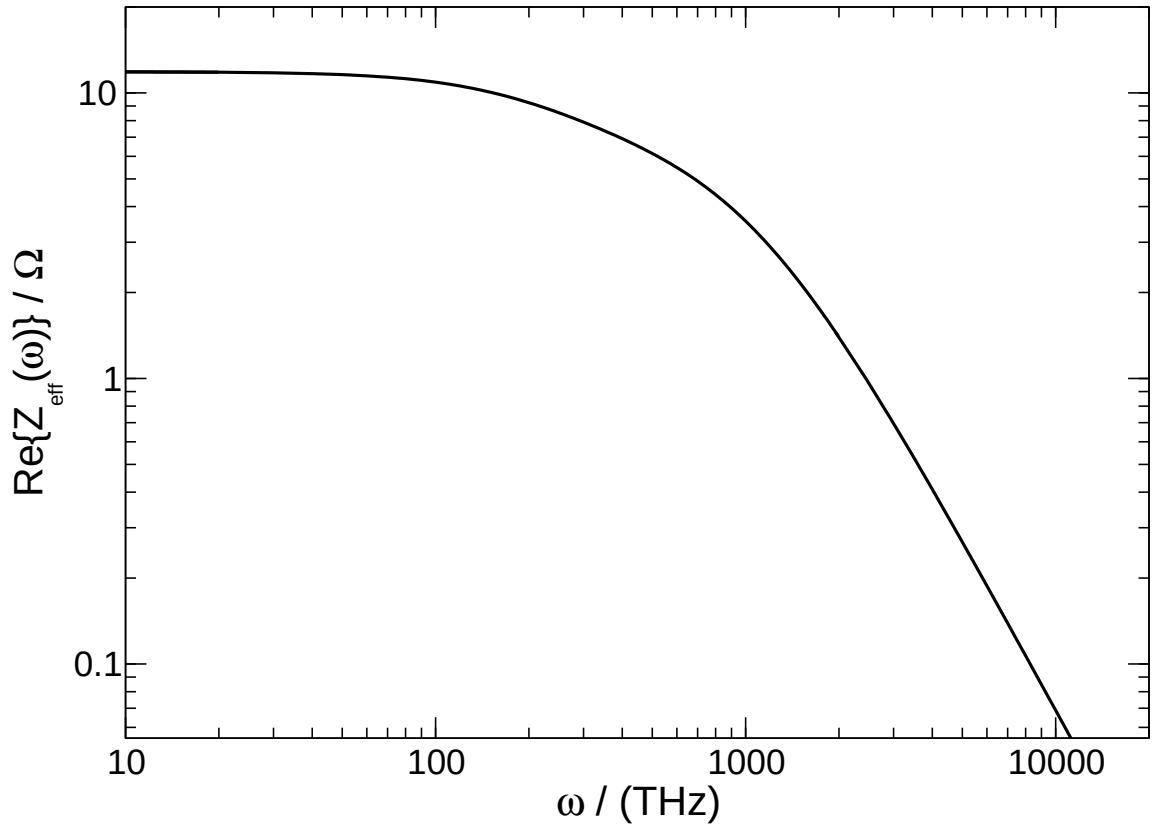

Figure 6.1: General behaviour of the real part of the effective impedance seen by one junction as a function of frequency from equation (6.1), plotted on a double logarithmic scale (for the circuit parameters as denoted in appendix A.1.1). Notice that $\mathrm{Re}\{Z_{\mathrm{eff}}(\omega)\}$ stays constant for lower than the cut-off frequencies $\sqrt{|z_j|}$. For higher frequencies, it drops. This can be understood as capacitances that become transmissive at certain frequencies, therefore reducing the effective impedance.

The plot of the real part of the effective impedance as a function of frequency is shown in figure 6.1 for a reasonable choice of the parameters (as provided in appendix A.1.1). Notice that $\mathrm{Re}\{Z_{\mathrm{eff}}(\omega)\}$ stays constant for low frequencies. For higher frequencies, it drops. This can be understood as capacitances that become transmissive at certain frequencies, therefore reducing the effective impedance. The frequencies, for which the effective impedance drops, are called cut-off frequencies $\sqrt{|z_j|}$.

Note that the cutoff frequencies are quite large, as they are in the order if THz. This verifies our approximation of $\hbar\sqrt{|z_j|} \gg E_{\mathrm{therm}}, E_C$, as the cut-off frequencies correspond to energies $\hbar\sqrt{|z_j|} \gg$ meV, both thermal and charging energy are in the order of 0.1meV for typical temperatures of 1K and typical charging energies of 0.1fF.

Most of the tunneling rates, that will be calculated using the effective impedance derived here, are fully determined by its value at low frequencies. However, to ensure convergence of the full theory, an ultra-violet cut-off, as it is given through equation (6.1), is essential [33].

6.2 $P(E)$ in Semi-classical Approximation

We want to study the function $P(E)$ for the semi-classical limit, which is obtained for high thermal energies compared to system energies $\hbar\omega \ll 2kT$,.

In this limit, we can approximate $\coth\left(\frac{\hbar\omega}{2kT}\right) \approx \frac{2kT}{\hbar\omega}$. Thus the correlation function (equation (5.11)) becomes

$$K(t) = \sum_{j=1}^{3} \frac{A_j}{R_k} \int_{-\infty}^{\infty} \frac{d\omega}{\omega(\omega^2 + |z_j|)} \left[\frac{2kT}{\hbar\omega}(\cos(\omega t) - 1) - i\sin(\omega t) \right]. \tag{6.4}$$

Due to our assumption the contribution of the $\sin(\omega t)$ term to the integral can be neglected and we obtain after some algebra

$$K(t) = -\sum_{j=1}^{3} \frac{A_j}{R_k} \frac{2kT}{\hbar} \int_0^{t''} dt' \int_0^{t'} dt \int_{-\infty}^{\infty} \frac{d\omega \cos(\omega t)}{\omega(\omega^2 + |z_j|)}. \tag{6.5}$$

We assume the cut-off frequencies to be large $\sqrt{|z_j|} \gg \frac{E_C}{\hbar}$. Therefore we approximate the last integral by

$$\int_{-\infty}^{\infty} \frac{d\omega \cos(\omega t)}{\omega(\omega^2 + |z_j|)} = \frac{2\pi}{|z_j|}\delta(t). \tag{6.6}$$

It can be shown that this approximations is valid, although the integral runs over all frequencies, but as this is a highly oscillating function, high frequencies do not contribute. Therefore we obtain for the correlation function

$$\begin{aligned} K(t) &= -\sum_{j=1}^{3} \frac{A_j}{R_k} \frac{2kT}{\hbar} \int_0^{t''} dt' \int_0^{t'} dt \frac{2\pi}{|z_j|}\delta(t) \\ &= -\frac{\omega_1}{g}|t|, \end{aligned} \tag{6.7}$$

where we inserted the dimensionless conductance (equation (6.3)) and the first Bose-Matsubara frequency $\omega_1 = \frac{2\pi kT}{\hbar}$.

Inserting this result into the function $P(E)$ yields

$$
\begin{aligned}
P(E) &= \frac{1}{2\pi\hbar}\int_{-\infty}^{\infty} dt \exp\left[-\frac{\omega_1}{g}|t| + \frac{iEt}{\hbar}\right] \\
&= \frac{1}{\pi\hbar}\mathrm{Re}\left\{\int_0^{\infty} dt \exp\left[-\left(\frac{\omega_1}{g} + \frac{iE}{\hbar}\right)t\right]\right\} \\
&= \frac{1}{\pi\hbar\omega_1}\mathrm{Re}\left\{\frac{1}{\frac{1}{g} + \frac{iE}{\hbar\omega_1}}\right\} \qquad (6.8) \\
&= \frac{1}{\pi}\frac{\frac{\hbar\omega_1}{g}}{\left(\frac{\hbar\omega_1}{g}\right)^2 + E^2}. \qquad (6.9)
\end{aligned}
$$

In appendix A.2 we derive the semi-classical approximation from the full calculation of $P(E)$ for a consistency check and obtain exactly the same result (see equation (A.90).

The function $P(E)$ is a Lorentzian which is centred around $E = 0$ and has the width $\frac{2\hbar\omega_1}{g}$. Although the properties of a Lorentzian are well known, figure 6.2 shows a plot of $P(E)$ to illustrate the impact of the environment for different parameters of the effective impedance, expressed in terms of $\frac{1}{g}$, and fixed temperature. One can understand this behaviour, as the function $P(E)$ describes the possible absorption and emission of photons for the environment. For the semi-classical limit, which is reached when $\frac{E}{\hbar\omega_1} \ll 1$, the environment can both absorb (contribution in $P(E)$ for positive energies) and emit (contribution in $P(E)$ for negative energies) photons. And, as expected, as we increase the effective impedance, i.e. increasing $\frac{1}{g}$, the peak broadens and its maximum is decreased. If we increase the effective impedance, the peak width is reduced and its height is increased. In the limit of an infinitesimally small environment this leads to the reduction of $P(E)$ to a δ-function, as is expected from its definition [11].

As the only dependence of the function $P(E)$ on the temperature and effective impedance is, where both parameters appear together in a product, the behaviour for changing the temperature while keeping $\frac{1}{g}$ fixed is the same as changing $\frac{1}{g}$ for fixed T. This means for increasing the temperature $P(E)$ the peak height drops and the peak broadens. This is also due to the absorption and emission properties of $P(E)$.

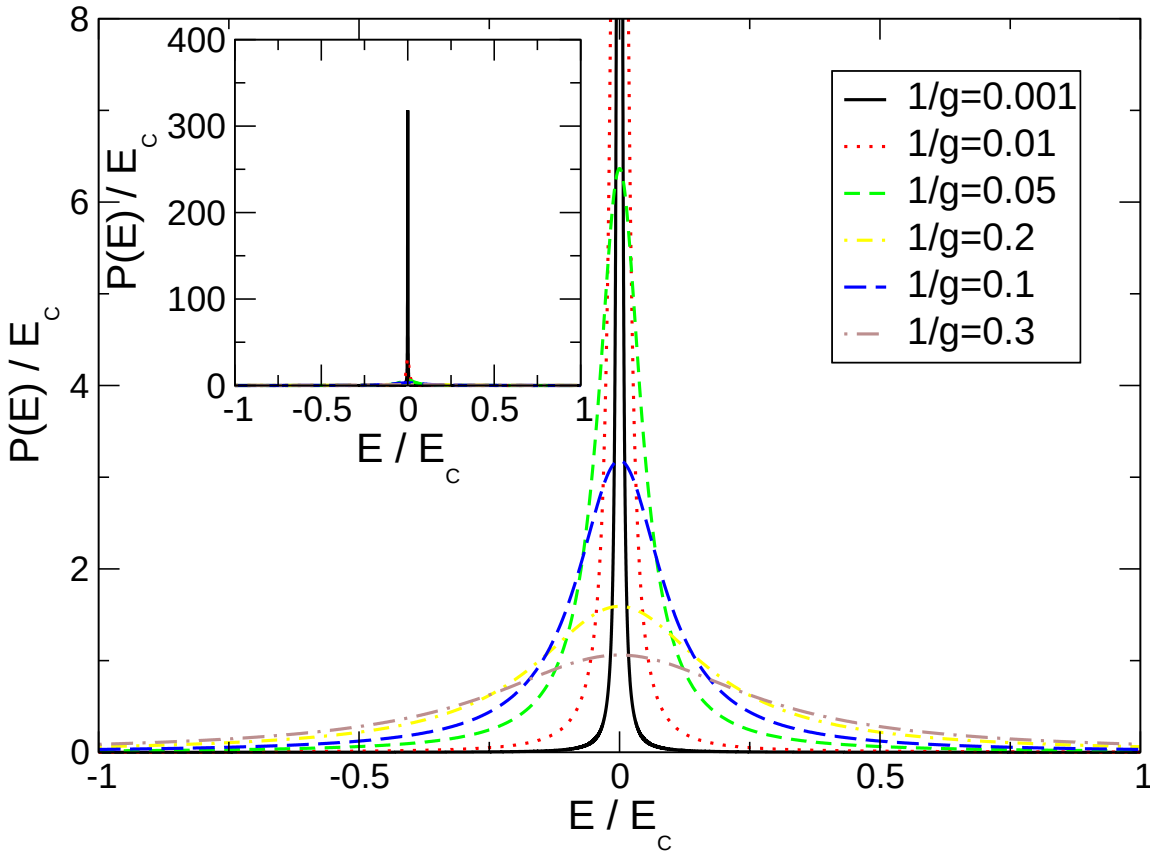

Figure 6.2: $P(E)$ for constant temperature $k_BT = 1$ varying the effective impedance of the environment from $\frac{1}{g} = 0.001$ to 0.3. This is a Lorentzian, centred around $E = 0$ with a width proportional to temperature and effective impedance. As we increase the effective impedance, i.e. increasing $\frac{1}{g}$, the peak broadens and its maximal value is decreased. The inset shows the actual height of the plots. This plot is for illustration.

Chapter 7

Master Equation

In the following we want to explicitly study the JQP resonance. Therefore we use a master equation approach, which modifies the master equations derived by Averin and Aleshkin in [1] to include an environment.

7.1 Master Equation of Averin and Aleshkin [1]

Averin and Aleshkin derived a set of master equations for a double junction system, where the gate can be taken into account through an induced charge. So basically this approach describes an SET, but without the electro-magnetic environment. They also apply perturbation theory in the tunneling Hamiltonian and only take density matrix elements into account, for which the difference in charging energy $\delta(Q)$ before and after the transition of a Cooper pair is small compared to E_C.

So the set of equations is

$$\begin{aligned}
\dot{\sigma}(Q) &= -E_J \mathrm{Im}[\rho(Q, Q+2e)] + F_T\{\sigma(Q)\}, && (7.1)\\
\dot{\sigma}(Q+2e) &= E_J \mathrm{Im}[\rho(Q+2e, Q)] + F_T\{\sigma(Q+2e)\}, && (7.2)\\
\dot{\rho}(Q, Q+2e) &= \frac{iE_J}{2}[\sigma(Q) - \sigma(Q+2e)] - \frac{(i\delta+\nu)}{\hbar}\rho(Q, Q+2e), && (7.3)
\end{aligned}$$

where the diagonal elements of the density matrices are defined as $\sigma(Q) = \rho(Q, Q)$. The contributions from the tunneling of quasi-particles is contained in

$$F_T\{\sigma(Q)\} = \sum_{j,\pm}[\sigma(Q \pm e)\Gamma_j^{\mp}(Q \pm e) - \sigma(Q)\Gamma_j^{\pm}(Q)]. \quad (7.4)$$

The tunneling rates $\Gamma_j^{\pm}(Q)$ describe the tunneling of a quasi-particle onto (plus-sign) or off (minus-sign) the island across the j-th junction, if there was an initial charge of Q on the island.

This defines the decay rate

$$\nu = \hbar \sum_{j,\pm}[\Gamma_j^{\pm}(Q) + \Gamma_j^{\pm}(Q+2e)] \quad (7.5)$$

and δ is the difference in charging energy, which corresponds to a dephasing rate.

7.2 Relevant States for the Master Equation Describing the JQP Cycle

To work out which rates have to be taken into account for the master equation, we calculate differences in charging energy for all processes close to the desired one and show that they do not contribute. The charging energy difference is calculated analogous to the approach of Averin and Aleshkin. We get the condition for the initial charge on the island from the requirement of the Cooper pair transition being resonant and the voltage from the quasi-particle transitions being allowed. For this calculation we use the definition for the charging energy given in [1]

$$U(n_L, n_R) = \frac{Q^2}{2C_\Sigma} - \frac{eV}{C_\Sigma} C(n_R + n_L), \tag{7.6}$$

where this notation refers to n_L (n_R) electrons, that already tunnelled through the left (right) junction from left to right, a voltage V applied across the SCT and equal junction capacitances $C = C_L = C_R$. The island charge is defined as

$$Q = e(n_L - n_R) + Q_0, \tag{7.7}$$

where Q_0 is the offset charge. This can be used to take a gate voltage into account.

We want to consider a JQP process, where the Cooper pair tunneling is resonant in the left junction and the quasi-particle tunnels out of the island across the right junction. The requirement, that the difference in the charging energy for a Cooper pair tunneling onto the island across the left junction has to be zero

$$U(n, n) - U(n + 2, n) = \frac{2e}{C_\Sigma}(CV - Q - e) = 0, \tag{7.8}$$

determines the charge in terms of the voltage

$$Q = CV - e. \tag{7.9}$$

The two quasi-particle transitions determine the minimal voltage that has to be applied. For the first quasi-particle tunneling off the island the difference in charging energy is

$$U(n + 2, n) - U(n + 2, n + 1) = \frac{2C}{C_\Sigma} eV + E_C, \tag{7.10}$$

where we inserted the charge from equation (7.9). In order to allow this tunneling process the energy difference has to be larger than 2Δ, which is the energy needed to create an additional quasi-particle on both island and left lead, as there is only an additional Cooper pair on the island.

For the second quasi-particle tunneling off the island the difference in charging energy is

$$U(n + 2, n + 1) - U(n + 2, n + 2) = \frac{2C}{C_\Sigma} eV - E_C. \tag{7.11}$$

This energy difference has to be larger than Δ to allow the transition. Here the gap energy only appears once, as there is already one quasi-particle on the island, and we have to excite only one quasi-particle on the left junction.

Both these energy differences have to be larger than their threshold in order to allow both transitions, therefore we get as a lower bound for the voltage the condition

$$eV > \max\left\{\frac{C_\Sigma}{2C}(E_C+\Delta), \frac{C_\Sigma}{2C}(2\Delta - E_C)\right\}. \tag{7.12}$$

This is the known threshold for the JQP process. For the size of the gap energy compared to the charging energy we assume

$$2\Delta > E_C. \tag{7.13}$$

To be able to set up the correct set of master equations, we now have to determine which other tunneling processes, i.e. which other charge states of the island contribute. So I will show, that all other possible charge states of the island can be neglected. We need to consider only tunneling processes, that are of first order, i.e. there are only single particles that tunnel in one process. Processes that involve for instance a Cooper pair and a quasi-particle in one process,which are of higher order and their tunnel coupling constant is quite small, can be neglected. In the following the states with charges Q, $Q+e$ or $Q+2e$ on the island are referred to as JQP-states $|Q\rangle$, $|Q+e\rangle$ and $|Q+2e\rangle$. The strategy is to calculate, if there can be other states occupied, starting from any JQP state using transitions that involve only one particle that tunnels. If there are no possible states involved, then we are done (because if there was a possible transition from one of these states into one of the JQP states, it would only appear once and will never be reoccupied later). Basically this means that we have to show, that the JQP process is a closed cycle and if it is started, there are no transitions that go out of it.

Consider processes that use the first JQP state with a charge Q on the island as initial state. The tunneling processes of quasi-particles are allowed, if they gain energy, i.e. if the energy difference between the initial and the final state is larger than the energy needed to overcome the energy gap (depending on the initial state of the island this can be Δ or 2Δ. The tunneling of a quasi-particle across the left junction onto the island with an energy difference

$$U(n,n) - U(n+1,n) = E_C < 2\Delta, \tag{7.14}$$

because of 7.13, and off the island with

$$U(n,n) - U(n-1,n) = -3E_C < 0 < 2\Delta \tag{7.15}$$

are energetically forbidden. The tunneling of a quasi-particle across the right junction onto the island with an energy difference

$$U(n,n) - U(n,n-1) = -\frac{2C}{C_\Sigma}eV + E_C < 2\Delta \tag{7.16}$$

is forbidden considering equation (7.13) and $V > 0$ (see equation (7.12)).

The tunneling of a quasi-particle across the right junction off the island with an energy difference

$$U(n,n) - U(n,n+1) = \frac{2C}{C_\Sigma} eV - 3E_C \tag{7.17}$$

defines an upper bound to the voltage. This transition is forbidden, if the energy difference is smaller than zero, therefore the voltage has to obey

$$eV < \frac{C_\Sigma}{2C}(3E_C + 2\Delta). \tag{7.18}$$

The transitions of Cooper pairs are resonant processes. This means, that they are only allowed, if they almost within their line width conserve energy. The finite line width arises from quasi-particle tunneling and from the environment.

The transition for a Cooper pair across the left junction discharging the island with an energy difference

$$U(n,n) - U(n-2,n) = -8E_C \neq 0 \tag{7.19}$$

is forbidden. Also the Cooper pair transition across the right junctions charging the island with an energy difference

$$U(n,n) - U(n,n-2) = -\frac{4C}{C_\Sigma} eV \neq 0 \tag{7.20}$$

is forbidden.

For discharging the island across the right junctions with a Cooper pair transition the difference in energy is

$$U(n,n) - U(n,n+2) = \frac{4C}{C_\Sigma} eV - 8E_C. \tag{7.21}$$

This transition would be possible, if $eV = \frac{2C_\Sigma}{C} E_C$. For the suppression of this process, we have to exclude this value of the voltage, therefore requiring

$$eV \neq \frac{2C_\Sigma}{C} E_C. \tag{7.22}$$

Now we want to consider processes starting from the JQP state with $Q + e$ charges on the island, that was obtained by the first Cooper pair transition onto the island across the left junction.

The tunneling of a quasi-particle across the left junction onto the island with an energy difference

$$U(n+2,n) - U(n+3,n) = -3E_C < 0 < 2\Delta, \tag{7.23}$$

off the island with

$$U(n+2,n) - U(n+1,n) = E_C < 2\Delta, \tag{7.24}$$

due to 7.13, and across the right junction onto the island with an energy difference

$$U(n+2,n) - U(n+2,n-1) = -\frac{2C}{C_\Sigma}eV - 3E_C < 0 < 2\Delta, \tag{7.25}$$

are energetically forbidden.

The transitions for a Cooper pair across the left junction charging the island with an energy difference

$$U(n+2,n) - U(n+4,n) = -8E_C \neq 0 \tag{7.26}$$

and both Cooper transitions across the right junction, with an energy difference

$$U(n+2,n) - U(n+2,n-2) = -\frac{4C}{C_\Sigma}eV - 8E_C \neq 0 \tag{7.27}$$

for charging the island and with

$$U(n+2,n) - U(n+2,n+2) = \frac{4C}{C_\Sigma}eV \neq 0. \tag{7.28}$$

for discharging the island, are energetically forbidden.

But the transition of a Cooper pair across the left junction discharging the island with an energy difference

$$U(n+2,n) - U(n,n) = 0 \tag{7.29}$$

is also resonant. This is expected, as we chose the Cooper pair transition in the left junction from state $|Q\rangle$ to $|Q+2e\rangle$ to be resonant, due to symmetry the transition from state $|Q+2e\rangle$ to $|Q\rangle$ has to be resonant as well. So this is one transition rate, we have to take into account when setting up the master equations. As this transition goes back to the first JQP state (with Q charges on the island), it does not require new calculations, as we have already shown that the state $|Q\rangle$ only involves a transition to the second JQP state.

Finally, we consider possible transitions starting from the third JQP state with $Q+e$ charges on the island, that is occupied after the tunneling of the first quasi-particle across the right junction.

The tunnelling of a quasi-particle across the left junction onto the island with an energy difference

$$U(n+2,n+1) - U(n+3,n+1) = -E_C < 0 < \Delta, \tag{7.30}$$

off the island with

$$U(n+2,n+1) - U(n+1,n+1) = -E_C < 0 < \Delta \tag{7.31}$$

and across the right junction onto the island with an energy difference

$$U(n+2,n+1) - U(n+2,n) = -\frac{2C}{C_\Sigma}eV - E_C < 0 < \Delta, \tag{7.32}$$

are energetically forbidden.

The transitions for a Cooper pair across the left junction charging the island with an energy difference

$$U(n+2,n+1) - U(n+4,n+1) = -4E_C \neq 0 \tag{7.33}$$

and discharging the island with an energy difference

$$U(n+2,n+1) - U(n,n+1) = -4E_C \neq 0 \tag{7.34}$$

and the Cooper transition across the right junction charging the island with

$$U(n+2,n+1) - U(n+2,n-1) = -\frac{4C}{C_\Sigma}eV - 4E_C \neq 0 \tag{7.35}$$

are energetically forbidden.

The transitions for a Cooper pair across the right junction discharging the island with an energy difference

$$U(n+2,n+1) - U(n+2,n+3) = \frac{4C}{C_\Sigma}eV - 4E_C \tag{7.36}$$

would be resonant, if $eV = \frac{C_\Sigma}{C}E_C$. Thus we have to exclude such voltages requiring

$$eV \neq \frac{C_\Sigma}{C}E_C \tag{7.37}$$

in order to suppress this process.

Concluding, we have shown, that the states $|Q\rangle$, $|Q+e\rangle$ and $|Q+2e\rangle$ provide a closed cycle of transitions, and the only tunnelling rates that have to be taken into account are

- the rates for the Cooper pair transitions across the right junction that
  - charge the island from state $|Q\rangle$ to $|Q+2e\rangle$: $\Gamma^L_{Q\to Q+2e}$
  - and discharge the island from state $|Q+2e\rangle$ to state $|Q\rangle$: $\Gamma^L_{Q+2e\to Q}$
- and the rates for the quasi-particle transitions across the left junction that discharge the island
  - from state $|Q+2e\rangle$ to $|Q+e\rangle$: $\Gamma^R_{Q+2e\to Q+e}$

– and from $|Q+e\rangle$ to $|Q\rangle$: $\Gamma^R_{Q+e\to Q}$.

Here we introduced the notation for the tunnelling rates $\Gamma^{L/R}_{Q\to Q'}$, where the index L/R denotes across which junction the tunnelling occurs and the index $Q\to Q'$ denotes the change in the charge states of the island from $|Q\rangle$ to $|Q'\rangle$.

The voltage range where these are the only rates that we need to consider is set by equations (7.12), (7.18), (7.22) and (7.37)

$$\max\left\{\frac{C_\Sigma}{2C}(E_C+\Delta),\frac{C_\Sigma}{2C}(2\Delta-E_C)\right\}<eV<\frac{C_\Sigma}{2C}(3E_C+2\Delta) \tag{7.38}$$

$$\text{excluding voltages that obey } \left|eV-\frac{C_\Sigma}{C}E_C\right|\ll E_C,\ \left|eV-\frac{2C_\Sigma}{C}E_C\right|\ll E_C.$$

The charge for the JQP cycle is determined by equation (7.9).

7.3 Charging Energy around the Resonance

As we want to study not only the current of the JQP cycle exactly at resonance (for the tunnelling of Cooper pairs), but we are also interested in the change of the current around the resonance, we have to figure out the charging energy differences for this as well. For all rates that contribute, we keep the value of the charge that corresponds to a resonance constant as $Q=VC-e$ and vary the bias voltage slightly by δV, so $V_\delta=V+\delta V$. For a small change in the voltage away from the resonance the Cooper pair transition is still allowed, since it is a Lorentzian with an intrinsic width given by the tunnelling rates of quasi-particles [1] and, as we will see, the environment.

So the change in charging energies becomes

- for the tunnelling of a Cooper pair across the left junction
  - onto the island

$$U(n,n)-U(n+2,n)=\frac{2C}{C_\Sigma}e\delta V=\delta \tag{7.39}$$

  - off the island

$$U(n+2,n)-U(n,n)=-\frac{2C}{C_\Sigma}e\delta V=-\delta \tag{7.40}$$

- and for the tunnelling of a quasi-particle across the right junction off the island
  - changing the charge on the island from $Q+2e$ to $Q+e$

$$\begin{aligned}U(n+2,n)-U(n+2,n+1) &= \frac{2C}{C_\Sigma}eV+E_C+\frac{C}{C_\Sigma}e\delta V\\ &= \frac{2C}{C_\Sigma}eV+E_C+\frac{\delta}{2}\end{aligned} \tag{7.41}$$

– changing the charge on the island from $Q+e$ to Q

$$\begin{aligned} U(n+2,n+1)-U(n+2,n+2) &= \frac{2C}{C_\Sigma}eV - E_C + \frac{C}{C_\Sigma}e\delta V \\ &= \frac{2C}{C_\Sigma}eV - E_C + \frac{\delta}{2} \end{aligned} \tag{7.42}$$

Where we introduced the energy parameter

$$\delta = \frac{2C}{C_\Sigma}e\delta V \tag{7.43}$$

that denotes the change in charging energy, if we go away from the Cooper pair resonance with a voltage δV. This energy can be identified with the δ that will be defined in equation (7.55).

7.4 Modification of the Master Equations

Equations (7.1), (7.2) and (7.3) contain the contributions from Cooper pairs and quasi-particles in separate terms. We will treat their modifications separately in the following sections.

7.4.1 Cooper Pairs

In this section all density matrix elements contain only the Cooper pair part of the master equation, even if it is not specifically indicated. In the following, the density matrix elements are defined in the charge basis with states $|Q\rangle$, therefore $\rho(Q,Q') = |Q\rangle\langle Q'|$. If there is no index, this means we consider the Schrödinger picture and the total density matrix of system and environment. Later it is intended to separate environmental (index R) and system (index S) degrees of freedom, which should not be confused with the Schrödinger picture. The index I will denote the interaction picture. To introduce dissipation into the set of equations, we need to modify the equations with phase - terms and trace over the environmental degrees of freedom to obtain a $P(E)$-like function. We start from the Liouville equation

$$\dot{\rho} = \frac{i}{\hbar}[\rho, H] \ , \tag{7.44}$$

which describes the dynamics for a density matrix ρ. If we consider a Hamiltonian which diagonal elements are E_0 and the off-diagonal elements are the Josephson-coupling complemented by a phase-factor for the environment $\frac{E_J}{2}e^{\pm 2i\phi(t)}$, we get for the time evolution of the density matrix for a two state system with the states for Q and $Q+2e$ charges on the island

$$\begin{aligned} &\begin{pmatrix} \dot{\sigma}(Q) & \dot{\rho}(Q,Q+2e) \\ \dot{\rho}(Q+2e,Q) & \dot{\sigma}(Q+2e) \end{pmatrix} \\ = \ &\frac{i}{\hbar}\left[\begin{pmatrix} \sigma(Q) & \rho(Q,Q+2e) \\ \rho(Q+2e,Q) & \sigma(Q+2e) \end{pmatrix}, \begin{pmatrix} E_0 & \frac{E_J}{2}e^{2i\phi(t)} \\ \frac{E_J}{2}e^{-2i\phi(t)} & E_0 \end{pmatrix}\right] \\ = \ &\frac{iE_J}{2\hbar}\begin{pmatrix} e^{-2i\phi(t)}\rho(Q,Q+2e) - e^{2i\phi(t)}\rho(Q+2e,Q) & e^{2i\phi(t)}(\sigma(Q)-\sigma(Q+2e)) \\ e^{-2i\phi(t)}(\sigma(Q+2e)-\sigma(Q)) & e^{2i\phi(t)}\rho(Q+2e,Q) - e^{-2i\phi(t)}\rho(Q,Q+2e) \end{pmatrix} \end{aligned} \tag{7.45}$$

This gives the Liouvillian part of the master equation, basically it describes the coherent dynamics of the Cooper pairs. So one can add the appropriate phase factors to the Cooper pair part of equations (7.1), (7.2) and (7.3) (where the quasi-particle part is left out here, its contributions are discussed in section 7.4.2).

$$\begin{aligned}
\dot{\sigma}(Q) &= \frac{iE_J}{2\hbar}(e^{-2i\phi(t)}\rho(Q,Q+2e) - e^{2i\phi(t)}\rho(Q+2e,Q)) && (7.46)\\
&= -\frac{E_J}{\hbar}\mathrm{Im}[e^{-2i\phi(t)}\rho(Q,Q+2e)] \\
\dot{\sigma}(Q+2e) &= \frac{iE_J}{2\hbar}(e^{2i\phi(t)}\rho(Q+2e,Q) - e^{-2i\phi(t)}\rho(Q,Q+2e)) && (7.47)\\
&= \frac{E_J}{\hbar}\mathrm{Im}[e^{-2i\phi(t)}\rho(Q,Q+2e)] \\
\dot{\rho}(Q,Q+2e) &= \frac{iE_J}{2\hbar}e^{2i\phi(t)}(\sigma(Q)-\sigma(Q+2e)) - \frac{(i\delta+\nu)}{\hbar}\rho(Q,Q+2e) && (7.48)\\
\dot{\rho}(Q+2e,Q) &= [\dot{\rho}(Q,Q+2e)]^* && (7.49)
\end{aligned}$$

In the next step we want to eliminate the off-diagonal elements in 7.46 and 7.47 with 7.48 and 7.49. By this we use a generalised interaction picture (see Appendix B for definitions) to transform the δ and ν dependence into phase factors which allow us to define a generalised $P(E)$ function that is valid for complex energy arguments. This can be viewed as solving the homogeneous equation for $i\delta + \nu = 0$ in the interaction picture and then turn back to the Schrödinger picture to solve the inhomogeneous equation. To introduce the interaction picture for these master equations, we set the Hamiltonian

$$H = H_0 + H_J \tag{7.50}$$

consisting of the time-independent part that contains the Hamiltonian for quasi-particle tunneling and charging energy

$$H_0 = H_{\mathrm{Ch}} + H_{\mathrm{QP}} \tag{7.51}$$

and the time-dependent Josephson part

$$H_J = \frac{E_J}{2}e^{\pm 2i\phi(t)}. \tag{7.52}$$

The action of the charging Hamiltonian H_{Ch} on a charge state $|Q\rangle$ is to give the respective charging energy

$$H_{\mathrm{Ch}}|Q\rangle = H_{\mathrm{Ch}}(Q)|Q\rangle. \tag{7.53}$$

and the action of the quasi-particle Hamiltonian H_{QP} is to give the respective quasi-particle energy

$$H_{\mathrm{QP}}|Q\rangle = H_{\mathrm{QP}}(Q)|Q\rangle. \tag{7.54}$$

The difference in eigenenergies of H_0 can be expressed in terms of δ and ν

$$\delta = H_{\mathrm{Ch}}(Q) - H_{\mathrm{Ch}}(Q+2e). \tag{7.55}$$

(Note that this is the same δ as was introduced in 7.43 to express the difference in charging energy for the Copper pair state.)

$$\nu = i(H_{\rm QP}(Q) - H_{\rm QP}(Q+2e)). \tag{7.56}$$

Note that ν is imaginary and has the meaning of a quasi-particle - induced dephasing rate. Thus we are using a generalisation of the interaction picture to finite life-time, which is mathematically based on the variation of constants approach.

The unitary evolution operator becomes

$$U = e^{-\frac{iH_0 t}{\hbar}} = e^{-\frac{iH_{\rm Ch} t}{\hbar}} e^{-\frac{iH_{\rm QP} t}{\hbar}} \tag{7.57}$$

as $[H_{\rm Ch}, H_{\rm QP}] = 0$.

To transform equation (7.48) into the generalised interaction picture we consider the density matrix element $\rho(Q, Q+2e)$ in the interaction picture

$$\begin{aligned}
\rho_I(Q,Q+2e) &= e^{\frac{iH_0 t}{\hbar}} \rho(Q,Q+2e) e^{-\frac{iH_0 t}{\hbar}} \\
&= e^{\frac{iH_{\rm QP} t}{\hbar}} e^{\frac{iH_{\rm Ch} t}{\hbar}} \rho(Q,Q+2e) e^{-\frac{iH_{\rm Ch} t}{\hbar}} e^{-\frac{iH_{\rm Ch} t}{\hbar}} \\
&= e^{\frac{iH_{\rm QP}(Q) t}{\hbar}} e^{\frac{iH_{\rm Ch}(Q) t}{\hbar}} |Q\rangle\langle Q+2e| e^{-\frac{iH_{\rm Ch}(Q+2e) t}{\hbar}} e^{-\frac{iH_{\rm QP}(Q+2e) t}{\hbar}} \\
&= e^{\frac{i(H_{\rm Ch}(Q) - H_{\rm Ch}(Q+2e)) t}{\hbar}} e^{\frac{i(H_{\rm QP}(Q) - H_{\rm QP}(Q+2e)) t}{\hbar}} |Q\rangle\langle Q+2e| \\
&= e^{\frac{(i\delta+\nu) t}{\hbar}} |Q\rangle\langle Q+2e| \\
&= e^{\frac{i(\delta - i\nu) t}{\hbar}} \rho(Q,Q+2e)
\end{aligned} \tag{7.58}$$

where the second-last step holds, as the charge states are eigenstates of the charging and quasi-particle Hamiltonian due to equations (7.53), (7.54). So the off-diagonal elements acquire a phase factor.

The diagonal elements of the density matrix are the same in both Schrödinger and interaction picture as can be easily shown

$$\begin{aligned}
\sigma_I(Q) &= e^{\frac{iH_0 t}{\hbar}} \sigma(Q) e^{-\frac{iH_0 t}{\hbar}} \\
&= e^{\frac{iH_{\rm QP}(Q) t}{\hbar}} e^{\frac{iH_{\rm Ch}(Q) t}{\hbar}} |Q\rangle\langle Q| e^{-\frac{iH_{\rm Ch}(Q) t}{\hbar}} e^{-\frac{iH_{\rm QP}(Q) t}{\hbar}} \\
&= |Q\rangle\langle Q| = \sigma(Q).
\end{aligned} \tag{7.59}$$

Now one can rewrite equation (7.48)

$$\begin{aligned}
\frac{d}{dt}\rho(Q,Q+2e) + \frac{(i\delta+\nu)}{\hbar}\rho(Q,Q+2e) &= \frac{iE_J}{2\hbar} e^{2i\phi(t)} (\sigma(Q) - \sigma(Q+2e)) \\
&\Longleftrightarrow \\
e^{-\frac{t}{\hbar}(i\delta+\nu)} \frac{d\rho_I(Q,Q+2e)}{dt} &= \frac{iE_J}{2\hbar} e^{2i\phi(t)} (\sigma_I(Q) - \sigma_I(Q+2e)) \\
&\Longleftrightarrow \\
\frac{d\rho_I(Q,Q+2e)}{dt} &= \frac{iE_J}{2\hbar} e^{2i\phi(t)} e^{\frac{t}{\hbar}(i\delta+\nu)} (\sigma_I(Q) - \sigma_I(Q+2e))
\end{aligned} \tag{7.60}$$

.

One can formally solve this equation in the stationary case, I.e. when the diagonal terms of the density matrix, the occupation probabilities, are constant in time. This results in

$$\rho_I(Q,Q+2e,t) = \frac{iE_J}{2\hbar}\int_0^t dt' e^{2i\phi(t')} e^{\frac{t'}{\hbar}(i\delta+\nu)}(\sigma_I(Q)-\sigma_I(Q+2e)). \tag{7.61}$$

This can be transformed back into the Schrödinger picture

$$\begin{aligned}
\rho(Q,Q+2e) &= U\rho_I(Q,Q+2e,t)U^+ = e^{-\frac{i(\delta-i\nu)t}{\hbar}}\rho_I(Q,Q+2e,t) \\
&= e^{-\frac{i(\delta-i\nu)t}{\hbar}}\frac{iE_J}{2\hbar}\int_0^t dt' e^{2i\phi(t')} e^{\frac{t'}{\hbar}(i\delta+\nu)}(\sigma_I(Q)-\sigma_I(Q+2e)) \\
&= e^{-\frac{i(\delta-i\nu)t}{\hbar}}\frac{iE_J}{2\hbar}\int_0^t dt' e^{2i\phi(t')} e^{\frac{t'}{\hbar}(i\delta+\nu)}(\sigma(Q)-\sigma(Q+2e)) \qquad (7.62)
\end{aligned}$$

where the complex conjugate of this density matrix

$$\rho(Q+2e,Q) = \rho^*(Q,Q+2e) \tag{7.63}$$

is to be inserted into the set of equations (7.46) and (7.47).

$$\dot\sigma(Q) = -\frac{E_J^2}{4\hbar^2}2\mathrm{Re}\left\{e^{-2i\phi(t)}e^{-\frac{i(\delta-i\nu)t}{\hbar}}\int_0^t dt' e^{2i\phi(t')}e^{\frac{t'}{\hbar}(i\delta+\nu)}(\sigma(Q)-\sigma(Q+2e))\right\} \tag{7.64}$$

$$\dot\sigma(Q+2e) = \frac{E_J^2}{4\hbar^2}2\mathrm{Re}\left\{(e^{2i\phi(t)}e^{\frac{i(\delta+i\nu)t}{\hbar}}\int_0^t dt' e^{-2i\phi(t')}e^{\frac{t'}{\hbar}(-i\delta+\nu)}(\sigma(Q)-\sigma(Q+2e))\right\} \tag{7.65}$$

$$= -\dot\sigma(Q). \tag{7.66}$$

From the last equation, we see that it is sufficient to consider equation (7.64) only.

As one is interested in the change of the system part of the density matrix, while it is influenced by an environment, but is not interested in the actual changes in the environment, we separate the density matrix operator into the system part (index S) and an environmental part (index R)

$$\sigma(Q) = \sigma_S(Q)\otimes\sigma_R(Q). \tag{7.67}$$

The system part of the density operator is then given by tracing out the bath degrees of freedom, described by states $|R\rangle$

$$\begin{aligned}
\dot\sigma_S(Q) &= \mathrm{tr}_R\{\dot\sigma(Q)\} \\
&= -\frac{E_J^2}{4\hbar^2}\mathrm{tr}_R\left\{2\mathrm{Re}\left\{e^{-2i\phi(t)}e^{-\frac{i(\delta-i\nu)t}{\hbar}}\int_0^t dt' e^{2i\phi(t')}e^{\frac{t'}{\hbar}(i\delta+\nu)}\right\}\times\right. \\
&\quad \left.\times(\sigma_S(Q)\otimes\sigma_R(Q)-\sigma_S(Q+2e)\otimes\sigma_R(Q+2e))\right\} \\
&\quad . \qquad (7.68)
\end{aligned}$$

We assume that the occupation of the bath states is given by the equilibrium distribution

$$\sigma_R(Q) = \sigma_R(Q+2e) = \frac{e^{-\beta H_{\text{Bath}}}}{Z_\beta} \tag{7.69}$$

then we get

$$\begin{aligned}\dot{\sigma}_S(Q) &= -\frac{E_J^2}{4\hbar^2} 2\text{Re}\left\{ e^{-\frac{i(\delta - i\nu)t}{\hbar}} \int_0^t dt' \frac{1}{Z_\beta} \sum_R \langle R| e^{-2i\phi(t)} e^{2i\phi(t')} e^{-\beta H_{\text{Bath}}} |R\rangle e^{\frac{t'}{\hbar}(i\delta+\nu)} \right\} \times \\ &\quad \times (\sigma_S(Q) - \sigma_S(Q+2e)) \end{aligned} \tag{7.70}$$

as the trace operation is a linear operation and only acts on the environmental degrees of freedom. The environmental degrees of freedom are contained in the bath correlation function, therefore we can write

$$\dot{\sigma}_S(Q) = -\frac{E_J^2}{4\hbar^2} 2\text{Re}\left\{ e^{-\frac{i(\delta - i\nu)t}{\hbar}} \int_0^t dt' \langle e^{-2i\phi(t)} e^{2i\phi(t')} \rangle_\beta e^{\frac{t'}{\hbar}(i\delta+\nu)} \right\} (\sigma_S(Q) - \sigma_S(Q+2e)) \tag{7.71}$$

and by using the identities C.4, C.6 this can be rewritten as

$$\dot{\sigma}_S(Q) = -\frac{E_J^2}{4\hbar^2} 2\text{Re}\left\{ e^{-\frac{i(\delta - i\nu)t}{\hbar}} \int_0^t dt' \langle e^{2i\phi(t-t')} e^{-2i\phi(0)} \rangle_\beta e^{\frac{t'}{\hbar}(i\delta+\nu)} \right\} (\sigma_S(Q) - \sigma_S(Q+2e)) \tag{7.72}$$

To evaluate the integral we substitute $\tau = t - t'$, therefore

$$\begin{aligned}\int_0^t dt' \langle e^{2i\phi(t-t')} e^{-2i\phi(0)} \rangle_\beta e^{\frac{t'}{\hbar}(i\delta+\nu)} &= \int_0^t d\tau \langle e^{2i\phi(\tau)} e^{-2i\phi(0)} \rangle_\beta e^{\frac{t-\tau}{\hbar}(i\delta+\nu)} \\ &= \int_0^t d\tau \exp\left[4K(\tau) - \frac{i\tau}{\hbar}(\delta - i\nu) \right] e^{\frac{it}{\hbar}(\delta - i\nu)} \end{aligned} \tag{7.73}$$

where we identified the correlation function $K(\tau)$.
Therefore

$$\begin{aligned}\dot{\sigma}_S(Q) &= -\frac{E_J^2}{4\hbar^2} 2\text{Re}\left\{ e^{-\frac{i(\delta - i\nu)t}{\hbar}} \int_0^t d\tau \exp\left[4K(\tau) - \frac{i\tau}{\hbar}(\delta - i\nu) \right] e^{\frac{it}{\hbar}(\delta - i\nu)} \right\} (\sigma_S(Q) - \sigma_S(Q+2e)) \\ &= -\frac{E_J^2}{4\hbar^2} 2\text{Re}\left\{ \int_0^t d\tau \exp\left[4K(\tau) - \frac{i\tau}{\hbar}(\delta - i\nu) \right] \right\} (\sigma_S(Q) - \sigma_S(Q+2e)). \end{aligned} \tag{7.74}$$

Now for going to the long-time limit $t \to \infty$, we can introduce $\tilde{P}'(E)$ as a generalisation of $P'(E)$ to the complex plane

$$\tilde{P}'(E) = 2\mathrm{Re}\left\{ \int_0^\infty \frac{d\tau}{2\pi\hbar} \exp\left[4K(\tau) + \frac{i\tau}{\hbar}(E)\right] \right\} \tag{7.75}$$

so the rate equation becomes

$$\dot{\sigma}_S(Q) = -\frac{E_J^2\pi}{2\hbar}\tilde{P}'(i\nu - \delta)(\sigma_S(Q) - \sigma_S(Q+2e)) \tag{7.76}$$

and with equation (7.66)

$$\dot{\sigma}_S(Q+2e) = \frac{E_J^2\pi}{2\hbar}\tilde{P}'(i\nu - \delta)(\sigma_S(Q) - \sigma_S(Q+2e)). \tag{7.77}$$

7.4.2 Quasi-particles

To modify the contribution for quasi-particles $F_T\{\sigma(Q)\}$ we have to introduce a phase factor that takes the voltage fluctuations, caused by the environment, into account and trace over the bath degrees of freedom to get the system part. But this is exactly the same as the derivation for the $P(E)$-theory (see chapter 5.1). So we can just write down the quasi-particle contribution

$$\tilde{F}_T\{\sigma_S(Q)\} = \sum_{j,\pm}[\sigma_S(Q \pm e)\tilde{\Gamma}_j^{\mp}(Q \pm e) - \sigma_S(Q)\tilde{\Gamma}_j^{\pm}(Q)]. \tag{7.78}$$

The tunneling rates depend on the difference in charging energy for each process and contain $P(E)$. They are the same as defined in equation (5.9), but replacing the difference in the chemical potentials eV by the differences in charging energy calculated in section 7.3. As the notation of [1] corresponds to our notation via

$$\tilde{\Gamma}_j^{\pm}(Q) = \Gamma^j_{Q \to Q \pm e}, \tag{7.79}$$

where $j = L, R$, we can rewrite the formula as

$$\tilde{F}_T\{\sigma_S(Q)\} = \sum_{j=L/R} [\sigma_S(Q+e)\Gamma^j_{Q+e\to Q} + \sigma_S(Q-e)\Gamma^j_{Q-e\to Q} - \sigma_S(Q)\Gamma^j_{Q\to Q+e} - \sigma_S(Q)\Gamma^j_{Q\to Q-e}] \tag{7.80}$$

This can be simplified by considering, that most of the involved tunneling rates are actually zero, as the corresponding transitions are forbidden (see section 7.2). Therefore we can simplify the quasi-particle contributions to

$$\tilde{F}_T\{\sigma_S(Q)\} = \sigma_S(Q+e)\Gamma^R_{Q+e\to Q} \tag{7.81}$$

$$\tilde{F}_T\{\sigma_S(Q+2e)\} = -\sigma_S(Q+2e)\Gamma^R_{Q+2e\to Q+e}. \tag{7.82}$$

7.5 Master Equation for the JQP-Process

Now by combining the contribution for Cooper pairs and quasi-particles we can write down the set of master equations.

$$\begin{aligned}
\dot{\sigma}_S(Q) &= -\frac{E_J^2\pi}{2\hbar}\tilde{P}'(i\nu-\delta)(\sigma_S(Q)-\sigma_S(Q+2e))+\tilde{F}_T\{\sigma_S(Q)\} \\
&= -\frac{E_J^2\pi}{2\hbar}\tilde{P}'(i\nu-\delta)(\sigma_S(Q)-\sigma_S(Q+2e))+\sigma_S(Q+e)\Gamma^R_{Q+e\to Q} \qquad (7.83)\\
\dot{\sigma}_S(Q+2e) &= \frac{E_J^2\pi}{2\hbar}\tilde{P}'(i\nu-\delta)(\sigma_S(Q)-\sigma_S(Q+2e))+\tilde{F}_T\{\sigma_S(Q+2e)\} \\
&= \frac{E_J^2\pi}{2\hbar}\tilde{P}'(i\nu-\delta)(\sigma_S(Q)-\sigma_S(Q+2e))-\sigma_S(Q+2e)\Gamma^R_{Q+2e\to Q+e} \qquad (7.84)
\end{aligned}$$

The third equation for $\dot{\sigma}(Q+e)$ can be inferred from the other two by the condition, that we want a non-trivial stationary solution.

$$\dot{\sigma}_S(Q+e)=\sigma_S(Q+2e)\Gamma^R_{Q+2e\to Q+e}-\sigma_S(Q+e)\Gamma^R_{Q+e\to Q} \qquad (7.85)$$

We can write down the system in matrix representation

$$\dot{\sigma}=T\sigma \qquad (7.86)$$

$$\text{with } T=\begin{pmatrix} -\frac{E_J^2\pi}{2\hbar}\tilde{P}'(i\nu-\delta) & \Gamma^R_{Q+e\to Q} & \frac{E_J^2\pi}{2\hbar}\tilde{P}'(i\nu-\delta) \\ 0 & -\Gamma^R_{Q+e\to Q} & \Gamma^R_{Q+2e\to Q+e} \\ \frac{E_J^2\pi}{2\hbar}\tilde{P}'(i\nu-\delta) & 0 & -\frac{E_J^2\pi}{2\hbar}\tilde{P}'(i\nu-\delta)-\Gamma^R_{Q+2e\to Q+e} \end{pmatrix}$$

$$\text{and } \sigma=\begin{pmatrix} \sigma_S(Q) \\ \sigma_S(Q+e) \\ \sigma_S(Q+2e) \end{pmatrix}.$$

As want to calculate a stationary current for the JQP process, we solve the system for the stationary state

$$\dot{\sigma}=0. \qquad (7.87)$$

As we constructed the system such that it has a non-trivial solution, $\det(T)=0$. Because the density matrix elements describe occupation probabilities, they have to satisfy the following condition

$$\sigma_S(Q)+\sigma_S(Q+e)+\sigma_S(Q+2e)=1. \qquad (7.88)$$

Inserting equations (7.87) and (7.88) into equation (7.86) gives the solution

$$\sigma=\begin{pmatrix} \sigma_S(Q) \\ \sigma_S(Q+e) \\ \sigma_S(Q+2e) \end{pmatrix}=\frac{1}{\Gamma_{\text{tot}}}\begin{pmatrix} \Gamma^R_{Q+e\to Q}\left(\Gamma^R_{Q+2e\to Q+e}+\frac{E_J^2\pi}{2\hbar}\tilde{P}'(i\nu-\delta)\right) \\ \Gamma^R_{Q+2e\to Q+e}\frac{E_J^2\pi}{2\hbar}\tilde{P}'(i\nu-\delta) \\ \Gamma^R_{Q+e\to Q}\frac{E_J^2\pi}{2\hbar}\tilde{P}'(i\nu-\delta) \end{pmatrix}, \qquad (7.89)$$

with

$$\Gamma_{\text{tot}} = \Gamma^R_{Q+e\to Q}\Gamma^R_{Q+2e\to Q+e} + 2\Gamma^R_{Q+e\to Q}\frac{E_J^2\pi}{2\hbar}\tilde{P}'(i\nu-\delta) + \Gamma^R_{Q+2e\to Q+e}\frac{E_J^2\pi}{2\hbar}\tilde{P}'(i\nu-\delta). \quad (7.90)$$

Using equations (7.5) and (7.79) and the considerations in section 7.2 which rates contribute, we can write down the decay rate ν as

$$\nu = \hbar\Gamma^R_{Q+2e\to Q+e}, \quad (7.91)$$

which is actually given by only a single tunneling rate setting the bottleneck for the decay through quasi-particles.

7.6 Current for the JQP-Process

The current I is given by the current flowing through both junctions. Because the two junctions can be viewed as series connection, the current has to be the same through each of them.

The current that flows through the left junction stems from purely Cooper pair transitions and is given as

$$I_L = 2e\left(\sigma(Q)\Gamma^L_{Q\to Q+2e} - \sigma(Q+2e)\Gamma^L_{Q+2e\to Q}\right) \quad (7.92)$$

where we assume, that the current flows from left to right (as we did for all the assumptions that went in the calculations before).

The current that flows through the right junction is due to the tunneling of quasi-particles off the island

$$I_R = e\sigma(Q+e)\Gamma^R_{Q+e\to Q} + e\sigma(Q+2e)\Gamma^R_{Q+2e\to Q+e}. \quad (7.93)$$

For the tunneling rates for Cooper pairs we use the result from equation (5.12) substituting $P(E)$ by the generalised $\tilde{P}'(i\nu-\delta)$

$$\Gamma^L_{Q\to Q+2e} = \Gamma^L_{Q+2e\to Q} = \frac{\pi E_J^2}{2\hbar}\tilde{P}'(i\nu-\delta). \quad (7.94)$$

Here the same energy argument in $\tilde{P}'(E)$ is used for both tunneling rates, even if the differences in the charging energy have opposite sign. This is allowed, because we are going to use the high temperature limit for $\tilde{P}'(i\nu-\delta)$ which is symmetric in δ around zero.

Inserting 7.89 and 7.94 into 7.92 yields

$$I_L = 2e\frac{\Gamma^R_{Q+e\to Q}\Gamma^R_{Q+2e\to Q+e}}{\Gamma_{\text{tot}}}\frac{\pi E_J^2}{2\hbar}\tilde{P}'(i\nu-\delta) \quad (7.95)$$

and inserting 7.89 into 7.93 yields

$$I_R = 2e\frac{\Gamma^R_{Q+e\to Q}\Gamma^R_{Q+2e\to Q+e}}{\Gamma_{\text{tot}}}\frac{\pi E_J^2}{2\hbar}\tilde{P}'(i\nu-\delta) \quad (7.96)$$

so we confirm as expected

$$I = I_L = I_R. \quad (7.97)$$

Chapter 8

Results

8.1 Semi-classical Approximation for the Complex $P(E)$ for Cooper Pairs

As we already evaluated the semi-classical approximation for $P(E)$ for real values of the energy in section 6.2 and derived the generalised function $\tilde{P}'(E)$ for complex arguments in section 7.4, we can now proceed with the semi-classical approximation for this generalised $\tilde{P}'(E)$. If we consider the derivation of $P(E)$ in appendix A.2, we recognise, that the generalised $\tilde{P}'(E)$ is the same as the $P'(E)$, but taking only the long-time limit of the correlation function into account (see equation (A.67)). $P'(E)$ for Cooper pairs emerges from $P(E)$ for quasi-particles by rescaling the effective charge to $2e$. The semi-classical approximation for $P(E)$ in section 6.2 corresponds to the derivation in A.2, were we already considered the contribution of the correlation function for long times only. Thus we can take equation (6.8) as a starting point and insert the complex energy argument

$$\tilde{P}'(i\nu - \delta) \approx \frac{1}{\pi\hbar\omega_1}\mathrm{Re}\left\{\frac{1}{\frac{1}{g} - \frac{i(i\nu-\delta)}{\hbar\omega_1}}\right\}. \tag{8.1}$$

Working out the real part, this becomes

$$\tilde{P}'(i\nu - \delta) \approx \frac{1}{\pi}\frac{\frac{4\hbar\omega_1}{g} + \nu}{\left(\frac{4\hbar\omega_1}{g} + \nu\right)^2 + \delta^2}. \tag{8.2}$$

This is valid for the assumptions made section 6.2 i.e. for $\frac{(i\nu-\delta)}{\hbar\omega_1} \ll 1$ and $\frac{E_C}{\hbar\sqrt{|z_j|}} \ll 1$.

This function is again a Lorentzian, if plotted against the difference in charging energy δ, but unlike $P(E)$, its width does not only depend on the effective impedance of the environment, which is proportional to $\frac{1}{g}$, and the temperature T, but also on the energy scale ν set by the rates for tunnelling of quasi-particles. So the total width is given by the sum of these contributions as $w_{FWHM} = \frac{8\hbar\omega_1}{g} + 2\nu = \frac{16\pi kT}{g} + 2\nu$.

Note that the dependence of the function $\tilde{P}'(i\nu - \delta)$ on temperature T and on the environment, described by the parameter $\frac{1}{g}$, only enters in a form, where both values appear together in the parameter $\frac{8\pi kT}{g}$. As the energy scale for system energies the charging energy E_C, we introduce the new dimensionless parameter $a = \frac{gE_C}{\hbar\omega_1}$, which will be used to describe the influence of the environment in the next sections.

8.2 Explicit Calculation of the Current for the JQP Process

For the particular calculation of the current for the JQP process we choose the relevant parameters to satisfy both equations (7.13) and (7.39), thus $\Delta = 2E_C$, and $eV = 5.5E_C$. And we assume $2C = C_\Sigma$, which is equivalent to assuming $C_G \ll C$ and equal capacitances. But, as we have seen from the discussion of the working principle of the SCT, adding the gate with a finite gate voltage only shifts the bias voltage we have to apply to reach the same working point. Again, condition 7.39 allows us to vary the voltage smoothly in a range of $4E_C < eV + e\delta V < 7E_C$, and as $e\delta V = \frac{\delta}{2}$ we can vary the energy around the Cooper pair resonance by $-3E_C < \delta < 3E_C$. The thermal energy is assumed to be $kT = 0.1E_C$.

8.2.1 Quasi-particle Tunnelling Rates

To be able to calculate the current at resonance, we first have to work out the tunnelling rates for the two possible quasi-particle transitions $\Gamma^R_{Q+e\to Q}$ and $\Gamma^R_{Q+2e\to Q+e}$. So we start with the rate $\Gamma^R_{Q+e\to Q}$ and use the definition for tunnelling rates (equation (5.9)), where the electrostatic energy is substituted by the difference in charging energy occurring for this transition that were calculated in section 7.3. For this particular choice of parameters we have $U(n+2,n+1) - U(n+2,n+2) = 4.5E_C + \frac{\delta}{2}$ and $U(n+2,n) - U(n+2,n+1) = 6.5E_C + \frac{\delta}{2}$.

Therefore

$$\begin{aligned}\Gamma^R_{Q+e\to Q} &= \frac{2\pi}{\hbar}|T|^2 \int_{-\infty}^{\infty} dE\, dE'\, f(E)[1-f(E')]N_S(E)N_S(E') \times \\ &\quad \times P(E - E' + U(n+2,n+1) - U(n+2,n+2)). \end{aligned} \tag{8.3}$$

As we consider sufficiently low temperatures, we can approximate the Fermi-distributions by its shape for zero temperature, which is a step-function. Inserting this and the density of states for superconductors from equation (2.6) the integral becomes

$$\begin{aligned}\Gamma^R_{Q+e\to Q} &= \frac{2\pi}{\hbar}|T|^2 N_N(0)^2 \int_{-\infty}^{\infty} dE\, dE'\, \theta(-E)\theta(E')\frac{|E|}{\sqrt{E^2-\Delta^2}}\frac{|E'|}{\sqrt{E'^2-\Delta^2}}\theta(|E|-\Delta)\theta(|E'|-\Delta) \times \\ &\quad \times P(E - E' + U(n+2,n+1) - U(n+2,n+2)) \end{aligned} \tag{8.4}$$

which by working out the θ functions and substituting $E \to -E$ yields

$$\begin{aligned}\Gamma^R_{Q+e\to Q} &= \frac{2\pi}{\hbar}|T|^2 N_N(0)^2 \int_{\Delta}^{\infty} dE \int_{\Delta}^{\infty} dE' \frac{E}{\sqrt{E^2-\Delta^2}}\frac{E'}{\sqrt{E'^2-\Delta^2}} \times \\ &\quad \times P(-E - E' + U(n+2,n+1) - U(n+2,n+2)). \end{aligned} \tag{8.5}$$

Inserting the approximation for $P(E)$ from equation (6.9) this becomes

$$\Gamma^R_{Q+e\to Q} = \frac{2}{\hbar}|T|^2 N_N(0)^2 \int_\Delta^\infty dE \int_\Delta^\infty dE' \frac{E}{\sqrt{E^2-\Delta^2}} \frac{E'}{\sqrt{E'^2-\Delta^2}} \times \\ \times \frac{\frac{g}{\hbar\omega_1}}{1+\left(\frac{g}{\hbar\omega_1}\right)^2 (-E-E'+U(n+2,n+1)-U(n+2,n+2))^2} \tag{8.6}$$

and inserting the parameters chosen above, but instead of inserting $\hbar\omega_1 = 2\pi kT = 0.2\pi E_C$, we use the dimensionless parameter $a = \frac{gE_C}{\hbar\omega_1}$, which can be assumed to be $a \gg 1$ as we are looking at small values of $\frac{1}{g}$, and substituting $E = xE_C$, $E' = yE_C$ to make the integral dimensionless, we obtain

$$\Gamma^R_{Q+e\to Q} = \frac{2}{\hbar}|T|^2 N_N(0)^2 E_C \int_2^\infty dx \int_2^\infty dy \frac{x}{\sqrt{x^2-4}} \frac{y}{\sqrt{y^2-4}} \frac{a}{1+a^2(-x-y+4.5+\delta')^2} \\ = \frac{2}{\hbar}|T|^2 N_N(0)^2 E_C S_1(\delta'), \tag{8.7}$$

where we introduced the dimensionless energy $\delta' = \frac{\delta}{2E_C}$ and the dimensionless integral $S_1(\delta')$

$$S_1(\delta') = \int_2^\infty dx \int_2^\infty dy \frac{x}{\sqrt{x^2-4}} \frac{y}{\sqrt{y^2-4}} \frac{a}{1+a^2(-x-y+4.5+\delta')^2}. \tag{8.8}$$

This is the tunnelling rate for quasi-particles, which depends on δ', i.e. on how much one shifts the energy away from the Cooper pair resonance. This integral is hard to evaluate both analytically and numerically. If we assume $a \gg 1$, then it can be approximated analytically. The integration of the dimensionless integral $S_1(\delta')$ is discussed in the appendix A.3 and results in equation (A.100).

Therefore we get for the tunnelling rate in terms of δ

$$\Gamma^R_{Q+e\to Q}(\delta) = \frac{4\pi}{\hbar}|T|^2 N_N(0)^2 E_C (2.25+\frac{\delta}{4E_C}) E\left(\frac{0.25+\frac{\delta}{4E_C}}{2.25+\frac{\delta}{4E_C}}\right) \theta(-\delta-1) \tag{8.9}$$

with $E(k)$ denoting the complete elliptic integral of the second kind, which is defined in equation (A.99).

The tunnelling rate

$$\Gamma^R_{Q+2e\to Q+e} = \frac{2\pi}{\hbar}|T|^2 \int_{-\infty}^\infty dE\, dE'\, f(E)[1-f(E')]N_S(E)N_S(E') \times \\ \times P(E-E'+U(n+2,n)-U(n+2,n+1)) \tag{8.10}$$

$$= \frac{2}{\hbar}|T|^2 N_N(0)^2 E_C S_2(\delta') \tag{8.11}$$

differs from the one just calculated only in the difference of the charging energies. This can be absorbed in shifting δ' to $\tilde{\delta}' = \delta' + 2$, so we get for the integral

$$S_2(\delta') = 2\pi(3.25 + \frac{\delta'}{2})E\left(\frac{1.25 + \frac{\delta'}{2}}{3.25 + \frac{\delta'}{2}}\right)\theta(-\delta' - 2.5) \tag{8.12}$$

and therefore for the tunnelling rate

$$\Gamma^R_{Q+2e\to Q+e}(\delta) = \frac{4\pi}{\hbar}|T|^2 N_N(0)^2 E_C(3.25 + \frac{\delta}{4E_C})E\left(\frac{1.25 + \frac{\delta}{4E_C}}{3.25 + \frac{\delta}{4E_C}}\right)\theta(-\delta - 5). \tag{8.13}$$

For the tunnel matrix element, which is defined as

$$|T|^2 = \frac{\hbar}{2\pi e^2 R_t N_N(0)^2}, \tag{8.14}$$

we assume the ideal BCS case, where the Ambegaokar-Baratoff-formula [22] can be used to determine the tunnelling resistance in terms of the Josephson energy and gap energy as $R_t = \frac{\hbar\Delta}{8e^2E_J}$ and for our choice of Δ one obtains

$$|T|^2 = \frac{E_J}{\pi^2 E_C N_N(0)^2}. \tag{8.15}$$

Thus using the critical current $I_C = \frac{2eE_J}{\hbar}$ the tunnelling rates become

$$\begin{aligned}
\Gamma^R_{Q+e\to Q}(\delta) &= \frac{I_C}{e\pi^2}S_1\left(\frac{\delta}{2E_C}\right) && (8.16)\\
&= \frac{2I_C}{e\pi}\left(2.25 + \frac{\delta}{4E_C}\right)E\left(\frac{0.25 + \frac{\delta}{4E_C}}{2.25 + \frac{\delta}{4E_C}}\right)\theta(-\delta - 1)\\
\Gamma^R_{Q+2e\to Q+e}(\delta) &= \frac{I_C}{e\pi^2}S_2\left(\frac{\delta}{2E_C}\right) && (8.17)\\
&= \frac{2I_C}{e\pi}\left(3.25 + \frac{\delta}{4E_C}\right)E\left(\frac{1.25 + \frac{\delta}{4E_C}}{3.25 + \frac{\delta}{4E_C}}\right)\theta(-\delta - 5).
\end{aligned}$$

A plot for both tunnelling rates is shown in figure 8.1 as a function of the energy shift δ from the Cooper pair resonance. This shows the increase of the tunnelling rates with the increasing additional bias voltage ($\delta = 2e\delta V$), as expected from theory of quasi-particle tunnelling. The rate is zero for bias voltages below the gap. As we consider two rates it different charging energy differences, they become zero for distinct voltage shifts. They, of course, have the same gap energy, as we consider only one tunnel junction. The rates to are not influenced on the environment for our assumption of large $\frac{gE_C}{\hbar\omega} = \frac{gE_C}{2\pi kT}$. This is because quasi-particle tunnelling is already an incoherent process, an additional environment would just increase its incoherence [34]. But as we consider only small effective impedances of the environment, this additional effect is quite small, and is of the order that was neglected in the calculation, as we only considered the dominant contribution to the integral.

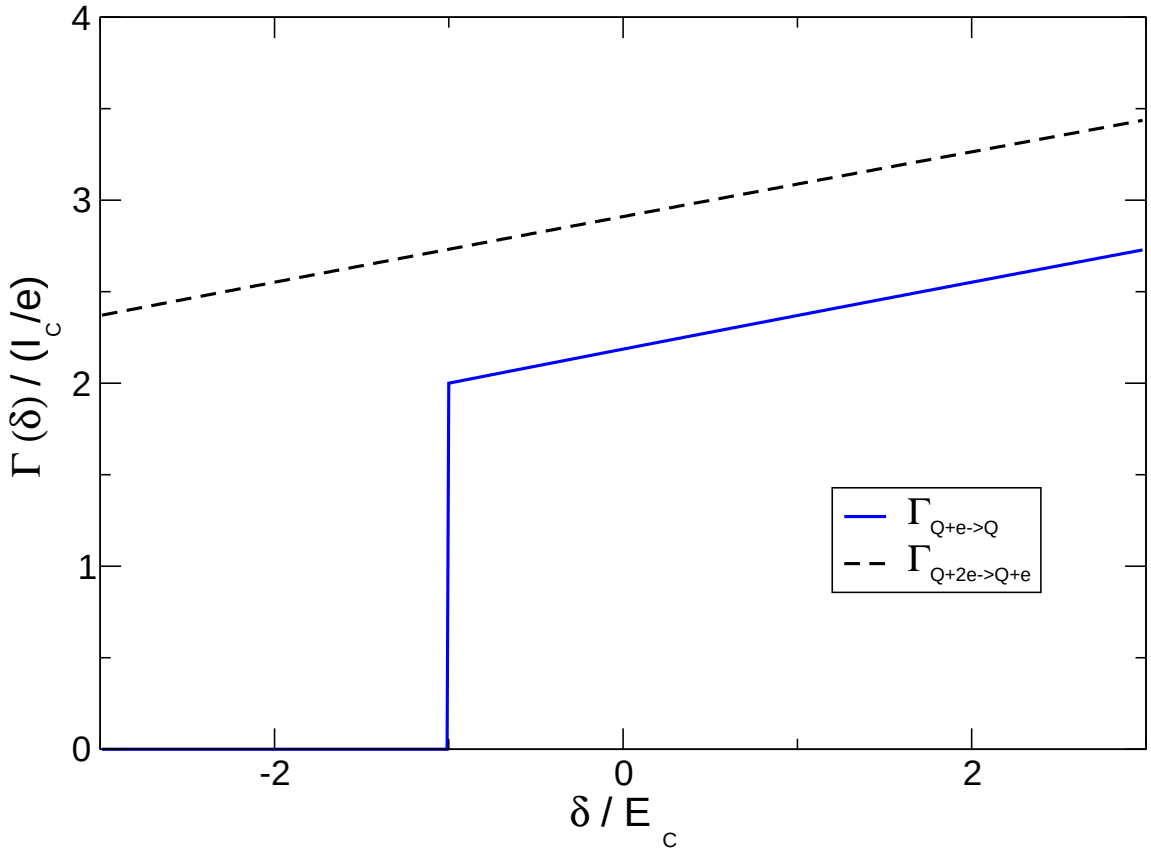

Figure 8.1: Quasi-particle Tunnelling Rates $\Gamma^R_{Q+e\to Q}(\delta)$ and $\Gamma^R_{Q+e\to Q}(\delta)$ (calculated from equations (8.16) and (8.16)) plotted against the energy δ (which corresponds to the voltage we tune the system away from the resonance for Cooper pair tunnelling being resonant in the left junction). Parameters are as chosen in this section. This rate is independent of temperature and environment, as we assume $\frac{gE_C}{2\pi kT} \gg 1$.

8.2.2 Generalised $\tilde{P}'(E)$ for Cooper Pairs

We can now calculate the generalised $\tilde{P}'(E)$ for Cooper pairs by using its approximation from equation (8.2). By inserting the quasi-particle energy ν from equation (7.91) we obtain

$$\tilde{P}'(i\nu - \delta) = \tilde{P}'(\delta) = \frac{1}{\pi} \frac{\frac{4\hbar\omega_1}{g} + \hbar\Gamma^R_{Q+2e\to Q+e}}{\left(\frac{4\hbar\omega_1}{g} + \hbar\Gamma^R_{Q+2e\to Q+e}\right)^2 + \delta^2}. \tag{8.18}$$

Now we can insert equation (8.17) to obtain

$$\tilde{P}'(\delta) = \frac{1}{\pi} \frac{\frac{4\hbar\omega_1}{g} + \frac{2E_J}{\pi^2} S_2\left(\frac{\delta}{2E_C}\right)}{\left(\frac{4\hbar\omega_1}{g} + \frac{2E_J}{\pi^2} S_2\left(\frac{\delta}{2E_C}\right)\right)^2 + \delta^2}. \tag{8.19}$$

and express $\tilde{P}'(\delta)$ in terms of E_C by using the dimensionless parameter $a = \frac{gE_C}{\hbar\omega_1}$ and reexpress the critical current in terms of the Josephson energy

$$\tilde{P}'(\delta) = \frac{1}{E_C}\frac{1}{\pi}\frac{\frac{4}{a}+\frac{2}{\pi}\frac{E_J}{E_C}S_2\left(\frac{\delta}{2E_C}\right)}{\left(\frac{4}{a}+\frac{2}{\pi}\frac{E_J}{E_C}S_2\left(\frac{\delta}{2E_C}\right)\right)^2+\left(\frac{\delta}{E_C}\right)^2} \tag{8.20}$$

$$= \frac{1}{E_C}\tilde{P}'_d(\delta) \tag{8.21}$$

where we introduced the dimensionless function $\tilde{P}'_d(\delta)$. This function describes the response of the Cooper pair transition to the environment in the presence of quasi-particle tunnelling, that empty the Cooper pair state on the island. From equation (8.20) we see that the generalised $P(E)$ would be a Lorentzian, if one assumes the tunnelling rate to be constant with respect to δ. Thus its width is given by

$$\delta_{\mathrm{FWHM}} = \frac{8}{a}+\frac{4}{\pi}\frac{E_J}{E_C}S_2\left(\delta=0\right) \tag{8.22}$$

which is a sum of the decoherence broadening $\frac{4}{a}$, which can be changed through the environment (for fixed temperature), and the life-time broadening, determined by the quasi-particles tunnelling off the island. The tunnel coupling for quasi-particles is proportional to $\frac{E_J}{E_C}$ which appears here again. This is due to using the Ambegaokar-Baratoff formula. Its maximum height depends on the same parameters, as it is given as

$$H = \frac{1}{\pi E_C}\frac{1}{w}. \tag{8.23}$$

Note that the approximation of constant tunnelling rates fails for large values of the dimensionless Josephson coupling $\frac{E_J}{E_C} \gg 1$, because then the plot covers a broader range of δ, where the tunnelling rates change. But we are only interested in a small Josephson coupling $\frac{E_J}{E_C} \ll 1$, as this is the regime, where the perturbation theory holds.

In the following we study the dependence of the generalised $\tilde{P}'(\delta)$ on the Josephson coupling and on the environment separately for different regimes. This is crucial, because the full rates entering equation (8.20) are actually not at all constant, see figure 8.1. Thus, deviations from the ideal Lorentzian shape can occur.

Firstly, we investigate the dependence of $\tilde{P}'(\delta)$ on the ratio of the Josephson coupling for a fixed environment. (Although $\tilde{P}'(\delta)$ is a Lorentzian (if the tunnelling rates are assumed to be constant), which is a well known function, we plot it for illustrating the analysis.) A plot for $a = 100$, which corresponds to a reasonable small effective impedance of the environment, is shown in figure 8.2. As expected from equation (8.20) it broadens with an increasing Josephson coupling. For increasing $\frac{E_J}{E_C}$ one enhances the tunnelling rate of quasi-particles, which decreases the life-time of a Cooper pair on the island. This in turn corresponds to a reduced life-time of the doubly charged state. Therefore we label the term $\frac{E_J}{E_C}S_2\left(\frac{\delta}{2E_C}\right)$ life time broadening. As $\tilde{P}'(\delta)$ is normalised, the height reduces.

For a larger value of the parameter a, i.e. a smaller contribution of the environment, the general behaviour of the function remains the same, although its maximum is increased and the function is narrowed, which is due to increasing a.

A characteristic parameter for $\tilde{P}'(\delta)$ is its width δ_{FWHM}, which is defined in equation 8.22. Its values from a Lorentzian fit to $\tilde{P}'(\delta)$ compared to the theoretical result from equation 8.22 are plotted for $a = 100$ in figure 8.3 and for $a = 1000$, i.e. a smaller effective impedance of the environment, in figure 8.4.

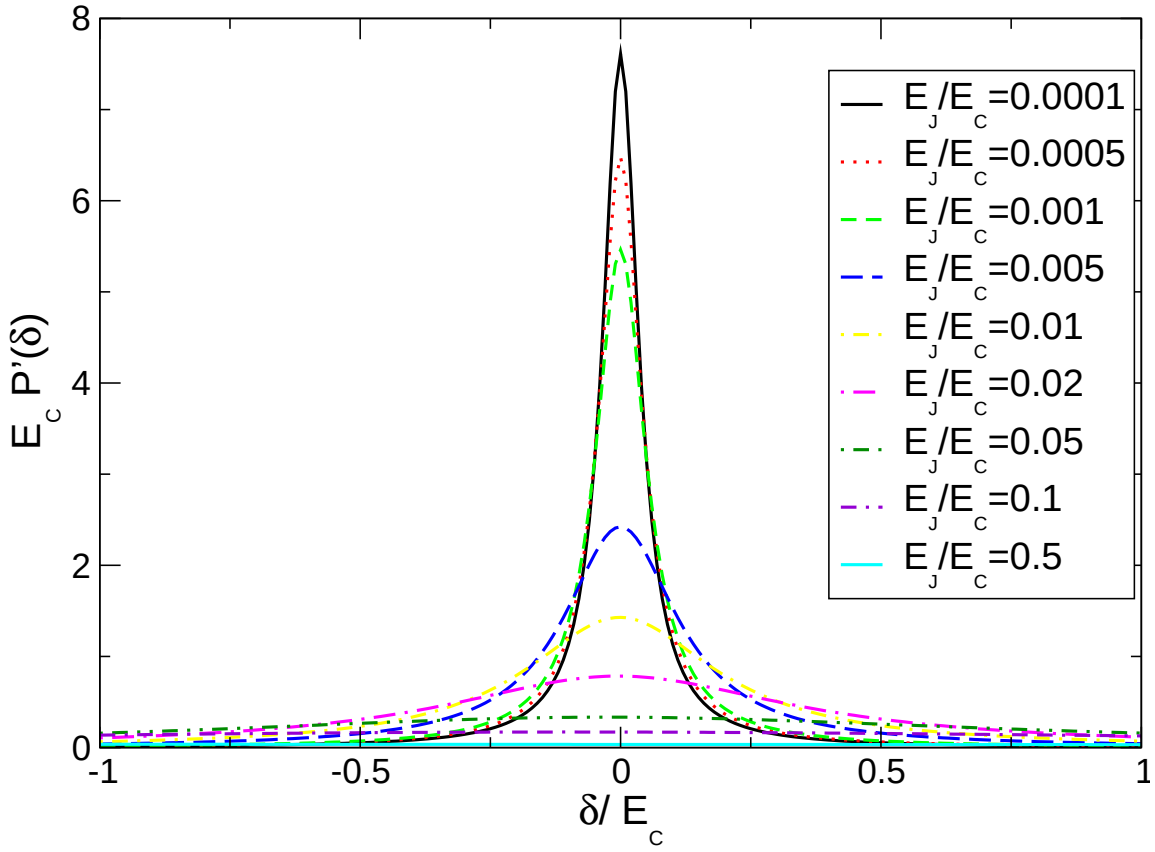

Figure 8.2: Dimensionless generalised $\tilde{P}'(\delta)$ as a function of the energy difference from the Cooper pair resonance for $a = 100$ and dimensionless Josephson couplings between $\frac{E_J}{E_C} = 0.0001$ and $\frac{E_J}{E_C} = 0.5$ (from top to bottom) calculated using equation (8.20). This plot is shown to illustrate the effect of the dimensionless Josephson coupling on $\tilde{P}'(\delta)$. The function is broadened for an increase in Josephson energy with respect to the charging energy due to life-time broadening.

For the limit of $\frac{E_J}{E_C} \to 0$ we see that the width saturates for both plots at a finite value, which is entirely determined by the environment, as expected from equation 8.22. Furthermore we see, that the increase of the width with respect to the dimensionless Josephson coupling is well described with the assumption of a constant tunneling rate.

Next we study in detail the influence of the effective impedance on the function $\tilde{P}'(E)$ for a fixed Josephson coupling. The plot for a reasonable large Josephson coupling $\frac{E_J}{E_C} = 0.02$ is shown in figure 8.5. Here the environment changes the peak width only little, the dependence of the peak height is strong for larger environment, but as we decrease the effective impedance (i.e. we increase a), the height saturates. This is also expected from equation (8.23), which for $a \to \infty$ depends on the quasi-particle rate only.

For small dimensionless Josephson coupling $\frac{E_J}{E_C}$ the function depends strongly on the change of the effective impedance. This is also clear from the definition of $\tilde{P}'(\delta)$, as for $\frac{E_J}{E_C} \to 0$ its shape is dominated by a. As we consider a regime of $\frac{E_J}{E_C} \ll 1$, the phase coherence of the Cooper pairs is very good, so it will be sensitive to small fluctuations of the environment. This explains the dramatic drop in peak height with an increase of the environment.

We plot the dependence of the peak width on the parameter a for the different regimes

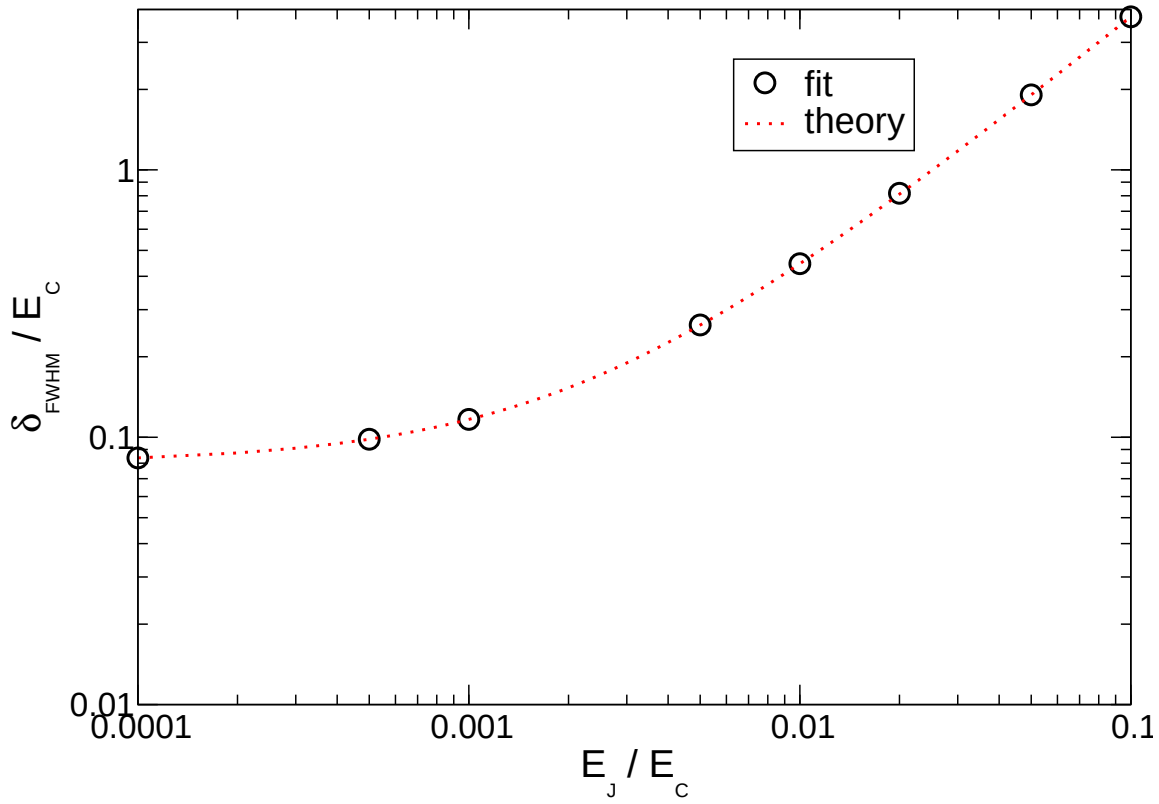

Figure 8.3: Full width at half maximum δ_{FWHM} for the dimensionless generalised $\tilde{P}'(\delta)$ as a function of the dimensionless Josephson couplings for $a = 100$ on a double logarithmic scale. This was obtained from fitting a Lorentzian to $\tilde{P}'(\delta)$ (circles denote the fitted values). This agrees well with the width for the assumption of a constant tunneling rate, calculated using equation (8.22) (dotted line).

of the Josephson coupling in figures 8.6 and 8.7. The values were extracted from plots of $\tilde{P}'(\delta)$ by fitting a Lorentzian to it. Again, they compare well with the assumption of constant tunneling rates, as the Josephson coupling is small.

In conclusion, the assumption of a constant tunneling rate is justified for our choice of parameters.

8.3 JQP Current

Finally, one can insert the formulas for the quasi-particle rates (equations (8.16) and (8.17)) and the generalised $\tilde{P}'(E)$ (equation (8.21)) into the stationary current for the JQP process (equations (7.96) and (7.97)) and obtain after some algebra

$$I(\delta) = I_C \frac{\pi}{2} \frac{E_J}{E_C} \frac{S_1\left(\frac{\delta}{2E_C}\right) S_2\left(\frac{\delta}{2E_C}\right) \tilde{P}'_d(\delta)}{S_1\left(\frac{\delta}{2E_C}\right) S_2\left(\frac{\delta}{2E_C}\right) + \frac{\pi^3}{4}\frac{E_J}{E_C}\left(2S_1\left(\frac{\delta}{2E_C}\right) + S_2\left(\frac{\delta}{2E_C}\right)\right) \tilde{P}'_d(\delta)}. \tag{8.24}$$

The current scales with E_J^2 (as $I_C \sim E_J$) which is characteristic for the incoherent tunneling of Cooper pairs, while the current for the coherent tunneling of Cooper pairs scales with E_J.

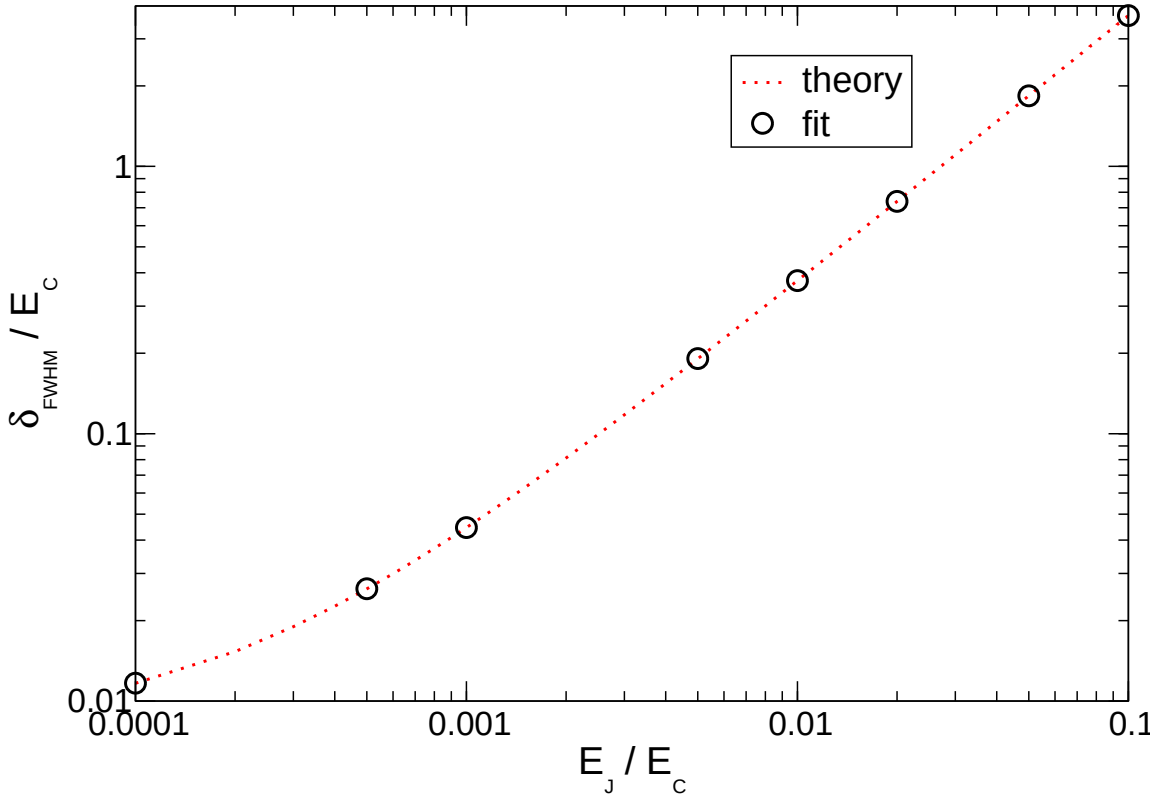

Figure 8.4: Full width at half maximum δ_{FWHM} for the dimensionless generalised $\tilde{P}'(\delta)$ as a function of the dimensionless Josephson couplings for $a = 1000$ on a double logarithmic scale. This was obtained from fitting a Lorentzian to $\tilde{P}'(\delta)$ (circles denote the fitted values). This agrees well with the width for the assumption of a constant tunneling rate, calculated using equation (8.22) (dotted line).

As we remember from section 3.3, in the JQP process an incoherent transition of a Cooper pair is involved, which causes this dependence. The current depends on the two parameters a (through the function $\tilde{P}'(\delta)$) and on the ratio of Josephson to charging energy $\frac{E_J}{E_C}$, i.e. on the Josephson coupling. The dependence on these parameters is discussed in the following. If one considers only regimes were the Josephson energy is small compared to the charging energy, we expect to observe a current which shape is dominated by the function $\tilde{P}'(\delta)$. Because in this regime, if we go just slightly away from the resonance for Cooper pair tunneling, $\tilde{P}'(\delta)$ is small compared to the tunneling rates. Therefore we can approximate the current as

$$I(\delta) \approx I_C \frac{\pi}{2} \frac{E_J}{E_C} \tilde{P}'_d(\delta). \tag{8.25}$$

For a full study of the current from equation 8.24, we investigate the resonance properties systematically.

The plot of the current for the JQP process for constant $a = 1000$ which means a reasonably small effective impedance of the environment ($\frac{1}{g} = \frac{1}{200\pi}$ for $kT = 0.1E_C$) and for different Josephson couplings can be seen in figure 8.8. The current is a symmetrically broadened peak around $\delta = 0$ for small values of the Josephson coupling $\frac{E_J}{E_C}$. The total current (in units of the critical current in a superconductor) increases with the increase of the Josephson coupling. This is, because the JQP process involves a Cooper pair transition. The incoherent tunneling

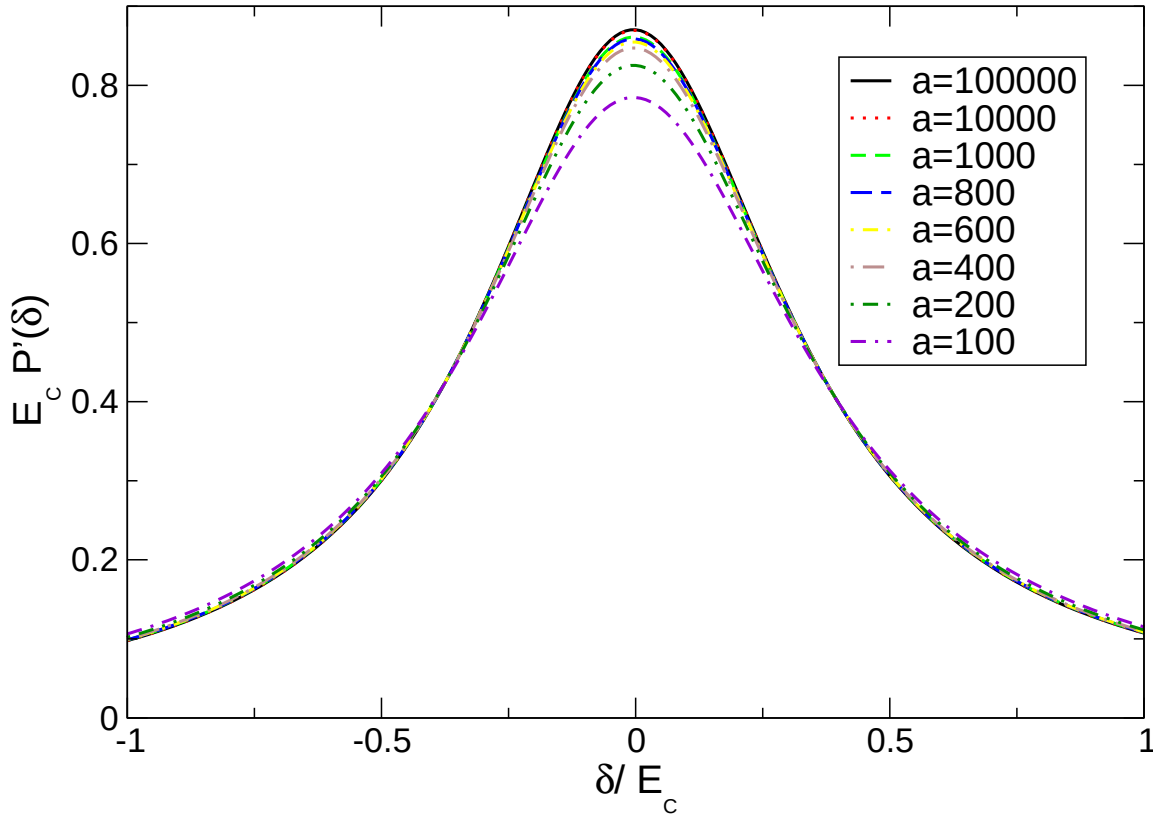

Figure 8.5: Dimensionless generalised $\tilde{P}'(\delta)$ as a function of the energy difference from the Cooper pair resonance for $\frac{E_J}{E_C} = 0.02$ and varying the parameter describing the environment from $a = 100$ to $a = 100000$ (from bottom to top) calculated using equation (8.20). This plot is shown to illustrate the effect of the environment on $\tilde{P}'(\delta)$. As the effective impedance of the environment is increased, i.e. a is decreased, the peak slightly broadens due to decoherence broadening by the environment.

of Cooper pairs increases with the Josephson coupling. For small values of the Josephson coupling the peak shape is dominated by the function $\tilde{P}'(\delta)$ as expected . The observed shift of the peak maximum away from the resonance point is due to the energy dependence of the quasi-particle tunneling rates becoming dominant.

Note that the regime $\frac{E_J}{E_C} \sim 0.1$ is in principle beyond perturbation theory. To actually take this regime into account one would have to consider more charge states and they can not be considered as eigenstates any more, because for large values of $\frac{E_J}{E_C}$ the phase becomes a well defined quantity instead of the charge. But this should only cause quantitative changes.

To confirm the prediction, that the current in this regime is proportional to the function $\tilde{P}'_d(\delta)$, we scale the plot of the current by the ratio of Josephson to charging energy. This shows a Lorentzian shaped function which indeed confirms our prediction. From this one can also extract the full width at half maximum δ_{FWHM} of the peak by fitting a Lorentzian to each of the plot. The width as a function of the Josephson coupling is shown in figure 8.9. From there we obtain a linear dependence of the width on $\frac{E_J}{E_C}$. The width of $\tilde{P}'(\delta)$ is shown on the same graph for comparison. The slope is the same, but there is a systematic deviation between both plots. This means that $\tilde{P}'(\delta)$ determines the global shape of the current, but a too small width, as in equation (8.24, quasi-particle rates provide additional broadening.

Considering a regime of larger coupling to the environment, we plot the current for $a = 100$

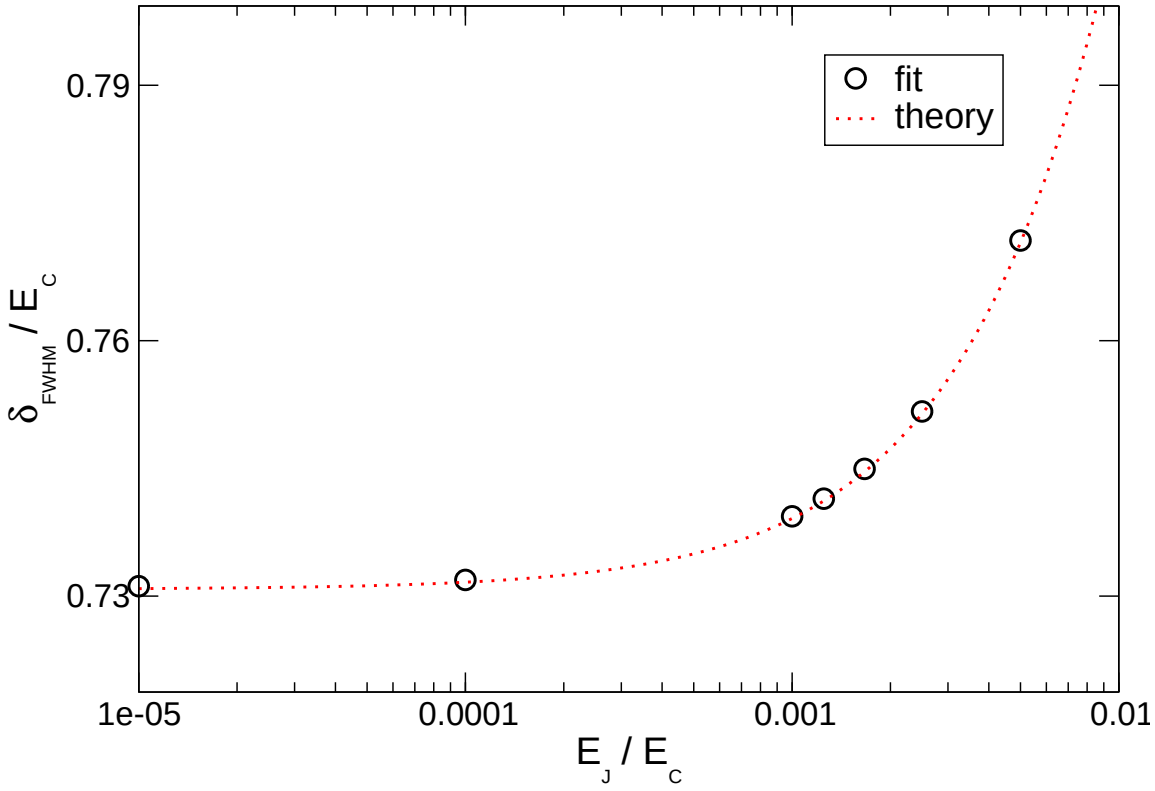

Figure 8.6: Full width at half maximum δ_{FWHM} for the dimensionless generalised $\tilde{P}'(\delta)$ as a function of the parameter a, which describes the influence of the environment for $\frac{E_J}{E_C} = 0.02$ on double logarithmic scales. This was obtained from fitting a Lorentzian to $\tilde{P}'(\delta)$ (circles denote the fitted values). It compares well with the width for the assumption of a constant tunneling rate, calculated from equation (8.22) (dotted line).

in units of the critical current in figure 8.10. The behaviour is similar compared to the plots for $a = 1000$, but the absolute value of the current is reduced for the same $\frac{E_J}{E_C}$ for small Josephson coupling. The current is more sensitive to the ratio of the Josephson to charging energy for larger environments, as this breaks the phase coherence more and more. Here one has to be careful with the interpretation of the current in the tails ($|\delta| > 0.2\pi E_C$), as the semi-classical approximation breaks down. So the interpretation given here is restricted to the regime, where $|\delta| \leq 0.2\pi E_C$.

For extracting the full width at half maximum δ_{FWHM} shown in figure 8.11 we again use a scaled plot and fit a Lorentzian to it which width is taken as δ_{FWHM} of the JQP current. As expected, this increases with a increasing $\frac{E_J}{E_C}$, too. As before, the width of the current compared to the width of $\tilde{P}'_d(\delta)$ is reduced, but the order of magnitude is the same.

Now, we investigate the dependence of the JQP peak on the environment in more detail. First we consider a regime of relatively large Josephson coupling (but still small enough to stay within the regime, where perturbation theory is valid). Thus we choose $\frac{E_J}{E_C} = 0.02$ and plot the current for different a in figure 8.12. We observe, that basically only the magnitude of the current changes by varying the effective impedance of the environment. This could be already suspected from the behaviour of $\tilde{P}'_d(\delta)$ as shown in figure 8.5. This occurs because the dimensionless Josephson coupling is already quite large and causes a large life time broadening. Compared to this effect, the change in the effective impedance of the environment is quite small

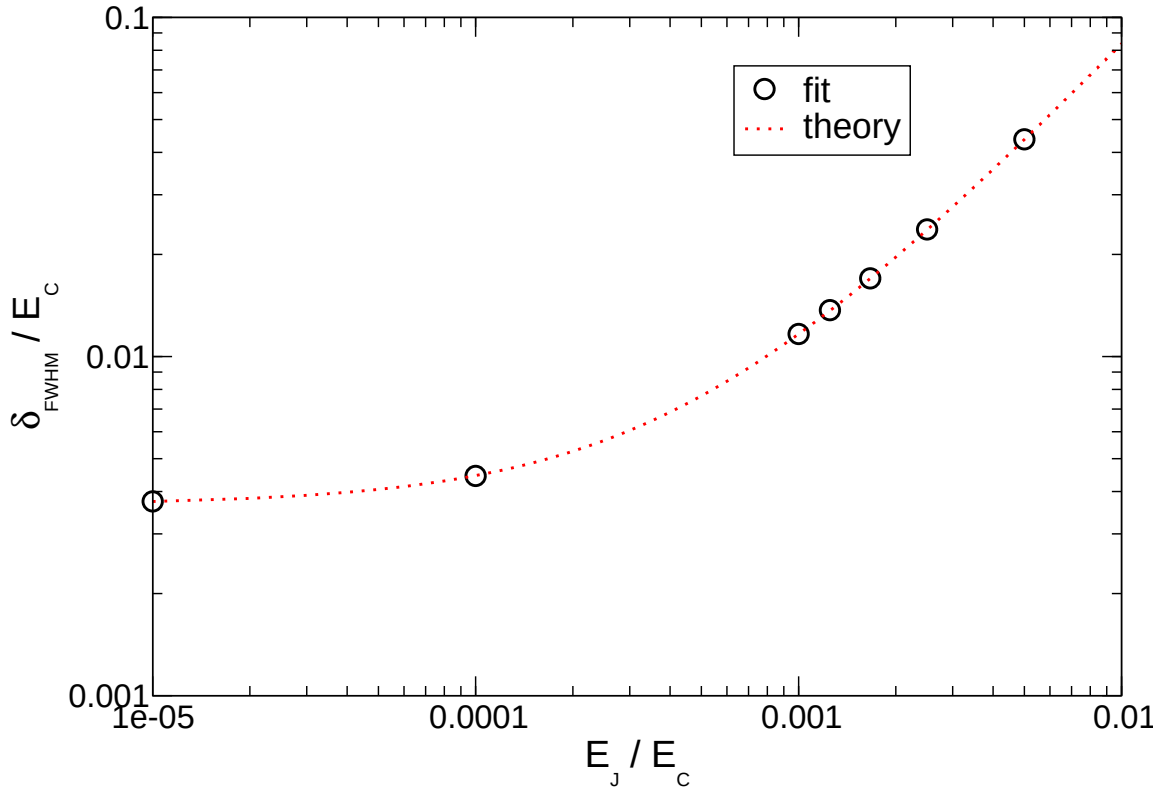

Figure 8.7: Full width at half maximum δ_{FWHM} for the dimensionless generalised $\tilde{P}'(\delta)$ as a function of the parameter a, which describes the influence of the environment for $\frac{E_J}{E_C} = 0.0001$ on double logarithmic scales. This was obtained from fitting a Lorentzian to $\tilde{P}'(\delta)$ (circles denote the fitted values). It compares well with the width for the assumption of a constant tunneling rate, calculated from equation (8.22) (dotted line).

and so is the decoherence broadening. Again, one has to be careful with the interpretation for the regime beyond $|\delta| \approx 0.2\pi E_C$.

We also scale the plots with respect to the Josephson coupling which is used to extract the peak width δ_{FWHM} shown in figure 8.13). This time we fit a scaled Lorentzian $f(x) = \frac{A}{\pi} \frac{\frac{\delta_{\mathrm{FWHM}}}{2}}{\frac{\delta_{\mathrm{FWHM}}}{2}+x^2}$ with fitting parameters A (shown in the inset of figure 8.14) and δ_{FWHM}, as these current are not normalised. From there we get the peak height at $\delta = 0$ as $H_0 = \frac{2}{\pi}\frac{A}{\delta_{\mathrm{FWHM}}}$, which is shown in figure 8.14. The peak width increases on a small scale if we increase the environment. It saturates in the limit of no environment at a value, which is entirely determined by the tunneling life-time of the quasi-particles. As the quasi-particle tunneling rate scales with $\frac{E_J}{E_C}$, which is a large value in this plot, they cause a huge broadening of the JQP peak. Therefore the peak width has a finite offset for $\frac{1}{a} \to 0$. The width is only slightly smaller than the width of $\tilde{P}'(\delta)$. The peak height decreases on a small scale.

For a significantly smaller Josephson coupling $\frac{E_J}{E_C} = 0.0001$, the behaviour is qualitatively the same, but it is much more prominent. In this regime the decoherence broadening is the dominant mechanism, which leads to a strong dependence of the current on the size of the effective impedance. As we decrease the induced dissipation (i.e. we increase a), the peak height increases dramatically. But the width of the peak is very small. This is because the lifetime of the Cooper pair is quite large, therefore the uncertainty in energy is only small,

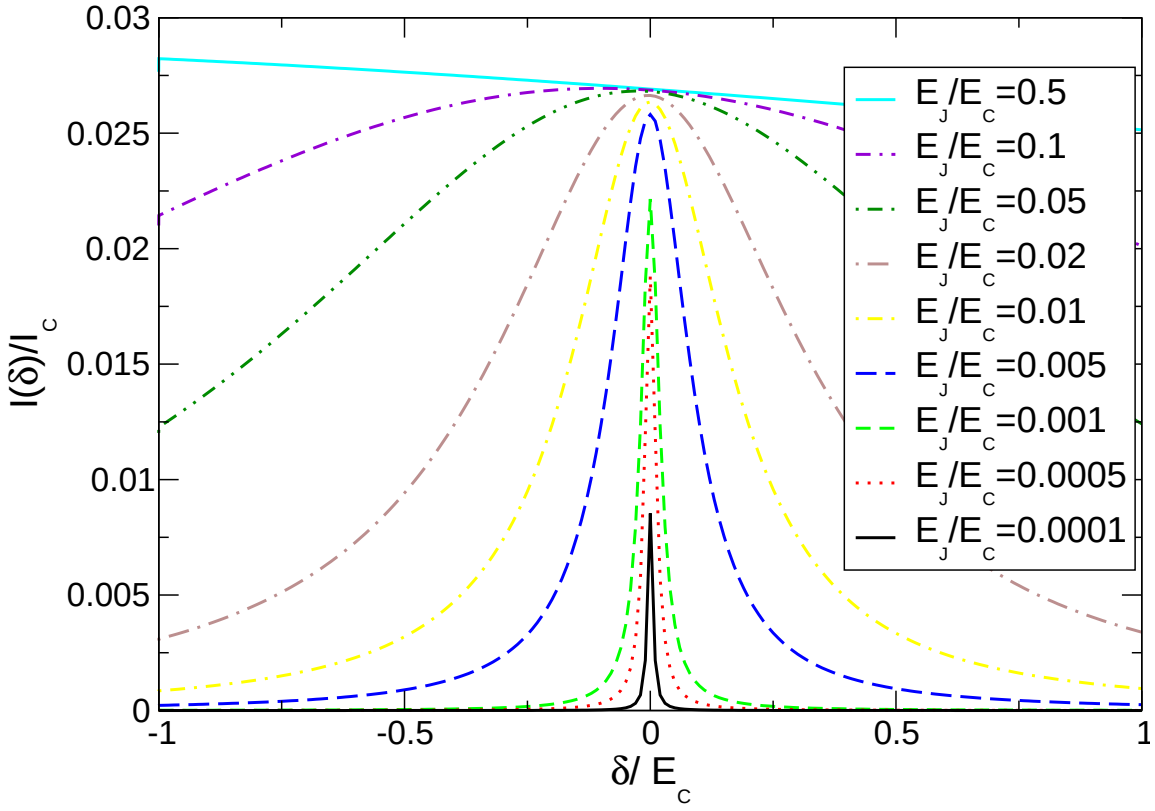

Figure 8.8: Current for the JQP cycle as a function of the energy difference from the Cooper pair resonance for $a = 1000$ and for different values of the dimensionless Josephson coupling from $\frac{E_J}{E_C} = 0.0001$ to $\frac{E_J}{E_C} = 0.5$ (from bottom to top). This was calculated, using equation (8.24). The current increases for the increasing dimensionless Josephson coupling, as an incoherent Cooper pair transition is involved. The peak is broadened by the shorter life-time of the doubly charged state, as quasi-particle transitions become more likely, if $\frac{E_J}{E_C}$ is increased.

therefore Cooper pair tunneling, which is a resonant process, is only allowed in a small voltage regime. For increasing dissipation the opposite happens. The current as a function of the energy difference from the Cooper pair resonance is plotted in figure 8.15. Both its magnitude and width are strongly dependent on the parameters of the environment.

Again, we extract the peak width (figure 8.16) and peak height (figure 8.17) from fitting a scaled Lorentzian (scaling parameter A is shown in the inset of figure 8.17) to the plot that is scaled by $\frac{E_J}{E_C}$. As before, the width saturates for $a \to \infty$ as well as the height. This time, the limit of small Josephson energies compared to charging energies is fulfilled sufficiently well, such that the peak width of the current nearly coincides with the peak with of $\tilde{P}'(\delta)$.

Concluding, we have seen, that the JQP current nearly shows Lorentzian shape. Its width is determined by both the decoherence broadening introduced by the environment and the life-time broadening, which is due to the quasi-particle transition that tunnels of the island of the SET in order to complete the JQP cycle. Depending on the actually size of the dimensionless Josephson coupling, the impact of the environment onto the system is different. For a large Josephson coupling $\frac{E_J}{E_C} \ll 1$, the width of the current peak is already determined by the decoherence broadening and the environment has only a very small additional broadening effect. But for small Josephson coupling $\frac{E_J}{E_C} < 1$, the impact of the environment on the system is huge and the peak width is mainly determined by the decoherence broadening.

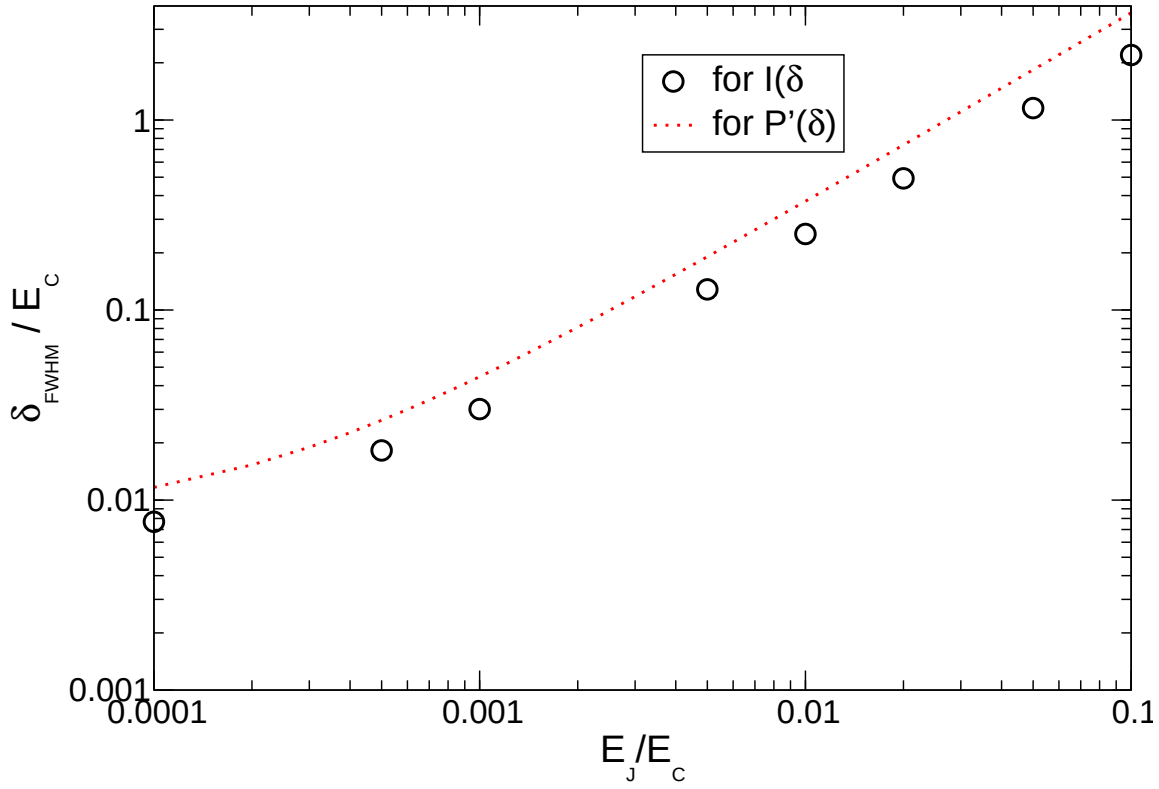

Figure 8.9: Full width at half maximum as a function of the dimensionless Josephson coupling for $a = 1000$ obtained from a Lorentzian fit to the current defined in equation (8.24) which was scaled by the factor $\frac{E_C}{E_J}$ (circles). The peak width increases due to life-time broadening while increasing the ratio of Josephson to charging energy. The dotted line shows the width of $\tilde{P}'(\delta)$ for comparison.

We also verified that for $\frac{E_J}{E_C} \ll 1$ the current is well determined by the function $\tilde{P}'(\delta)$.

Finally, we want to mention, that so far, we only discussed the behaviour of the current with the variation of the parameter a by the impact of the environment (described by the parameter $\frac{1}{g}$) on the system for constant temperature. As $a \sim \frac{g}{T}$ the change in temperature for constant effective impedance causes the same effects.

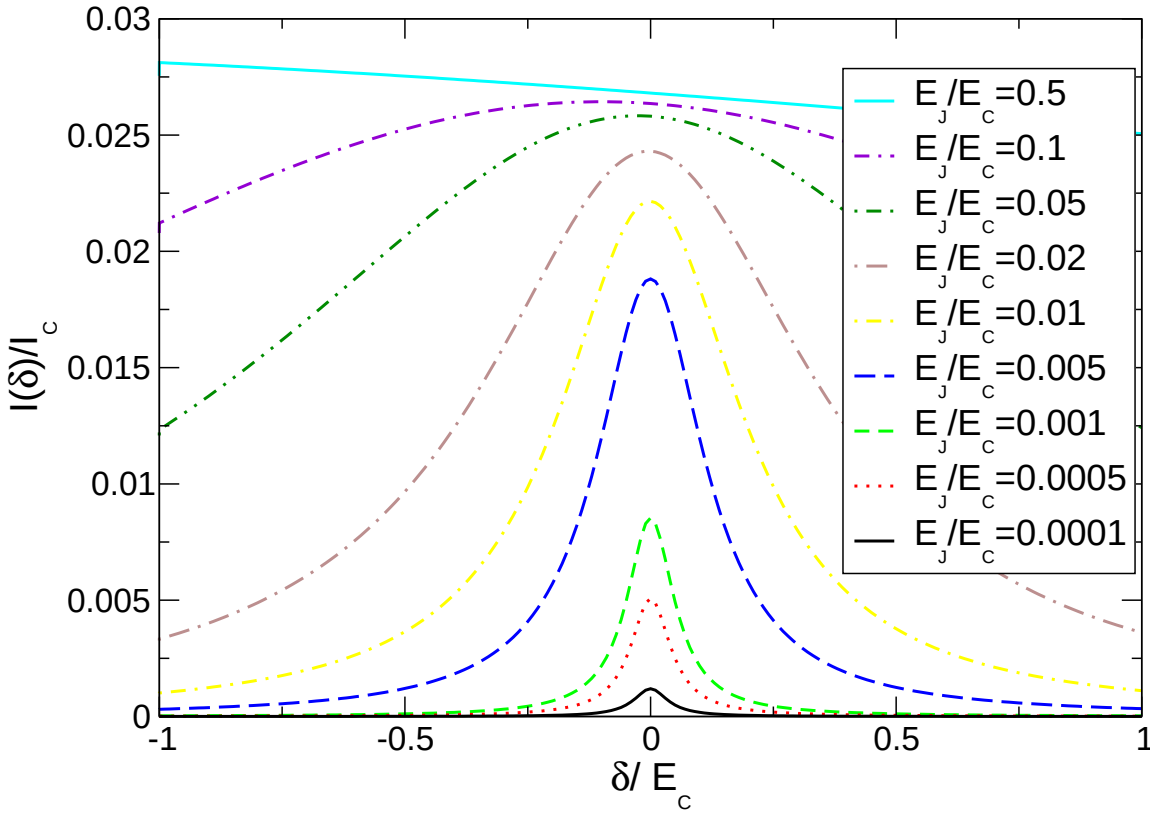

Figure 8.10: Current for the JQP cycle as a function of the energy difference from the Cooper pair resonance for $a = 100$ and different values of the dimensionless Josephson coupling from $\frac{E_J}{E_C} = 0.0001$ to $\frac{E_J}{E_C} = 0.5$ (from bottom to top) determined from equation (8.24). It exhibits life-time broadening like figure 8.8. But here the peak is broader, as we chose a larger effective impedance of the environment, which increases the decoherence broadening.

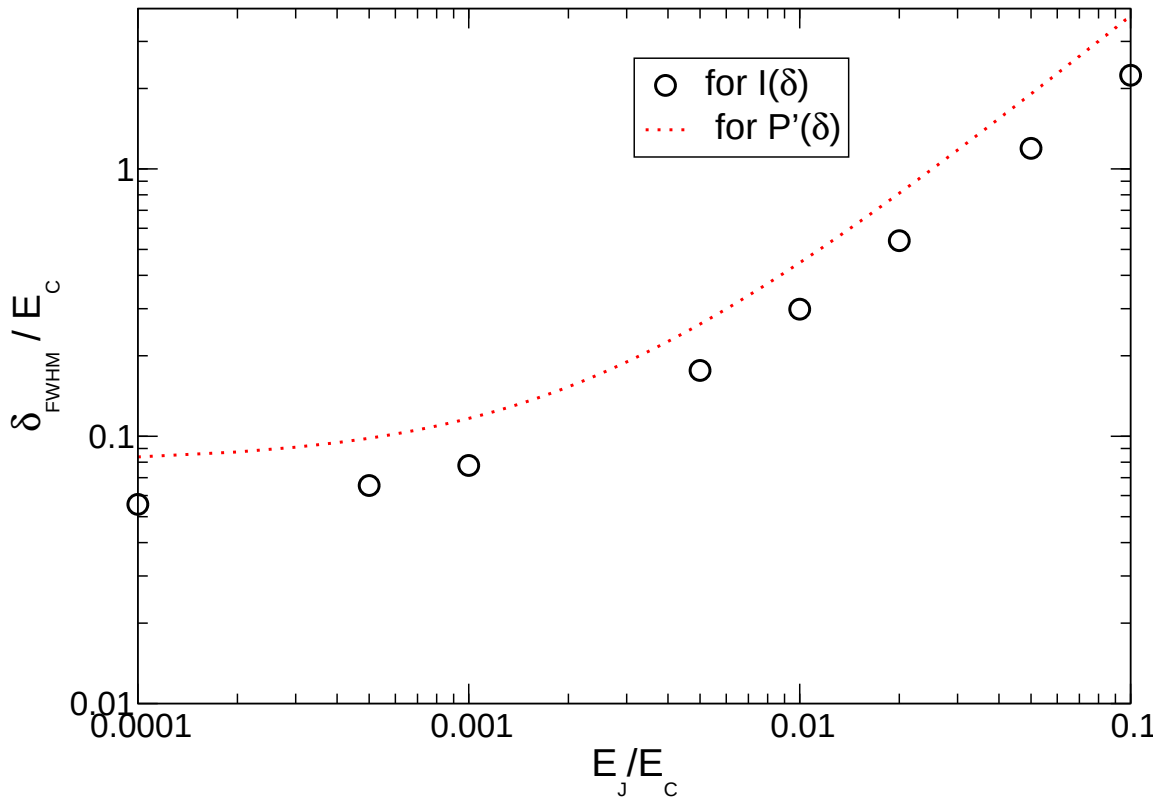

Figure 8.11: Full width at half maximum as a function of the dimensionless Josephson coupling for $a = 100$, extracted from a Lorentzian fir to the current defined by equation (8.24) which was scaled by the factor $\frac{E_C}{E_J}$ (circles). The peak width increases due to life-time broadening while increasing the ratio of Josephson to charging energy. The saturation value for $\frac{E_J}{E_C} \to 0$ is larger than the one shown in figure 8.9 due to the larger effect of the environment. The dotted line shows the width of $\tilde{P}'(\delta)$ for comparison.

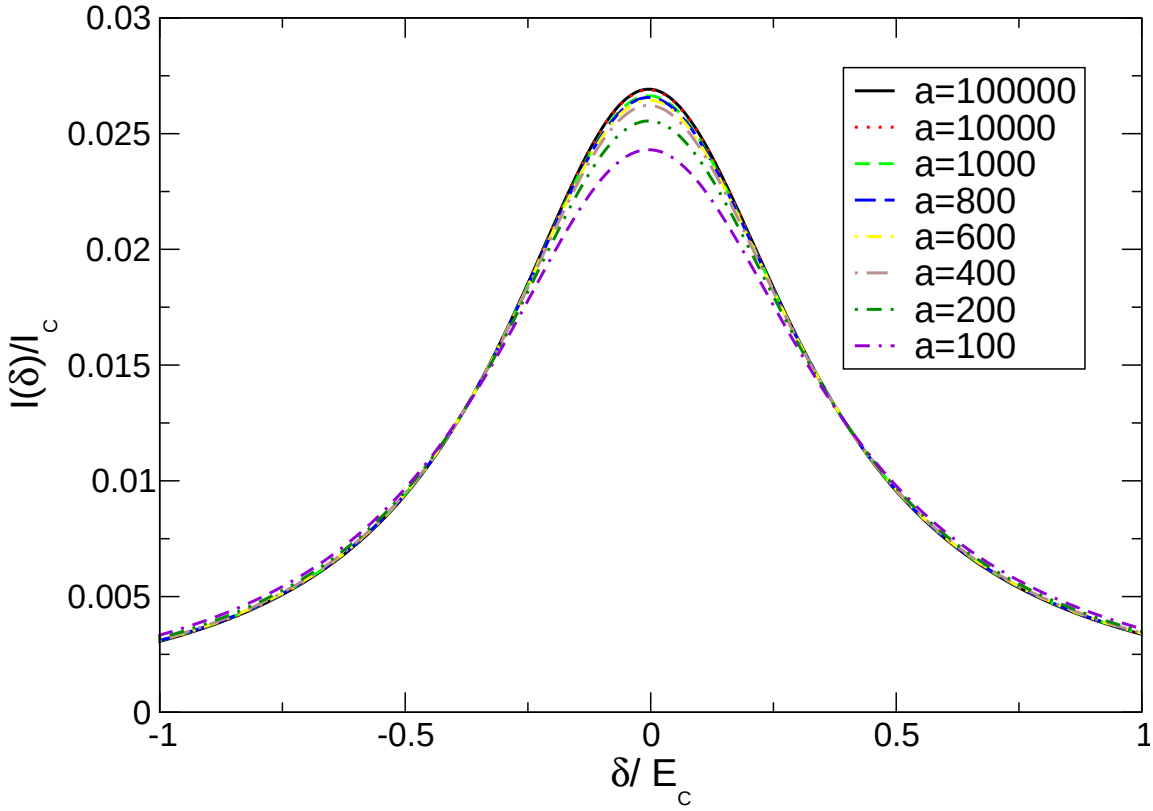

Figure 8.12: Current for the JQP cycle as a function of the energy difference from the Cooper pair resonance for $\frac{E_J}{E_C} = 0.02$ and for different valued of the parameter that describes the influence of the environment from $a = 100$ to $a = 100000$ (from bottom to top). This was calculated, using equation (8.24). The current increases for decreasing the effective impedance of the environment and the peak gets narrower, as the decoherence broadening is reduced. As the Josephson coupling is already quite large, the additional changes for different environments are only small.

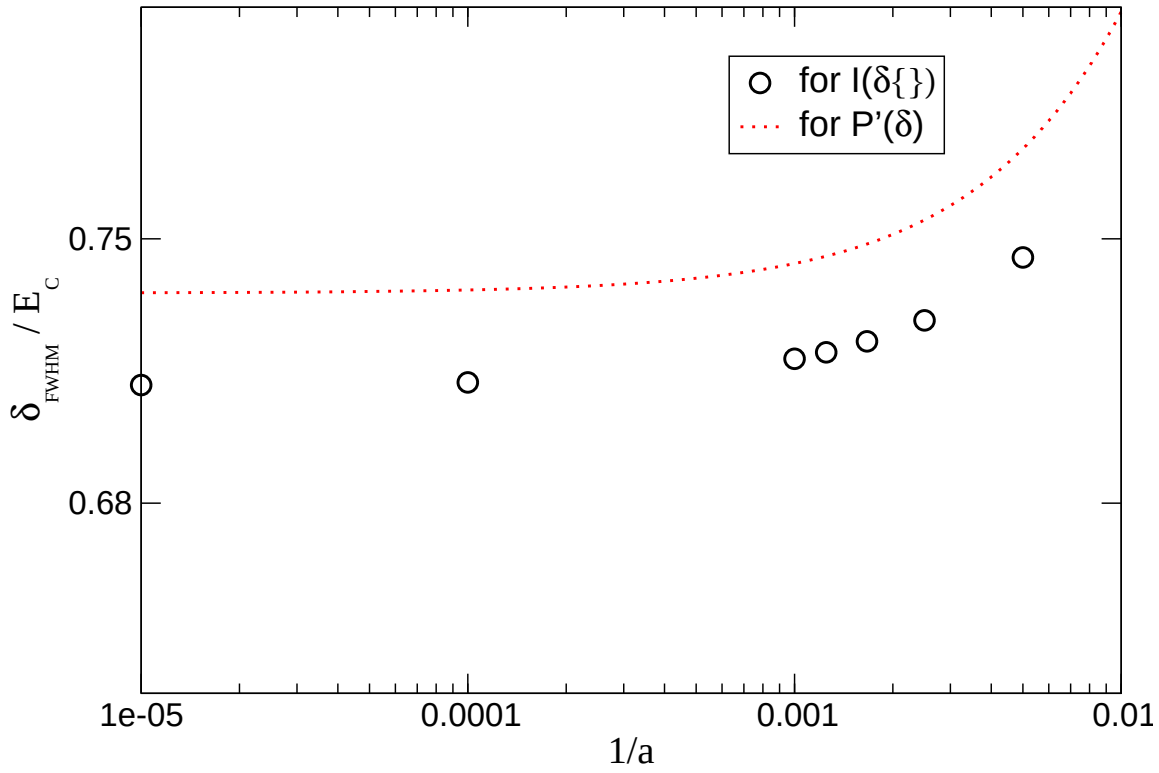

Figure 8.13: Full width at half maximum for $\frac{E_J}{E_C} = 0.02$ as a function of the parameter $\frac{1}{a}$, extracted from a scaled Lorentzian fit to the current defined by equation (8.24) which was scaled by the factor $\frac{E_C}{E_J}$ (circles). The peak width decreases slightly due to decoherence broadening. The saturation value is already large due to the dominant contribution of the life-time broadening. The dotted line shows the width of $\tilde{P}'(\delta)$ for comparison.

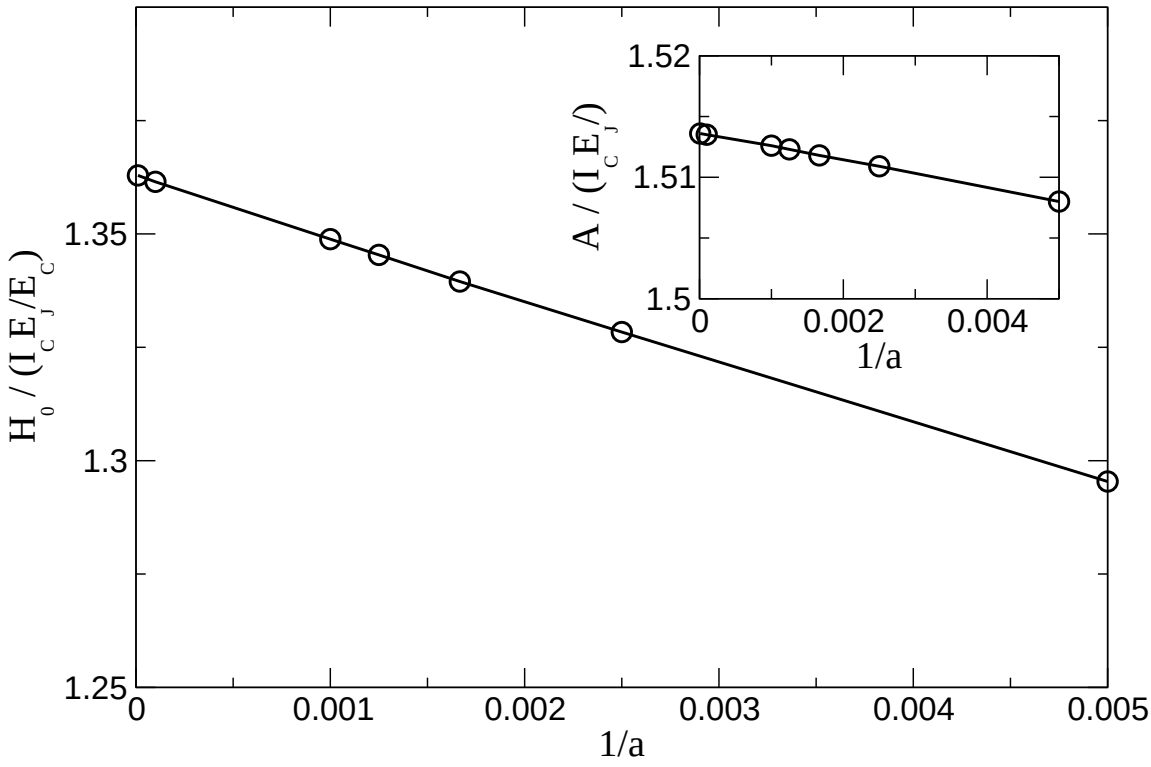

Figure 8.14: Peak Height at $\delta = 0$ for $\frac{E_J}{E_C} = 0.02$ as a function of the parameter $\frac{1}{a}$, extracted from a scaled Lorentzian fit to the current defined by equation (8.24) which was scaled by the factor $\frac{E_C}{E_J}$. The peak height is reduced, if the environment is increased. This is again due to the environment, which increases the decoherence in the system. The inset shows the fitting Parameter A.

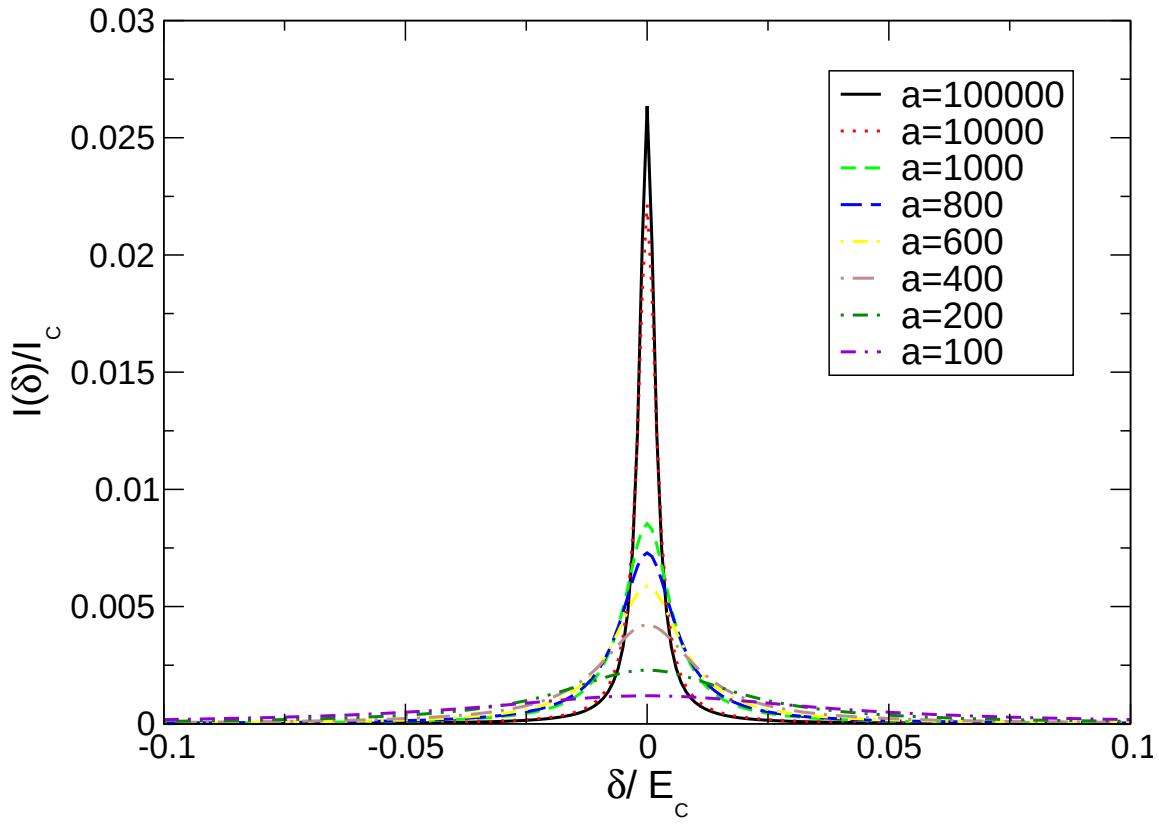

Figure 8.15: Current for the JQP cycle as a function of the energy difference from the Cooper pair resonance for $\frac{E_J}{E_C} = 0.0001$ and for different values of the parameter that describes the influence of the environment from $a = 100$ to $a = 100000$ (from bottom to top).This was calculated, using equation (8.24). Increasing the environment strongly broadens the peak, as the Josephson coupling is so small.

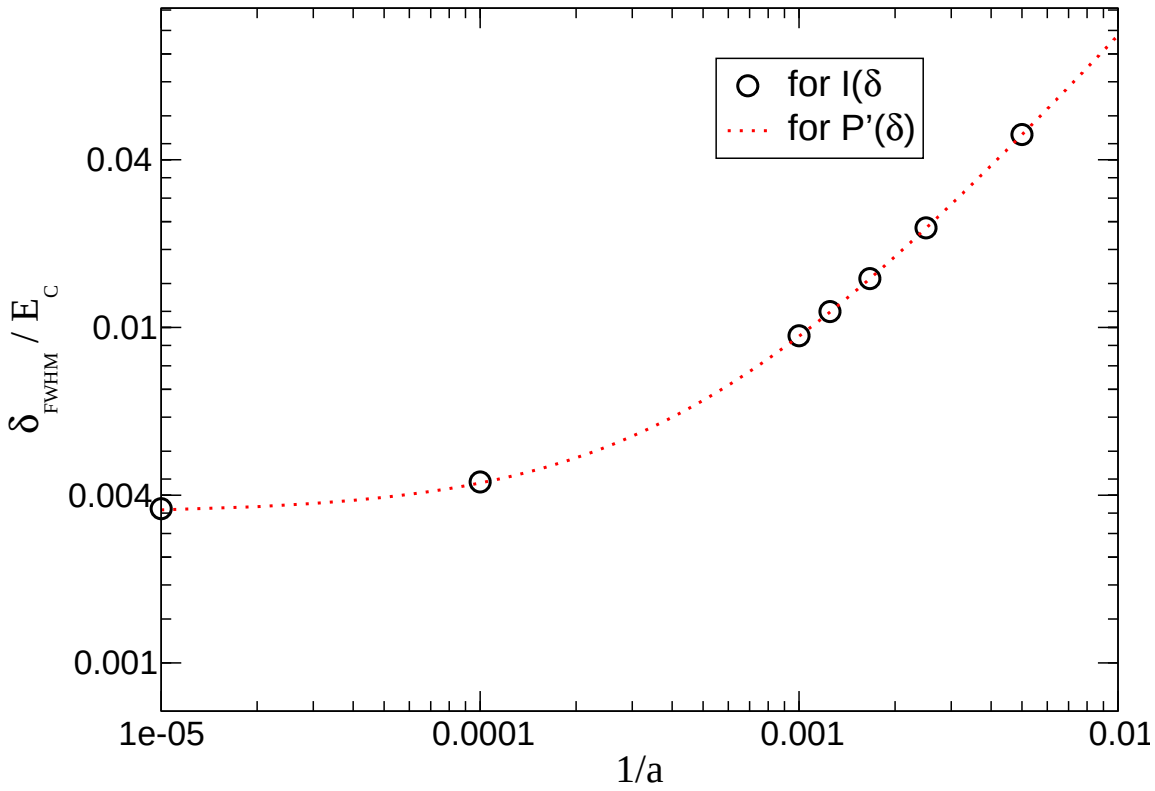

Figure 8.16: Full width at half maximum for $\frac{E_J}{E_C} = 0.0001$ as a function of the parameter $\frac{1}{a}$, extracted from a scaled Lorentzian fit to the current defined by equation (8.24) which was scaled by the factor $\frac{E_C}{E_J}$ (circles). The peak width decreases rapidly with the increase of the effective impedance of the environment. The saturation value is quite small due to the small ratio of Josephson to charging energy. Note the good agreement with the width of $\tilde{P}'(\delta)$ (dotted line).

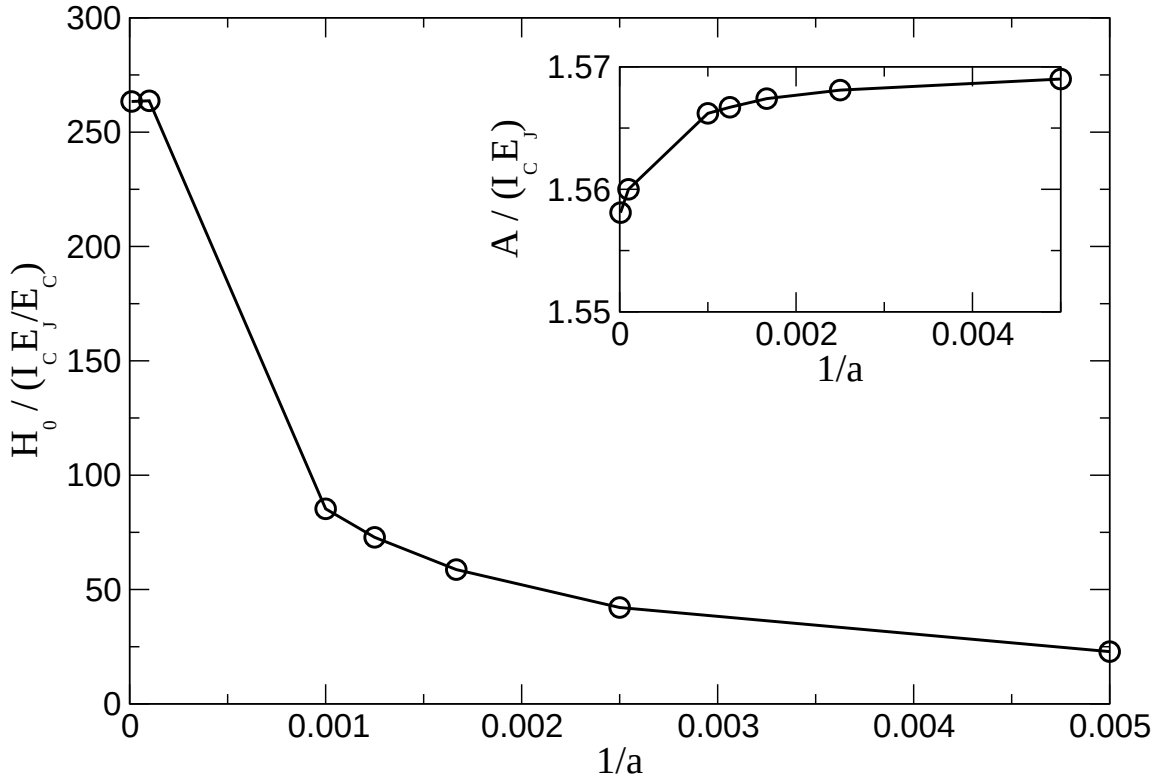

Figure 8.17: Peak height at $\delta = 0$ for $\frac{E_J}{E_C} = 0.0001$ as a function of the parameter $\frac{1}{a}$, extracted from a scaled Lorentzian fit to the current defined by equation (8.24) which was scaled by the factor $\frac{E_C}{E_J}$. The peak height is drastically reduced, as the environment is increased. This is again due to the decoherence broadening, which is the dominant contribution here. The fitting parameter A is shown in the inset.

Chapter 9

Concluding Remarks

We investigated an all superconducting single charge transistor that is coupled to an electromagnetic environment that couples capacitively to the SCT. We calculated the function $P(E)$ for quasi-particles and Cooper pairs for this particular circuit model. We approximated these functions in the semi-classical limit. They depend on the product of the contribution from the effective impedance of the environment and the thermal energy.

We have derived a modification of the master equation by [1] to include the effect of an environment. After solving these set of equations for a stationary current, we have investigated the current for a high bias voltage in a regime where, considering only single particle tunnelling processes, the current is entirely carried by the Josephson quasi-particle cycle. For the semi-classical assumption of a small product of temperature and effective impedance, the current can be calculated analytically. In the limit of small Josephson coupling its behaviour is dominated by the generalised function $\tilde{P}'(\delta)$, which describes the influence of the environment for Cooper pairs in the presence of quasi-particle tunnelling.

The current is largest for a large Josephson coupling and a small impact of the environment (i.e. a small effect of dissipation). We studied the dependence on the dimensionless Josephson coupling and on the environment separately.

We found for the dependence of the current on the dimensionless Josephson coupling for a fixed effective impedance that the width and height of the current are increased for increasing the Josephson coupling. For larger effective impedance the effect is more prominent, as the peak width approximately scales with the lifetime broadening caused by the presence of quasi-particle transitions, which is proportional to the Josephson coupling and it is limited by the decoherence broadening, which is proportional to the effective impedance of the environment.

For the dependence of the current on the effective impedance for fixed dimensionless Josephson coupling, we found that the peak height is increased as the environment is decreased and the width is broadened. This is significantly more prominent for small Josephson couplings, because then the life-time broadening gives only a small contribution to the peak width and height.

The overall shape of the current is basically Lorentzian, with notable deviations due to the energy-dependence of the quasi-particle rates. As mentioned in the introduction, for the JQP process as a sensitive read-out process one has to obtain sharply peaked $I - V$ curves. For the parameters chosen in the analysis we found that one either has to tune into a regime, where the Josephson coupling is small, actually requiring $\frac{E_J}{E_C} \ll 1$. Then one has to chose the effective impedance to be quite small to obtain sharply peaked response curves. As in this regime larger impedances reduce the slope of the current with respect to the applied voltage remarkably. Or one can tune into a regime of larger Josephson coupling (still obeying $\frac{E_J}{E_C} \ll 1$

for justifying our approach which uses perturbation theory in the Josephson coupling). Then the slope of the peak is reasonably steep and changes only slightly for sweeping the effective impedance through the parameter range, we have studied.

For maximally profiting from the high sensitivity of the JQP resonance in an SCT as a read-out process, we determine a lower threshold for the effective impedance of the system of $\mathrm{Re}Z_{\mathrm{eff}} \ll \frac{R_K E_C}{2\pi kT}$ for small Josephson couplings $\frac{E_J}{E_C} \ll 1$.

Instead of decreasing the impedance one can also increase the temperature to obtain the same effect.

This analysis was basically limited by the semi-classical assumption, which allowed us to calculate the current analytically. To extend the analysis to a more general choice of parameters, it is necessary to use numerical methods.

Finally, it would be interesting to compare our results with experiments. Unfortunately, there was no systematic study of the dependence of the width of the JQP current on the effective impedance of the environment, so far. This should be done in the future, as soon as such data will be provided.

Appendix A

Explicit Calculations and Further Details

This appendix shows all the details of the calculations that finally produce the function $P(E)$. Furthermore, the connection between the constants used in the formulas and its expressions in terms of experimental measurable quantities are denoted.

A.1 Effective Impedance $\mathrm{Re}\{Z_{\mathrm{eff}}(\omega)\}$

A.1.1 Choice of the Parameters

For calculations of the effective impedance in numbers, the parameters of the setup of the SET including the environment were chosen as follows

$$R_{\mathrm{2DEG}}^{(L)} = R_{2DEG}^{(R)} = 20\Omega \tag{A.1}$$
$$R_t = 50\mathrm{k}\Omega \tag{A.2}$$
$$C_0 = 350\mathrm{aF} \tag{A.3}$$
$$C_{\mathrm{Lead}} = 3.5\mathrm{fF} \tag{A.4}$$
$$C_t = 120\mathrm{aF} \tag{A.5}$$

This choice of parameters is done to model the set-up of the Rimberg group [9] as well as possible.

A.1.2 Calculation of the Effective Impedance $Z_{\mathrm{eff}}(\omega)$

In the following the resistance seen by the left junction is calculated. From this one can easily get the impedance seen by the right junction by just exchanging indices L and R. For simplicity we assume that both tunnel junctions have the same resistances $R_t = R_L = R_R$ and the same capacitances $C_t = C_L = C_R$.

Junction one sees in parallel:

- its own capacitance $Z_1 = \frac{1}{i\omega C_t}$
- a series connection Z_8 consisting of
  - capacitance C_0 between island and 2DEG: $Z_2 = \frac{1}{i\omega C_0}$

– a parallel connection Z_7 consisting of

  * series connection between the resistance of the 2DEG on the left hand side $R^{(L)}_{\rm 2DEG}$ and the capacitive coupling to the left lead $C_{\rm Lead}$: $Z_3 = R^{(L)}_{\rm 2DEG} + \frac{1}{i\omega C_{\rm Lead}}$
  * series connection Z_6 consisting of
    · series connection between the resistance of the 2DEG on the right hand side $R^{(R)}_{\rm 2DEG}$ and the capacitive coupling to the right lead $C_{\rm Lead}$: $Z_4 = R^{(R)}_{\rm 2DEG} + \frac{1}{i\omega C_{\rm Lead}}$
    · parallel connection between the tunnelling resistance and the capacitance of junction 2: $Z_5 = \frac{R_t}{1+i\omega R_t C_t}$

  $Z_6 = Z_4 + Z_5$

$Z_7 = \frac{Z_3 Z_6}{Z_3+Z_6}$

$Z_8 = Z_7 + Z_2$

Therefore the effective impedance seen by junction one is given by $Z_{\rm eff} = \frac{Z_1 Z_8}{Z_1+Z_8}$.

By inserting all the impedances this becomes a complicated expression

$$Z_{\rm eff}(\omega) = \frac{\frac{1}{i\omega C_t}\left(\frac{\left[R^{(L)}_{\rm 2DEG}+\frac{1}{i\omega C_{\rm Lead}}\right]\left[R^{(R)}_{\rm 2DEG}+\frac{1}{i\omega C_{\rm Lead}}+\frac{R_t}{1+i\omega R_t C_t}\right]}{R^{(L)}_{\rm 2DEG}+\frac{1}{i\omega C_{\rm Lead}}+R^{(R)}_{\rm 2DEG}+\frac{1}{i\omega C_{\rm Lead}}+\frac{R_t}{1+i\omega R_t C_t}} + \frac{1}{i\omega C_0}\right)}{\frac{1}{i\omega C_t} + \frac{1}{i\omega C_0} + \frac{\left[R^{(L)}_{\rm 2DEG}+\frac{1}{i\omega C_{\rm Lead}}\right]\left[R^{(R)}_{\rm 2DEG}+\frac{1}{i\omega C_{\rm Lead}}+\frac{R_t}{1+i\omega R_t C_t}\right]}{R^{(L)}_{\rm 2DEG}+\frac{1}{i\omega C_{\rm Lead}}+R^{(R)}_{\rm 2DEG}+\frac{1}{i\omega C_{\rm Lead}}+\frac{R_t}{1+i\omega R_t C_t}}} \quad . \tag{A.6}$$

For further calculation one only needs the real part of the effective impedance $\mathrm{Re}\{Z_{\rm eff}(\omega)\} = (Z_{\rm eff}(\omega) + Z^*_{\rm eff}(\omega))/2$. This can be written in a simplified form as one can order numerator and denominator by powers of ω and evaluate the corresponding coefficients:

$$\mathrm{Re}\{Z_{\rm eff}(\omega)\} = \frac{C_1 + C_2\omega^2 + C_3\omega^4}{C_4 + C_5\omega^2 + C_6\omega^4 + C_7\omega^6} \quad . \tag{A.7}$$

The coefficients C_i $(i = 1, ..., 7)$ can be calculated from a specific experimental set-up as

$$\begin{aligned}
C_1 &= C_0^2 C_{\rm Lead}^2 (R^{(L)}_{\rm 2DEG} + R^{(R)}_{\rm 2DEG} + R_t) \\
C_2 &= C_0^2 C_{\rm Lead}^4 R^{(L)}_{\rm 2DEG}(R^{(R)}_{\rm 2DEG} + R_t)(R^{(L)}_{\rm 2DEG} + R^{(R)}_{\rm 2DEG} + R_t) \\
C_3 &= C_0^2 C_{\rm Lead}^4 C_t^2 R^{(L)}_{\rm 2DEG} R^{(R)}_{\rm 2DEG} R_t^2 (R^{(L)}_{\rm 2DEG} + R^{(R)}_{\rm 2DEG}) \\
C_4 &= 4C_{\rm Lead}(C_0 + C_t)\{C_0(C_{\rm Lead} + C_t) + C_{\rm Lead}C_t\} + C_0^2 C_t^2 \\
C_5 &= 2C_0 C_{\rm Lead}^2 (4C_0 + 3C_{\rm Lead}) C_t^2 R_t^2 + C_0 C_{\rm Lead}^4 (C_0 + 2C_t) R_t^2 \\
&\quad + C_{\rm Lead}^4 (C_0 + C_t)^2 (R^{(L)}_{\rm 2DEG} + R^{(R)}_{\rm 2DEG})(R^{(L)}_{\rm 2DEG} + R^{(R)}_{\rm 2DEG} + 2R_t) \\
&\quad + C_t^3\{6C_0^2(C_{\rm Lead} + C_t) + 2C_0 C_{\rm Lead}(7C_{\rm Lead} + 2C_t) + C_{\rm Lead}^2(4C_{\rm Lead} + 4C_t + C_{\rm Lead}^2 C_t)\} R_t^2 \\
&\quad + C_0 C_{\rm Lead}^2 C_t\{2C_{\rm Lead}C_t + C_0(2C_{\rm Lead} + C_t)\}((R^{(L)}_{\rm 2DEG})^2 + (R^{(L)}_{\rm 2DEG})^2 + 5R_t^2) \\
C_6 &= C_{\rm Lead}^2 C_t^2\{2C_0 C_{\rm Lead} C_t\{(2C_0 + 2C_{\rm Lead} + C_t)(R^{(L)}_{\rm 2DEG})^2 + 2C_{\rm Lead}^2 R^{(L)}_{\rm 2DEG} R^{(R)}_{\rm 2DEG} \\
&\quad + C_{\rm Lead}(C_0 + C_{\rm Lead} + C_t)(R^{(R)}_{\rm 2DEG})^2\} R_t^2 + C_0^2\{C_t^2((R^{(L)}_{\rm 2DEG})^2 + (R^{(R)}_{\rm 2DEG})^2) R_t^2 \\
&\quad + C_{\rm Lead}^2\{R^{(R)}_{\rm 2DEG}(2R^{(L)}_{\rm 2DEG} + R^{(R)}_{\rm 2DEG}) R_t^2 + (R^{(L)}_{\rm 2DEG})^2((R^{(R)}_{\rm 2DEG})^2 + 2R^{(R)}_{\rm 2DEG} R_t + 4R_t^2)\}\} \\
&\quad C_{\rm Lead}^2 C_t^2 (R^{(L)}_{\rm 2DEG} + R^{(R)}_{\rm 2DEG})^2 R_t^2\} \\
C_7 &= C_0^2 C_{\rm Lead}^2 C_t^4 (R^{(L)}_{\rm 2DEG})^2 (R^{(R)}_{\rm 2DEG})^2 R_t^2 \quad .
\end{aligned} \tag{A.8}$$

For determining the quadratic roots of the denominator of $\mathrm{Re}\{Z_{\mathrm{eff}}(\omega)\}$ one has to solve the equation:

$$C_4 + C_5\omega^2 + C_6(\omega^2)^2 + C_7(\omega^2)^3 = 0 \ , \tag{A.9}$$

which is equivalent to solving the equation

$$z^3 + C_6/C_7 z^2 + C_5/C_7 z + C4/C_7 = 0 \ , \tag{A.10}$$

where we applied the substitution $z = \omega^2$. This is a polynomial of third power in z, therefore it can be solved by applying Cardan's formula with substituting $y = z + C_6/(3C_7)$ leading to the equation

$$y^3 + 3py + 2q = 0 \ , \tag{A.11}$$

with

$$q = \frac{1}{2}\left[\frac{2}{27}\left(\frac{C_6}{C_7}\right)^3 - \frac{1}{3}\frac{C_5C_6}{C_7^2} + \frac{C_4}{C_7}\right] \tag{A.12}$$

$$p = \frac{1}{3}\left[\frac{C_5}{C_7} - \left(\frac{C_6}{C_7}\right)^2\frac{1}{3}\right] \tag{A.13}$$

and the discriminant is given by

$$\begin{aligned} D &= p^3 + q^2 \\ &= \frac{1}{27}\left(\frac{C_5}{C_7}\right)^3 - \frac{1}{108}\frac{(C_5C_6)^2}{C_7^4} + \frac{1}{4}\left(\frac{C_4}{C_7}\right)^2 + \frac{1}{27}\frac{C_4C_6^3}{C_7^4} - \frac{1}{6}\frac{C_4C_5C_6}{C_7^3} \ . \end{aligned} \tag{A.14}$$

As $D < 0$ for an appropriately chosen parameter range, equation (A.11) has the three real solutions

$$\begin{aligned} y_1 &= \sqrt[3]{-q+\sqrt{D}} + \sqrt[3]{-q-\sqrt{D}} \\ y_2 &= \frac{1}{2}(-1+i\sqrt{3})\sqrt[3]{-q+\sqrt{D}} + \frac{1}{2}(-1-i\sqrt{3})\sqrt[3]{-q-\sqrt{D}} \\ y_3 &= \frac{1}{2}(-1-i\sqrt{3})\sqrt[3]{-q+\sqrt{D}} + \frac{1}{2}(-1+i\sqrt{3})\sqrt[3]{-q-\sqrt{D}} \ . \end{aligned} \tag{A.15}$$

Therefore our initial equation (A.10) is solved by setting

$$\begin{aligned} z_1(=\omega_1^2) &= y_1 - \frac{C_6}{3C_7} \\ z_2(=\omega_2^2) &= y_2 - \frac{C_6}{3C_7} \\ z_3(=\omega_3^2) &= y_3 - \frac{C_6}{3C_7} \ . \end{aligned} \tag{A.16}$$

These are the values that were cited in this thesis. For appropriate chosen parameters the z_j's are all negative. Therefore the corresponding frequencies ω_j are imaginary.

To simplify the following calculation of the correlation function (in particular we want to be able to use the residue theorem) $\mathrm{Re}\{Z_{\mathrm{eff}}(\omega)\}$ has to be expanded into partial fractions yielding

$$\mathrm{Re}\{Z_{\mathrm{eff}}(\omega)\} = \sum_{j=1}^{3} \frac{A_j}{\omega^2 - z_j} \,, \tag{A.17}$$

where the quadratic roots of the denominator z_j are given in equation (A.16) and the coefficients A_j are

$$\begin{aligned}
A_1 &= \frac{C_1C_7(z_2-z_3) + C_2C_7[z_1z_2 + (z_2-z_3)z_3] + C_3(z_2-z_3)[(1-C_7)z_1^2 + C_7z_3^2]}{C_7^2(z_1-z_3)(z_2-z_3)^2} \\
A_2 &= \frac{C_3[(-1+C_7)z_1^2 - C_7z_2^2](z_2-z_3) - C_2C_7z_2(z_1+z_2-z_3) + C_1C_7(-z_2+z_3)}{C_7^2(z_1-z_2)(z_2-z_3)^2} \\
A_3 &= \frac{C_1C_2(z_2-z_3) + C_2C_7[z_1z_2 + (z_2-z_3)z_3] + C_3(z_2-z_3)[(1-C_7)z_1^2 + C_7z_3^2]}{C_7^2(z_1-z_3)(z_2-z_3)^2}
\end{aligned} \tag{A.18}$$

However, the other tunnel resistance is part of the quantum system and not of the environment. Thus we consider the limits $R_t \to \infty$ and $\frac{C_{\mathrm{Lead}}}{C_0} \gg 1$, at which $\mathrm{Re}\{Z_{\mathrm{eff}}(\omega)\}$ approaches the resistance of the 2DEG for low frequencies with a soft cut-off at $\omega_C \approx \frac{1}{R_{\mathrm{2DEG}}C_0}$. For the evaluation of the real part of equation (A.6) using these assumptions and considering equal resistances of the 2DEG underneath both junctions ($R^{(L}_{\mathrm{2DEG}}) = R^{(R)}_{\mathrm{2DEG}} = R_{\mathrm{2DEG}}$)) we obtain

$$\mathrm{Re}\{Z_{\mathrm{eff}}(\omega)\} = R_{\mathrm{2DEG}} \frac{1 + 2(C_tR_{\mathrm{2DEG}})^2\omega^2}{1 + 2\frac{C_t}{C_0} + 18\frac{C_t}{C_0}(R_{\mathrm{2DEG}}C_t)^2\omega^2 + (C_tR_{\mathrm{2DEG}})^4\omega^4}, \tag{A.19}$$

A.2 Consistency Check for the Semi-Classical Approximation of $P(E)$

In order to verify the simple approximation of section 6.2 we are going to approximate $P(E)$ for the limit of high temperatures (compared to system energies) and small effective impedances of the environment using an essentially general calculation.

A.2.1 Calculation of the Correlation Function

To be able to use the residue theorem for evaluating the integral for $K(t)$ (equation (5.11)) one has to simplify the integration. Therefore one evaluates the derivative of the correlation function with respect to time t

$$\frac{dK(t)}{dt} = -\frac{1}{R_K}\int_{-\infty}^{\infty} d\omega \mathrm{Re}\{Z_{\mathrm{eff}}(\omega)\}\left[\coth\left(\frac{\hbar\omega}{2kT}\right)\sin(\omega t) + i\cos(\omega t)\right] \tag{A.20}$$

$$= -\sum_{j=1}^{3}\frac{A_j}{R_K}\int_{-\infty}^{\infty} d\omega \frac{1}{\omega^2 - z_j}\left[\coth\left(\frac{\hbar\omega}{2kT}\right)\sin(\omega t) + i\cos(\omega t)\right], \tag{A.21}$$

where we already inserted the real part of the effective impedance (equation (A.17)). One can rewrite equation (A.21) using exponential functions in the complex plane

$$\begin{aligned}\frac{dK(t)}{dt} &= -\sum_{j=1}^{3}\frac{A_j}{R_K}\int_{-\infty}^{\infty}d\omega\frac{1}{\omega^2-z_j}\left[\coth\left(\frac{\hbar\omega}{2kT}\right)\mathrm{Im}\left\{e^{i\omega t}\right\}+i\mathrm{Re}\left\{e^{i\omega t}\right\}\right]\\ &= -\sum_{j=1}^{3}\frac{A_j}{R_K}\mathrm{Im}\int_{-\infty}^{\infty}d\omega\frac{1}{\omega^2-z_j}\coth\left(\frac{\hbar\omega}{2kT}\right)e^{i\omega t}-\sum_{j=1}^{3}\frac{iA_j}{R_K}\mathrm{Re}\int_{-\infty}^{\infty}d\omega\frac{1}{\omega^2-z_j}e^{i\omega t}.\end{aligned} \tag{A.22}$$

We will evaluate the integrals

$$I_1 = \int_{-\infty}^{\infty}d\omega\frac{1}{\omega^2-z_j}\coth\left(\frac{\hbar\omega}{2kT}\right)e^{i\omega t} \tag{A.23}$$

$$I_2 = \int_{-\infty}^{\infty}d\omega\frac{1}{\omega^2-z_j}e^{i\omega t} \tag{A.24}$$

using the residue theorem. The closed integral over the functions $\frac{1}{\omega^2-z_j}\coth\left(\frac{\hbar\omega}{2kT}\right)\exp(i\omega t)$ and $\frac{1}{\omega^2-z_j}\exp(i\omega t)$ amounts to zero for $t>0$ if the contour of integration is along the upper half complex plane and for $t<0$ if it is along the lower half complex plane. Therefore

$$I_1(t) = \pm 2\pi i\sum_i \mathrm{Res}_{\omega_i}\frac{1}{\omega^2-z_j}\coth(\frac{\hbar\omega}{2kT})e^{i\omega t} \tag{A.25}$$

$$I_2(t) = \pm 2\pi i\sum_i \mathrm{Res}_{\omega_i}\frac{1}{\omega^2-z_j}e^{i\omega t}. \tag{A.26}$$

The plus sign is used for the integration along the mathematically positive oriented contour (e.g. for $t>0$) and the minus sign is used for the mathematically negative oriented contour (e.g. for $t<0$). There are poles for the function $\frac{1}{\omega^2-z_j}$ at $\omega=\pm\sqrt{z_j}=\pm i\sqrt{|z_j|}$, therefore

$$\mathrm{Res}_{\pm z_j}\frac{1}{\omega^2-z_j}=\lim_{\omega\to\pm\sqrt{z_j}}\frac{\omega\mp\sqrt{z_j}}{(\omega+\sqrt{z_j})(\omega-\sqrt{z_j})}=\pm\frac{1}{2\sqrt{z_j}}=\mp\frac{i}{2\sqrt{|z_j|}}. \tag{A.27}$$

For the function $\coth\left(\frac{\hbar\omega}{2kT}\right)$ there are poles at $\omega=i\omega_n=\frac{i\pi 2kT}{\hbar}n$, $n\epsilon\mathbb{Z}$ and one directly calculates the residue to

$$\mathrm{Res}_{\omega_n}\coth\left(\frac{\hbar\omega}{2kT}\right)=Res_0\left(\frac{2kT}{\hbar}\frac{1}{\omega}+\frac{\hbar\omega}{kT}\sum_{k=1}^{\infty}\frac{1}{\pi^2k^2+\left(\frac{\hbar\omega}{2kT}\right)^2}\right)=\frac{2kT}{\hbar}, \tag{A.28}$$

where we used the $\frac{i\pi 2kT}{\hbar}$ periodicity and the series representation

$$\coth(z) = 2z \sum_{k=1}^{\infty} \frac{1}{\pi^2 k^2 + z^2} + \frac{1}{z} \tag{A.29}$$

of the coth-function. One has to keep in mind for the following calculation that the pole at the real axis (at $\omega = 0$) only counts half of its value. Therefore for $t > 0$

$$\begin{aligned} I_1(t>0) &= 2\pi i \left(\mathrm{Res}_{i\sqrt{|z_j|}} + \sum_{n\epsilon\mathbb{N}} \mathrm{Res}_{i\omega_n} + \frac{1}{2}\mathrm{Res}_0 \right) \frac{1}{\omega^2 - z_j} \coth(\frac{\hbar\omega}{2kT}) e^{i\omega t} \qquad \text{(A.30)} \\ &= 2\pi i \left(-\frac{i}{2\sqrt{|z_j|}} \coth\left(\frac{i\hbar\sqrt{|z_j|}}{2kT} \right) e^{-\sqrt{|z_j|}t} - \frac{2kT}{\hbar} \sum_{n\epsilon\mathbb{N}} \frac{e^{-\omega_n t}}{\omega_n^2 + z_j} - \frac{1}{2z_j}\frac{2kT}{\hbar} \right) \\ I_2(t>0) &= 2\pi i \mathrm{Res}_{i\sqrt{|z_j|}} \frac{1}{\omega^2 - z_j} e^{i\omega t} \\ &= \frac{\pi}{\sqrt{|z_j|}} e^{-\sqrt{|z_j|}t} , \qquad \text{(A.31)} \end{aligned}$$

by using the expansion of the coth function into partial fractions (equation (A.29)), equation (A.30) can be rewritten as

$$I_1(t>0) = i\frac{4\pi kT}{\hbar} \left(\sum_{\omega_n} \frac{e^{-\sqrt{|z_j|}t} - e^{-\omega_n t}}{\omega_n^2 - |z_j|} + \frac{1 - e^{-\sqrt{|z_j|}t}}{2|z_j|} \right). \tag{A.32}$$

Finally, the derivative of the correlation function becomes for $t > 0$

$$\frac{dK_{t>0}(t)}{dt} = -\sum_{j=1}^{3} \frac{A_j}{R_k} \left\{ \frac{4\pi kT}{\hbar} \left(\sum_{\omega_n} \frac{e^{-\sqrt{|z_j|}t} - e^{-\omega_n t}}{\omega_n^2 - |z_j|} + \frac{1 - e^{-\sqrt{|z_j|}t}}{2|z_j|} \right) + \frac{i\pi}{\sqrt{|z_j|}} e^{-\sqrt{|z_j|}t} \right\} \tag{A.33}$$

For $t < 0$ the calculation is analogous:

$$\begin{aligned} I_1(t<0) &= -2\pi i \left(\mathrm{Res}_{-i\sqrt{|z_j|}} + \sum_{n\epsilon\mathbb{N}} \mathrm{Res}_{-i\omega_n} + \frac{1}{2}\mathrm{Res}_0 \right) \frac{1}{\omega^2 - z_j} \coth(\frac{\hbar\omega}{2kT}) e^{i\omega t} \qquad \text{(A.34)} \\ &= -2\pi i \left(\frac{i}{2\sqrt{|z_j|}} \coth\left(-\frac{i\hbar\sqrt{|z_j|}}{2kT} \right) e^{\sqrt{|z_j|}t} - \frac{2kT}{\hbar} \sum_{n\epsilon\mathbb{N}} \frac{e^{\omega_n t}}{\omega_n^2 + z_j} - \frac{1}{2z_j}\frac{2kT}{\hbar} \right) \\ I_2(t<0) &= -2\pi i \mathrm{Res}_{-i\sqrt{|z_j|}} \frac{1}{\omega^2 - z_j} e^{i\omega t} \\ &= \frac{\pi}{\sqrt{|z_j|}} e^{\sqrt{|z_j|}t} , \qquad \text{(A.35)} \end{aligned}$$

by using again the property A.29, equation (A.34) can be rewritten as

$$I_1(t<0) = -i\frac{4\pi kT}{\hbar} \left(\sum_{\omega_n} \frac{e^{\sqrt{|z_j|}t} - e^{\omega_n t}}{\omega_n^2 - |z_j|} + \frac{1 - e^{\sqrt{|z_j|}t}}{2|z_j|} \right). \tag{A.36}$$

Finally, the derivative of the correlation function becomes for $t < 0$

$$\frac{dK_{t<0}(t)}{dt} = -\sum_{j=1}^{3} \frac{A_j}{R_k} \left\{ \frac{4\pi kT}{\hbar} \left(\sum_{\omega_n} \frac{e^{\omega_n t} - e^{\sqrt{|z_j|}t}}{\omega_n^2 - |z_j|} + \frac{e^{\sqrt{|z_j|}t} - 1}{2|z_j|} \right) + \frac{i\pi}{\sqrt{|z_j|}} e^{\sqrt{|z_j|}t} \right\}. \quad \text{(A.37)}$$

The functions are continuous for $t \to 0$ with

$$\lim_{t\to 0} \frac{dK_{t>0}(t)}{dt} = \lim_{t\to 0} \frac{dK_{t<0}(t)}{dt} = -\sum_{j=1}^{3} \frac{A_j}{R_k} \frac{i\pi}{\sqrt{|z_j|}} \quad \text{(A.38)}$$

therefore one can generalise equations (A.33) and (A.37) for all times t to

$$\frac{dK(t)}{dt} = -\sum_{j=1}^{3} \frac{A_j}{R_k} \left\{ \frac{4\pi kT}{\hbar} \text{sign}(t) \left(\sum_{\omega_n} \frac{e^{-\sqrt{|z_j|}|t|} - e^{-\omega_n|t|}}{\omega_n^2 - |z_j|} + \frac{1 - e^{-\sqrt{|z_j|}|t|}}{2|z_j|} \right) + \frac{i\pi}{\sqrt{|z_j|}} e^{-\sqrt{|z_j|}|t|} \right\} \quad \text{(A.39)}$$

This can be straightforwardly integrated to calculate the correlation function. By using $K(t = 0) = 0$, one can substitute the constant of integration. Therefore

$$\begin{aligned} K(t) = & - \sum_{j=1}^{3} \frac{A_j}{R_k} \left\{ \frac{4\pi kT}{\hbar} \left[\sum_{\omega_n} \frac{1}{\omega_n^2 - |z_j|} \left(\frac{e^{-\omega_n|t|} - 1}{\omega_n} - \frac{e^{-\sqrt{|z_j|}|t|} - 1}{\sqrt{|z_j|}} \right) + \frac{e^{-\sqrt{|z_j|}|t|} - 1}{2|z_j|^{3/2}} + \frac{|t|}{2|z_j|} \right] \right. \\ & \left. - \frac{i\pi}{|z_j|} \left[e^{-\sqrt{|z_j|}|t|} - 1 \right] \text{sign}(t) \right\}. \end{aligned} \quad \text{(A.40)}$$

with $\omega_n = \frac{2\pi kT}{\hbar} n$, $n \epsilon \mathbb{N}$, the Bose-Matsubara frequencies.

A.2.2 Calculation of $P(E)$

The analytic calculation of $P(E)$ with this quite general $K(t)$ is not possible. Therefore one has to approximate $K(t)$ for long and short times and integrate over the respective times separately to get $P(E)$. A natural time scale is given by the inverse cutoff frequencies $\sqrt{|z_j|}$, which have been calculated in Appendix **??** for the particular circuit model considered in this thesis. The three cutoff-frequencies are different, which has to be taken into account by the evaluation of the integral for $P(E)$.

Approximation of the Correlation Function for long and short times

In this section we will approximate the correlation function for long and short time scales compared to the inverse cut-off frequencies.

Firstly, we can rewrite $K(t)$

$$\begin{aligned} K(t) = & -\sum_{j=1}^{3} \frac{A_j}{R_k} \frac{2\pi k}{\hbar |z_j|} \left[T|t| + \left(e^{-\sqrt{|z_j|}|t|} - 1 \right) \left(\frac{T}{\sqrt{|z_j|}} - \text{sign}(t) \frac{i\hbar}{2k} \right) \right. \\ & \left. - 2T \sum_{\omega_n} \frac{(e^{-\omega_n|t|} - 1)\frac{1}{\omega_n} - (e^{-\sqrt{|z_j|}|t|} - 1)\frac{1}{\sqrt{|z_j|}}}{1 - \frac{\omega_n^2}{|z_j|}} \right]. \end{aligned} \quad \text{(A.41)}$$

To obtain the short time behaviour for $|t| \ll \frac{1}{\sqrt{|z_j|}}$ of the correlation function $K_S(t)$ one expands the exponential function up to first order in $\sqrt{|z_j|}|t|$: $e^{-\sqrt{|z_j|}|t|} \approx 1 - \sqrt{|z_j|}|t|$. Applying this to equation (A.41) yields

$$\begin{aligned} K_S(t) &= -\sum_{j=1}^{3} \frac{A_j}{R_k} \frac{2\pi k}{\hbar |z_j|} \left[T|t| - \sqrt{|z_j|}|t| \left(\frac{T}{\sqrt{|z_j|}} - \mathrm{sign}(t) \frac{i\hbar}{2k} \right) - 2T \sum_{\omega_n} \frac{(e^{-\omega_n|t|} - 1)\frac{1}{\omega_n} + |t|}{1 - \frac{\omega_n^2}{|z_j|}} \right] \\ &= -\sum_{j=1}^{3} \frac{A_j}{R_k} \frac{2\pi k}{\hbar |z_j|} \left[\sqrt{|z_j|}|t| \mathrm{sign}(t) \frac{i\hbar}{2k} - 2T \sum_{\omega_n} \frac{(e^{-\omega_n|t|} - 1)\frac{1}{\omega_n} + |t|}{1 - \frac{\omega_n^2}{|z_j|}} \right] . \end{aligned} \tag{A.42}$$

Now we want to consider the term $\sum_{\omega_n} \frac{e^{-\omega_n|t|}}{\omega_n \left(1 - \frac{\omega_n^2}{|z_j|}\right)}$, which contributes for large enough values of $e^{-\omega_n|t|}$ only, therefore we can assume $\omega_n|t| \ll 1$. Then we can again expand the exponential function up to first order in $\omega_n|t|$: $e^{-\omega_n|t|} \approx 1 - \omega_n|t|$. Therefore

$$\sum_{\omega_n} \frac{(e^{-\omega_n|t|} - 1)\frac{1}{\omega_n} + |t|}{1 - \frac{\omega_n^2}{\sqrt{|z_j|}}} \approx \sum_{\omega_n} \frac{\frac{-\omega_n|t|}{\omega_n} + |t|}{1 - \frac{\omega_n^2}{\sqrt{|z_j|}}} = 0 . \tag{A.43}$$

So the short time limit of the correlation function becomes

$$K_S(t) = -\sum_{j=1}^{3} \frac{i\pi A_j}{|z_j| R_k} \mathrm{sign}(t)|t| = -\sum_{j=1}^{3} \frac{i\pi A_j}{|z_j| R_k} t . \tag{A.44}$$

In the long time limit one assumes the times to be much larger than the inverse cut-off frequencies, e.g. $|t| \gg \frac{1}{\sqrt{|z_j|}}$, therefore $e^{-\sqrt{|z_j|}|t|} \approx 0$. Therefore

$$K_L(t) = -\sum_{j=1}^{3} \frac{A_j}{R_k} \frac{2\pi k}{\hbar |z_j|} \left[T|t| - \frac{T}{\sqrt{|z_j|}} + \mathrm{sign}(t) \frac{i\hbar}{2k} - 2T \sum_{\omega_n} \frac{(e^{-\omega_n|t|} - 1)\frac{1}{\omega_n} + \frac{1}{\sqrt{|z_j|}}}{1 - \frac{\omega_n^2}{|z_j|}} \right] . \tag{A.45}$$

Again, the term $\sum_{\omega_n} \frac{e^{-\omega_n|t|}}{\omega_n \left(1 - \frac{\omega_n^2}{|z_j|}\right)}$ contributes only for $\omega_n|t| \ll 1$. But then $\frac{\omega_n}{\sqrt{|z_j|}} \ll 1$, and we can neglect the quadratic term in $\frac{\omega_n}{\sqrt{|z_j|}}$ in the denominator

$$\sum_{\omega_n} \frac{e^{-\omega_n|t|}}{\omega_n \left(1 - \frac{\omega_n^2}{|z_j|}\right)} \approx \sum_{\omega_n} \frac{e^{-\omega_n|t|}}{\omega_n} \tag{A.46}$$

and calculate (for $t > 0$)

$$\begin{aligned} \sum_{\omega_n} \frac{e^{-\omega_n t}}{\omega_n} &= -\int dt \sum_{\omega_n} e^{-\omega_n t} = -\int dt \sum_{n=1}^{\infty} \left(e^{-\omega_1 t}\right)^n = -\int dt \left(\sum_{n=0}^{\infty} \left(e^{-\omega_1 t}\right)^n - 1 \right) \\ &= -\int dt \left(\frac{1}{1 - e^{-\omega_1 t}} - 1 \right) = -\int dt \frac{1}{e^{\omega_1 t} - 1} = -\frac{1}{\omega_1} \ln\left[1 - e^{-\omega_1 t}\right] , \end{aligned} \tag{A.47}$$

where we used the formula for a geometrical series $\sum_{n=0}^{\infty}\left(e^{-\omega_1|t|}\right)^n = \frac{1}{1-e^{-\omega_1|t|}}$. Then

$$K_L(t) = -\sum_{j=1}^{3}\frac{A_j}{R_k}\frac{2\pi kT}{\hbar|z_j|}\left[|t| - \frac{1}{\sqrt{|z_j|}} + \mathrm{sign}(t)\frac{i\hbar}{2kT} + \frac{2}{\omega_1}\ln\left(1-e^{-\omega_1|t|}\right) + 2\sum_{\omega_n}\frac{\frac{1}{\omega_n} - \frac{1}{\sqrt{|z_j|}}}{1-\frac{\omega_n^2}{|z_j|}}\right] . \tag{A.48}$$

Now one can still rewrite the remaining sum. Therefore we introduce the digamma function $\Psi(z)$ which has the series representation

$$\Psi(1+z) = -\gamma + \sum_{n=1}^{\infty}\frac{z}{n(n+z)} , \tag{A.49}$$

which is valid for $z\epsilon\{\mathbb{C}\setminus(-\mathbb{N})\}$ and the reflection property

$$\Psi(1-z) = \Psi(z) + \pi\cot(\pi z) . \tag{A.50}$$

Using equation (A.49) we can replace the first part of the summation by

$$\sum_{n=1}^{\infty}\frac{1}{\omega_n\left(1-\frac{\omega_n^2}{|z_j|}\right)} = \frac{1}{\omega_1}\left[\frac{1}{2}\Psi\left(1+\frac{\sqrt{|z_j|}}{\omega_1}\right) + \frac{1}{2}\Psi\left(1-\frac{\sqrt{|z_j|}}{\omega_1}\right) + \gamma\right] . \tag{A.51}$$

Applying the series representation of the cotangent function

$$\cot(z) = \frac{1}{z} + 2z\sum_{k=1}^{\infty}\frac{1}{z^2-k^2\pi^2} , \tag{A.52}$$

which is valid for $z\epsilon\{(\mathbb{C}\setminus\mathbb{Z})\pi\}$.
One can replace the second part of the summation of equation (A.48) by

$$\sum_{n=1}^{\infty}\frac{1}{\sqrt{|z_j|}\left(1-\frac{\omega_n^2}{|z_j|}\right)} = \frac{\pi}{2\omega_1}\left[\cot\left(\frac{\pi\sqrt{|z_j|}}{\omega_1}\right) - \frac{\omega_1}{\pi\sqrt{|z_j|}}\right] . \tag{A.53}$$

Now combining both the results of equations (A.51) and (A.53) and using equation (A.50) the summation becomes

$$\begin{aligned}\sum_{n=1}^{\infty}\frac{\frac{1}{\omega_n} - \frac{1}{\sqrt{|z_j|}}}{1-\frac{\omega_n^2}{|z_j|}} &= \frac{1}{\omega_1}\left[\frac{1}{2}\Psi\left(1+\frac{\sqrt{|z_j|}}{\omega_1}\right) + \frac{1}{2}\Psi\left(1-\frac{\sqrt{|z_j|}}{\omega_1}\right) + \gamma - \frac{\pi}{2}\cot\left(\frac{\pi\sqrt{|z_j|}}{\omega_1}\right) + \frac{1}{2\sqrt{|z_j|}}\right] \\ &= \frac{1}{\omega_1}\left[\frac{1}{2}\Psi\left(1+\frac{\sqrt{|z_j|}}{\omega_1}\right) + \frac{1}{2}\Psi\left(\frac{\sqrt{|z_j|}}{\omega_1}\right) + \gamma + \frac{1}{2\sqrt{|z_j|}}\right] .\end{aligned} \tag{A.54}$$

So the long-time limit of the correlation function becomes

$$\begin{aligned} K_L(t) &= -\sum_{j=1}^{3} \frac{A_j}{R_k} \frac{2\pi kT}{\hbar |z_j|} \left\{ |t| + \frac{2}{\omega_1} \left[\ln\left(1 - e^{-\omega_1 |t|}\right) + \frac{1}{2}\Psi\left(1 + \frac{\sqrt{|z_j|}}{\omega_1}\right) + \frac{1}{2}\Psi\left(\frac{\sqrt{|z_j|}}{\omega_1}\right) + \gamma \right] \right. \\ &+ \left. \frac{i\hbar}{kT}\mathrm{sign}(t) \right\} \\ &= -\sum_{j=1}^{3} \frac{A_j}{R_k |z_j|} \left\{ \omega_1 |t| + 2 \left[\ln\left(1 - e^{-\omega_1 |t|}\right) + \frac{1}{2}\Psi\left(1 + \frac{\sqrt{|z_j|}}{\omega_1}\right) + \frac{1}{2}\Psi\left(\frac{\sqrt{|z_j|}}{\omega_1}\right) + \gamma \right] \right. \\ &+ \left. i\pi\,\mathrm{sign}(t) \right\} \ . \end{aligned} \tag{A.55}$$

Calculation of $P(E)$

Now we can calculate the function $P(E)$

$$\begin{aligned} P(E) &= \frac{1}{2\pi\hbar} \int_{-\infty}^{\infty} dt \exp\left(K(t) + \frac{iEt}{\hbar} \right) \\ &= \frac{1}{2\pi\hbar} \left[\int_{-\infty}^{-\max\left\{\frac{1}{\sqrt{|z_j|}}\right\}} dt \exp\left(K_L(t) + \frac{iEt}{\hbar} \right) + \int_{-\min\left\{\frac{1}{\sqrt{|z_j|}}\right\}}^{\min\left\{\frac{1}{\sqrt{|z_j|}}\right\}} dt \exp\left(K_S(t) + \frac{iEt}{\hbar} \right) \right. \\ &+ \left. \int_{\max\left\{\frac{1}{\sqrt{|z_j|}}\right\}}^{\infty} dt \exp\left(K_L(t) + \frac{iEt}{\hbar} \right) + \delta\left(\max\left\{ \frac{1}{\sqrt{|z_j|}} \right\} - \min\left\{ \frac{1}{\sqrt{|z_j|}} \right\} \right) \right] . \end{aligned} \tag{A.56}$$

If one assumes the cut-off frequencies $\sqrt{|z_j|}$ to be at the same order of magnitude, the last constant, which can be approximated by

$$\begin{aligned} & \delta \left(\max\left\{ \frac{1}{\sqrt{|z_j|}} \right\} - \min\left\{ \frac{1}{\sqrt{|z_j|}} \right\} \right) \\ \approx & \int_{-\max\left\{\frac{1}{\sqrt{|z_j|}}\right\}}^{-\min\left\{\frac{1}{\sqrt{|z_j|}}\right\}} dt \exp\left(K(t) + \frac{iEt}{\hbar} \right) + \int_{\min\left\{\frac{1}{\sqrt{|z_j|}}\right\}}^{\max\left\{\frac{1}{\sqrt{|z_j|}}\right\}} dt \exp\left(K(t) + \frac{iEt}{\hbar} \right) \end{aligned} \tag{A.57}$$

can be neglected. Define the short hand notation

$$\frac{1}{\sqrt{|z_{min}|}} = \max\left\{\frac{1}{\sqrt{|z_j|}}\right\} \text{ and } \frac{1}{\sqrt{|z_{max}|}} = \min\left\{\frac{1}{\sqrt{|z_j|}}\right\} \tag{A.58}$$

and the ratio of the quantum to the system impedance by

$$g_j = \frac{R_k|z_j|}{A_j} \tag{A.59}$$

$$\text{and for later purposes } \frac{1}{g} = \sum_{j=1}^{3}\frac{1}{g_j}\,. \tag{A.60}$$

Then we can solve the integration

$$\begin{aligned}\int_{-\infty}^{-\frac{1}{\sqrt{|z_{min}|}}} dt \exp\left[K_L(t) + \frac{iEt}{\hbar}\right] &= \exp\left[-\sum_{j=1}^{3}\frac{1}{g_j}\left(2\gamma + \Psi\left(1+\frac{\sqrt{|z_j|}}{\omega_1}\right) + \Psi\left(\frac{\sqrt{|z_j|}}{\omega_1}\right) - i\pi\right)\right] * \\ &\int_{-\infty}^{-\frac{1}{\sqrt{|z_{min}|}}} dt \exp\left[-\sum_{j=1}^{3}\frac{1}{g_j}\left(2\ln\left(1-e^{\omega_1 t}\right) - \omega_1 t\right)\right]\exp\left[\frac{iEt}{\hbar}\right].\end{aligned} \tag{A.61}$$

Consider the integral on the right hand side

$$\begin{aligned}&\int_{-\infty}^{-\frac{1}{\sqrt{|z_{min}|}}} dt \exp\left[-\sum_{j=1}^{3}\frac{1}{g_j}\left(2\ln\left(1-e^{\omega_1 t}\right) - \omega_1 t\right)\right]\exp\left[\frac{iEt}{\hbar}\right] = \\ &= \int_{-\infty}^{-\frac{1}{\sqrt{|z_{min}|}}} dt \left[1-e^{\omega_1 t}\right]^{-\sum_{j=1}^{3}\frac{2}{g_j}} \exp\left[t\left(\frac{iE}{\hbar} + \omega_1\sum_j\frac{1}{g_j}\right)\right].\end{aligned} \tag{A.62}$$

Now one can solve this integration by reducing it to a hyper-geometric function of the form

$$F(a,b,c,z) = \frac{\Gamma(c)}{\Gamma(b)\Gamma(c-b)}\int_0^1 dt t^{b-1}(1-tz)^{-a}(1-t)^{c-b-1} \tag{A.63}$$

by substituting $\xi = \frac{e^{\omega_1 t}}{e^{-\frac{\omega_1}{\sqrt{|z_{min}|}}}} = e^{\omega_1 t + \frac{\omega_1}{\sqrt{|z_{min}|}}}$. Therefore

$$\begin{aligned}&\int_{-\infty}^{-\frac{1}{\sqrt{|z_{min}|}}} dt \left[1-e^{\omega_1 t}\right]^{-\sum_{j=1}^{3}\frac{2}{g_j}} \exp\left[t\left(\frac{iE}{\hbar} + \omega_1\sum_j\frac{1}{g_j}\right)\right] = \\ &= \frac{\exp\left[-\frac{\omega_1}{\sqrt{|z_{min}|}}\left(\frac{1}{g}+\frac{iE}{\hbar\omega_1}\right)\right]}{\omega_1\left(\frac{1}{g}+\frac{iE}{\hbar\omega_1}\right)} F\left(\frac{2}{g}, \frac{1}{g}+\frac{iE}{\hbar\omega_1}, 1+\frac{1}{g}+\frac{iE}{\hbar\omega_1}, e^{-\frac{\omega_1}{\sqrt{|z_{min}|}}}\right).\end{aligned} \tag{A.64}$$

The contribution of the long time limit for positive times can be calculated in analogy but with the substitution $\xi = \frac{e^{-\omega_1 t}}{e^{-\frac{\omega_1}{\sqrt{|z_{min}|}}}} = e^{-\omega_1 t + \frac{\omega_1}{\sqrt{|z_{min}|}}}$, thus

$$\int\limits_{\frac{1}{\sqrt{|z_{min}|}}}^{\infty} dt \exp\left[K_L(t) + \frac{iEt}{\hbar}\right] = \exp\left[-\sum_{j=1}^{3}\frac{1}{g_j}\left(2\gamma + \Psi\left(1 + \frac{\sqrt{|z_j|}}{\omega_1}\right) + \Psi\left(\frac{\sqrt{|z_j|}}{\omega_1}\right) + i\pi\right)\right] * \int\limits_{\frac{1}{\sqrt{|z_{min}|}}}^{\infty} dt \exp\left[-\sum_{j=1}^{3}\frac{1}{g_j}\left(2\ln\left(1 - e^{-\omega_1 t}\right) + \omega_1 t\right)\right] \exp\left[\frac{iEt}{\hbar}\right] \quad \text{(A.65)}$$

Consider the integral on the right hand side

$$\begin{aligned}
&\int\limits_{\frac{1}{\sqrt{|z_{min}|}}}^{\infty} dt \exp\left[-\sum_{j=1}^{3}\frac{1}{g_j}\left(2\ln\left(1 - e^{-\omega_1 t}\right) + \omega_1 t\right)\right] \exp\left[\frac{iEt}{\hbar}\right] = \\
&= \int\limits_{\frac{1}{\sqrt{|z_{min}|}}}^{\infty} dt \left[1 - e^{-\omega_1 t}\right]^{-\sum_{j=1}^{3}\frac{2}{g_j}} \exp\left[t\left(\frac{iE}{\hbar} - \omega_1 \sum_j \frac{1}{g_j}\right)\right] \\
&= \frac{\exp\left[-\frac{\omega_1}{\sqrt{|z_{min}|}}\left(\frac{1}{g} - \frac{iE}{\hbar\omega_1}\right)\right]}{\omega_1\left(\frac{1}{g} - \frac{iE}{\hbar\omega_1}\right)} F\left(\frac{2}{g}, \frac{1}{g} - \frac{iE}{\hbar\omega_1}, 1 + \frac{1}{g} - \frac{iE}{\hbar\omega_1}, e^{-\frac{\omega_1}{\sqrt{|z_{min}|}}}\right).
\end{aligned} \quad \text{(A.66)}$$

The long time limit result for negative times is the complex conjugate of the long time limit for positive times, therefore for their contributions to $P(E)$ one gets twice the real part of the long time limit for positive times

$$
\begin{aligned}
&\int_{-\infty}^{-\frac{1}{\sqrt{|z_{min}|}}} dt \exp\left[K_L(t)+\frac{iEt}{\hbar}\right] + \int_{\frac{1}{\sqrt{|z_{min}|}}}^{\infty} dt \exp\left[K_L(t)+\frac{iEt}{\hbar}\right] \\
&= \left(\int_{\frac{1}{\sqrt{|z_{min}|}}}^{\infty} dt \exp\left[K_L(t)+\frac{iEt}{\hbar}\right]\right)^* + \int_{\frac{1}{\sqrt{|z_{min}|}}}^{\infty} dt \exp\left[K_L(t)+\frac{iEt}{\hbar}\right] \\
&= 2\mathrm{Re}\left\{\int_{\frac{1}{\sqrt{|z_{min}|}}}^{\infty} dt \exp\left[K_L(t)+\frac{iEt}{\hbar}\right]\right\} \qquad (A.67) \\
&= \exp\left[-\sum_{j=1}^{3}\frac{1}{g_j}\left(2\gamma+\Psi\left(1+\frac{\sqrt{|z_j|}}{\omega_1}\right)+\Psi\left(\frac{\sqrt{|z_j|}}{\omega_1}\right)\right)\right] * \\
&\quad 2\mathrm{Re}\left\{\exp\left[-\frac{i\pi}{g}\right]\frac{\exp\left[-\frac{\omega_1}{\sqrt{|z_{min}|}}\left(\frac{1}{g}-\frac{iE}{\hbar\omega_1}\right)\right]}{\omega_1\left(\frac{1}{g}-\frac{iE}{\hbar\omega_1}\right)}F\left(\frac{2}{g},\frac{1}{g}-\frac{iE}{\hbar\omega_1},1+\frac{1}{g}-\frac{iE}{\hbar\omega_1},e^{-\frac{\omega_1}{\sqrt{|z_{min}|}}}\right)\right\}.
\end{aligned}
$$

Now we can calculate the short-time contribution for $P(E)$

$$
\begin{aligned}
\int_{-\frac{1}{\sqrt{|z_{max}|}}}^{\frac{1}{\sqrt{|z_{max}|}}} dt \exp\left[K_S(t)+\frac{iEt}{\hbar}\right] &= \int_{-\frac{1}{\sqrt{|z_{max}|}}}^{\frac{1}{\sqrt{|z_{max}|}}} dt \exp\left[i\left(\frac{E}{\hbar}-\sum_{j=1}^{3}\frac{\pi\sqrt{|z_j|}}{g_j}\right)t\right] \\
&= \frac{2\sin\left(\frac{1}{\sqrt{|z_{max}|}}\left(\frac{E}{\hbar}-\sum_{j=1}^{3}\frac{\pi\sqrt{|z_j|}}{g_j}\right)\right)}{\frac{E}{\hbar}-\sum_{j=1}^{3}\frac{\pi\sqrt{|z_j|}}{g_j}}. \qquad (A.68)
\end{aligned}
$$

So the exact result for $P(E)$ is

$$
\begin{aligned}
P(E) &= \frac{1}{2\pi\hbar}\left[\exp\left[-\sum_{j=1}^{3}\frac{1}{g_j}\left(2\gamma+\Psi\left(1+\frac{\sqrt{|z_j|}}{\omega_1}\right)+\Psi\left(\frac{\sqrt{|z_j|}}{\omega_1}\right)\right)\right] * \right. \\
&\quad 2\mathrm{Re}\left\{\exp\left[-\frac{i\pi}{g}\right]\frac{\exp\left[-\frac{\omega_1}{\sqrt{|z_{min}|}}\left(\frac{1}{g}-\frac{iE}{\hbar\omega_1}\right)\right]}{\omega_1\left(\frac{1}{g}-\frac{iE}{\hbar\omega_1}\right)}F\left(\frac{2}{g},\frac{1}{g}-\frac{iE}{\hbar\omega_1},1+\frac{1}{g}-\frac{iE}{\hbar\omega_1},e^{-\frac{\omega_1}{\sqrt{|z_{min}|}}}\right)\right\} \\
&\quad \left.+\frac{2\sin\left(\frac{1}{\sqrt{|z_{max}|}}\left(\frac{E}{\hbar}-\sum_{j=1}^{3}\frac{\pi\sqrt{|z_j|}}{g_j}\right)\right)}{\frac{E}{\hbar}-\sum_{j=1}^{3}\frac{\pi\sqrt{|z_j|}}{g_j}}\right]. \qquad (A.69)
\end{aligned}
$$

This result holds for arbitrary temperatures, satisfying $\omega_1 \ll \sqrt{|z_{\min}|}$. (The parameters $\frac{1}{g}$, g_j, $\sqrt{|z_{\max}|}$ and $\sqrt{|z_{\min}|}$ were defined in equations A.58, A.59 and A.60.) If we had only one important capacitance in the circuit (which is the same as assuming all the cut-off frequencies exactly equal each other), this result would be the same as obtained by F. K. Wilhelm [35].

To calculate the $P'(E)$ function for Cooper pairs we use the property, that it differs from the $P(E)$ function for quasi-particles only by a factor of four in the correlation function, so

$$P'(E) = \frac{1}{2\pi\hbar} \int_{-\infty}^{\infty} dt \exp\left[4K(t) + \frac{iEt}{\hbar}\right]. \tag{A.70}$$

This can be absorbed in the factors g_j and g respectively for the contribution of the environment by exchanging $\frac{1}{g_j}$ by $\frac{4}{g_j}$ and $\frac{1}{g}$ by $\frac{4}{g}$ respectively. Thus $P'(E)$ for Cooper pairs becomes

$$\begin{aligned} P'(E) \;=\; & \frac{1}{2\pi\hbar}\left[\exp\left[-\sum_{j=1}^{3}\frac{4}{g_j}\left(2\gamma + \Psi\left(1+\frac{\sqrt{|z_j|}}{\omega_1}\right) + \Psi\left(\frac{\sqrt{|z_j|}}{\omega_1}\right)\right)\right] * \right. \\ & 2\mathrm{Re}\left\{\exp\left[-\frac{4\pi i}{g}\right]\frac{\exp\left[-\frac{\omega_1}{\sqrt{|z_{\min}|}}\left(\frac{4}{g}-\frac{iE}{\hbar\omega_1}\right)\right]}{\omega_1\left(\frac{4}{g}-\frac{iE}{\hbar\omega_1}\right)} F\left(\frac{8}{g}, \frac{4}{g}-\frac{iE}{\hbar\omega_1}, 1+\frac{4}{g}-\frac{iE}{\hbar\omega_1}, e^{-\frac{\omega_1}{\sqrt{|z_{\min}|}}}\right)\right\} \\ & \left. + \frac{2\sin\left(\frac{1}{\sqrt{|z_{\max}|}}\left(\frac{E}{\hbar} - \sum_{j=1}^{3}\frac{4\pi\sqrt{|z_j|}}{g_j}\right)\right)}{\frac{E}{\hbar} - \sum_{j=1}^{3}\frac{4\pi\sqrt{|z_j|}}{g_j}}\right]. \end{aligned} \tag{A.71}$$

A.2.3 Emergence of the Semi-classical Approximation

Now we can approximate $P(E)$ for the limit of high temperatures (compared to system energies) and small effective impedances of the environment, requiring

$$\frac{1}{g} \ll 1 \tag{A.72}$$

$$\text{and } \frac{E}{\hbar\omega_1} \ll 1. \tag{A.73}$$

As the cutoff-frequencies are quite large, we can assume $\frac{1}{\sqrt{|z_{min}|}} = 0$ and therefore neglect the contribution to $P(E)$ from the short-time limit $K_S(t)$ of the correlation function. And even if we are in the high temperature regime (which means still low temperatures compared to room temperature, as we want to retain superconductivity), the temperatures are small compared to the cutoff frequencies. So we can safely assume

$$\frac{\omega_1}{\sqrt{|z_j|}} \ll 1 \tag{A.74}$$

and approximate the exponential

$$\exp\left[-\frac{\omega_1}{\sqrt{|z_j|}}\left(\frac{1}{g}-\frac{iE}{\hbar\omega_1}\right)\right]\approx 1 \tag{A.75}$$

and the hyper-geometric function as

$$F\left(\frac{2}{g},\frac{1}{g}-\frac{iE}{\hbar\omega_1},1+\frac{1}{g}-\frac{iE}{\hbar\omega_1},e^{\frac{\omega_1}{\sqrt{|z_j|}}}\right)\approx F\left(\frac{2}{g},\frac{1}{g}-\frac{iE}{\hbar\omega_1},1+\frac{1}{g}-\frac{iE}{\hbar\omega_1},1\right)\ . \tag{A.76}$$

For this, one can apply the formula for special values

$$F(a,b,c,1)=\frac{\Gamma(c)\Gamma(c-a-b)}{\Gamma(c-a)\Gamma(c-b)}=\frac{\Gamma(c)\Gamma(1-a)}{\Gamma(c-a)}\ , \tag{A.77}$$

where the last step holds only for our special case of $c=b+1$.
Then we get

$$\begin{aligned}F\left(\frac{2}{g},\frac{1}{g}-\frac{iE}{\hbar\omega_1},1+\frac{1}{g}-\frac{iE}{\hbar\omega_1},1\right) &= \frac{\Gamma\left(1+\frac{1}{g}-\frac{iE}{\hbar\omega_1}\right)\Gamma\left(1-\frac{2}{g}\right)}{\Gamma\left(1-\frac{1}{g}-\frac{iE}{\hbar\omega_1}\right)}\\ &= \left(\frac{1}{g}-\frac{iE}{\hbar\omega}\right)\frac{\Gamma\left(\frac{1}{g}-\frac{iE}{\hbar\omega_1}\right)\Gamma\left(1-\frac{2}{g}\right)}{\Gamma\left(1-\frac{1}{g}-\frac{iE}{\hbar\omega_1}\right)}\\ &= \left(\frac{1}{g}-\frac{iE}{\hbar\omega}\right)B\left(\frac{1}{g}-\frac{iE}{\hbar\omega_1},1-\frac{2}{g}\right)\ ,\end{aligned} \tag{A.78}$$

where we introduced the beta-function $B(p,q)$ which is defined as $B(p,q)=\frac{\Gamma(p)\Gamma(q)}{\Gamma(p+q)}$.
For the following approximation we need the assumption of a small effective impedance of the environment (equation (A.72)).Consider the exponential prefactor

$$\exp\left[-\sum_j\frac{2}{g_j}\left(\gamma+\frac{1}{2}\left[\Psi\left(1+\frac{\sqrt{|z_j|}}{\omega_1}\right)+\Psi\left(\frac{\sqrt{|z_j|}}{\omega_1}\right)\right]\right)\right]\ . \tag{A.79}$$

As $\frac{\omega_1}{\sqrt{|z_j|}}\ll 1$ the argument of the digamma function becomes $\frac{\sqrt{|z_j|}}{\omega}\gg 1$, thus we can approximate

$$\frac{1}{2}\left[\Psi\left(1+\frac{\sqrt{|z_j|}}{\omega_1}\right)+\Psi\left(\frac{\sqrt{|z_j|}}{\omega_1}\right)\right]\approx\Psi\left(\frac{\sqrt{|z_j|}}{\omega_1}\right)\ , \tag{A.80}$$

which can be simplified by using the asymptotic expansion of the digamma-function $\Psi(x)\approx\ln(x)$ for large x yielding

$$\Psi(\frac{\sqrt{|z_j|}}{\omega_1}) \approx \ln\left(\frac{\sqrt{|z_j|}}{\omega_1}\right) \quad . \tag{A.81}$$

Therefore the exponential prefactor reduces to

$$\begin{aligned} & \exp\left[-\sum_j \frac{2}{g_j}\left(\gamma + \frac{1}{2}\left[\Psi\left(1+\frac{\sqrt{|z_j|}}{\omega_1}\right) + \Psi\left(\frac{\sqrt{|z_j|}}{\omega_1}\right)\right]\right)\right] \\ \approx\ & \exp\left[-\sum_j \frac{2\gamma}{g_j}\right] \exp\left[-\sum_j \frac{2}{g_j}\ln\left(\frac{\sqrt{|z_j|}}{\omega_1}\right)\right] \\ \approx\ & \exp\left[-\frac{2\gamma}{g}\right] \prod_j \left(\frac{\omega_1}{\sqrt{|z_j|}}\right)^{\frac{2}{g_j}} \\ \approx\ & 1 \ . \end{aligned} \tag{A.82}$$

Thus for applying the assumptions (A.72) and (A.74) to the exact result for the function $P(E)$ (equation (A.69)) this becomes

$$P(E) \approx \frac{1}{\pi\hbar\omega_1}\mathrm{Re}\left\{e^{-\frac{i\pi}{g}} B\left(\frac{1}{g} - \frac{iE}{\hbar\omega_1}, 1-\frac{2}{g}\right)\right\}. \tag{A.83}$$

For further approximations we use, in addition to the former assumptions, the semi-classical assumption (A.73). One can expand the Beta-function up to first order in $\frac{1}{g}$ and $\frac{E}{\hbar\omega_1}$ in numerator and denominator separately

$$\Gamma\left(\frac{1}{g} - \frac{iE}{\hbar}\omega_1\right) \approx \frac{1}{\frac{1}{g} - \frac{iE}{\hbar\omega_1}}, \tag{A.84}$$

$$\begin{aligned} \Gamma\left(1 - \frac{1}{g} - \frac{iE}{\hbar}\omega_1\right) &\approx \Gamma(1)\left[1 - \Gamma(1)\Psi(1)\left(\frac{1}{g} + \frac{iE}{\hbar\omega_1}\right)\right] \\ &= 1 + \gamma\left(\frac{1}{g} + \frac{iE}{\hbar\omega_1}\right), \end{aligned} \tag{A.85}$$

$$\Gamma\left(1 - \frac{2}{g}\right) \approx \Gamma(1) = 1 \tag{A.86}$$

as for small z one can approximate $\Gamma[z] \approx \frac{1}{z}$ and $\Psi(1) = -\gamma$. Therefore the Beta-function becomes

$$\begin{aligned} B\left(\frac{1}{g} - \frac{iE}{\hbar\omega}, 1-\frac{2}{g}\right) &= \frac{1}{\left(\frac{1}{g} - \frac{iE}{\hbar\omega_1}\right)\left(1 + \gamma\left(\frac{1}{g} + \frac{iE}{\hbar\omega_1}\right)\right)} \\ &= \frac{1}{\frac{1}{g} + \frac{\gamma}{g^2} - \frac{iE}{\hbar\omega_1} + \gamma\left(\frac{E^2}{\hbar\omega_1}\right)^2} \\ &\approx \frac{1}{\frac{1}{g} - \frac{iE}{\hbar\omega_1}} \end{aligned} \tag{A.87}$$

by keeping only terms up to first order in $\frac{1}{g}$ and $\frac{E}{\hbar\omega_1}$.
Applying again assumption (A.72) we can approximate

$$e^{-\frac{i\pi}{g}} \approx 1. \tag{A.88}$$

Finally $P(E)$ becomes

$$P(E) \approx \frac{1}{\pi\hbar\omega_1}\mathrm{Re}\left\{\frac{1}{\frac{1}{g}-\frac{iE}{\hbar\omega_1}}\right\} \tag{A.89}$$

$$= \frac{1}{\pi}\frac{\frac{\hbar\omega_1}{g}}{\left(\frac{\hbar\omega_1}{g}\right)^2+E^2}. \tag{A.90}$$

This is exactly the same result as obtained by the semi-classical approximation.

A.3 Evaluation of the Integral for the Quasi-particle Tunneling Rate

Consider the integral

$$S_1(\delta') = \int_2^\infty dx \int_2^\infty dy \, \frac{x}{\sqrt{x^2-4}}\frac{y}{\sqrt{y^2-4}}\frac{a}{1+a^2(-x-y+4.5+\delta')^2}. \tag{A.91}$$

For $a \ll 1$ its main contribution comes from a small strip (defined by $(x+y) \approx 4.5+\frac{\delta'}{2}$) in the region $2 < x, y < 2.5+\delta$. If we only consider this main contribution, the integral is only nonzero if the parameter $\delta' > -0.5$.

Considering this main contribution only, we can evaluate the integral within this new limits

$$S_1(\delta') = \int_2^{2.5+\delta'} dx \int_2^{2.5+\delta'} dy \, \frac{x}{\sqrt{x^2-4}}\frac{y}{\sqrt{y^2-4}}\frac{a}{1+a^2(x+y-4.5-\delta')^2}. \tag{A.92}$$

We can substitute $x' = x-2$, $y' = y-2$, therefore

$$S_1(\delta') = \int_0^{0.5+\delta'} dx' \int_0^{0.5+\delta'} dy' \, \frac{(x'+2)}{\sqrt{x'^2+2x'}}\frac{(y'+2)}{\sqrt{y'^2+2y'}}\frac{a}{1+a^2(x'+y'-0.5-\delta')^2}. \tag{A.93}$$

Now substituting $\rho = x'+y'-(0.5+\delta')$ and considering that the integral over ρ only contributes in a small range as $\rho \sim \frac{1}{a} \ll 1$, we can extend its limits of integration to infinity, thus obtaining

$$S_1(\delta') = \int_0^{0.5+\delta'} dx \int_{-\infty}^{\infty} d\rho \, \frac{(x+2)}{\sqrt{x^2+2x}}\frac{(\rho-x+2.5+\delta')}{\sqrt{(\rho-x+2.5+\delta')(\rho-x+0.5+\delta')}}\frac{a}{1+a^2\rho^2}. \tag{A.94}$$

As $\rho \ll 1$ this can be approximated by

$$S_1(\delta') = \int_0^{0.5+\delta'} dx \, \frac{(x+2)}{\sqrt{x^2+2x}} \frac{(-x+2.5+\delta')}{\sqrt{(-x+2.5+\delta')(-x+0.5+\delta')}} \int_{-\infty}^{\infty} d\rho \, \frac{a}{1+a^2\rho^2} \tag{A.95}$$

where we can straightforwardly evaluate the integral over ρ resulting in

$$\begin{aligned} S_1(\delta') &= \pi \int_0^{0.5+\delta'} dx \, \frac{(x+2)}{\sqrt{x^2+2x}} \frac{(-x+2.5+\delta')}{\sqrt{(-x+2.5+\delta')(-x+0.5+\delta')}} \\ &= \pi \int_0^{0.5+\delta'} dx \, \frac{\sqrt{x+2}}{\sqrt{x}} \frac{\sqrt{x-(2.5+\delta')}}{\sqrt{(x-(0.5+\delta'))}}. \end{aligned} \tag{A.96}$$

For symmetrization we substitute $y = x - \frac{0.5+\delta'}{2}$, thus

$$S_1(\delta') = \pi \int_{-0.25-\frac{\delta'}{2}}^{0.25+\frac{\delta'}{2}} dy \, \frac{\sqrt{y^2+(2.25+\frac{\delta'}{2})^2}}{\sqrt{y^2-(0.25+\frac{\delta'}{2})^2}}. \tag{A.97}$$

As the integrand is symmetric in y we can rewrite the integral in a form that allows us to use the Gradsteyn integral 3.169.14 [36]

$$\begin{aligned} S_1(\delta') &= 2\pi \int_0^{0.25+\frac{\delta'}{2}} dy \, \frac{\sqrt{y^2+(2.25+\frac{\delta'}{2})^2}}{\sqrt{y^2-(0.025+\frac{\delta'}{2})^2}} \\ &= 2\pi(2.25+\frac{\delta'}{2})E\left(\frac{0.25+\frac{\delta'}{2}}{2.25+\frac{\delta'}{2}}\right) \end{aligned} \tag{A.98}$$

where $E(k)$ is the complete elliptic integral of the second kind and is defined as

$$E(k) = \int_0^{\frac{\pi}{2}} d\phi \, \sqrt{1-k^2\sin^2(\phi)}. \tag{A.99}$$

By taking into account, that the tunneling rate is zero for $\delta' \leq -0.5$, we finally obtain

$$S_1(\delta') = 2\pi(2.25+\frac{\delta'}{2})E\left(\frac{0.25+\frac{\delta'}{2}}{2.25+\frac{\delta'}{2}}\right)\theta(-\delta'-0.5). \tag{A.100}$$

Appendix B

Interaction Picture

The interaction picture is used to describe the dynamics of a time dependent Hamiltonian. The Hamiltonian is separated into a time-independent part and a time-dependent perturbation

$$H(t) = H_0 + W(t) \ . \tag{B.1}$$

the time evolution is defined as

$$U_0(t) = e^{-\frac{iH_0t}{\hbar}}. \tag{B.2}$$

Then the state vector in the interaction picture becomes

$$|\Psi_I(t)\rangle = U_0^\dagger(t)|\Psi_S(t)\rangle \tag{B.3}$$

obeying the Schrödinger equation

$$i\hbar\frac{d}{dt}|\Psi_I(t)\rangle = W_I(t)|\Psi_I(t)\rangle \ , \tag{B.4}$$

where $|\Psi_S(t)\rangle$ defines the state vector in the Schrödinger picture and the interaction in the interaction picture is

$$W_I(t) = U_0^\dagger(t)W(t)U_0(t). \tag{B.5}$$

And the time evolution of the density operator can be derived as

$$\begin{aligned}
\frac{d\rho_I(t)}{dt} &= \frac{d}{dt}(U^\dagger(t)\rho_S(t)U(t)) \\
&= (\partial_t U^\dagger(t))\rho_S(t)U(t) + U^\dagger\rho_S(t)(\partial_t U(t)) + U^\dagger(t)(\partial_t\rho_S(t))U(t) \\
&= \frac{i}{\hbar}[H_0, \rho_I(t)] + [\partial_t\rho_S(t)]_I
\end{aligned} \tag{B.6}$$

Applying the unitary transform to the time-derivative of the diagonal terms ρ_{nn} just gives the time-derivative in the interaction picture

$$U^\dagger \dot{\rho}_{nn} U = \left[\frac{d\rho_n n}{dt}\right]_I = \frac{i}{\hbar}[H_0, \rho_{nn,I}] + \left[\frac{d\rho_{nn}}{dt}\right]_I = \frac{d\rho_{nn}}{dt}. \tag{B.7}$$

In our case this interaction picture is used in a more generalized fashion to take an imaginary part of the energy into account, where we describe a finite life time of the charge.

Appendix C

Bath Correlation Functions

This chapter aims to give an overview on properties of the bath correlation function used in this thesis (see [12]).

The definition of the bath correlation function is

$$\langle e^{i\phi(t)}e^{-i\phi(0)}\rangle_\beta = \frac{1}{Z_\beta}\mathrm{tr}\{e^{i\phi(t)}e^{-i\phi(0)}e^{-\beta H_{\mathrm{Bath}}}\} = \frac{1}{Z_\beta}\sum_R \langle R|e^{i\phi(t)}e^{-i\phi(0)}e^{-\beta H_{\mathrm{Bath}}}|R\rangle \tag{C.1}$$

with

$$Z_\beta = tr\{e^{-\beta H}\} \tag{C.2}$$

For a Hamiltonian H_{Bath} that is harmonic we get

$$\langle e^{i\phi(t)}e^{-i\phi(0)}\rangle_\beta = \exp\{\langle[\phi(t)-\phi(0)]\phi(0)\rangle_\beta\} \tag{C.3}$$

which by exchanging ϕ by $-\phi$ leads to the identity

$$\langle e^{i\phi(t)}e^{-i\phi(0)}\rangle_\beta = \langle e^{-i\phi(t)}e^{i\phi(0)}\rangle_\beta \tag{C.4}$$

and by using the cycling invariance of the trace operation one can show the following identity

$$\begin{aligned}
\langle e^{i\phi(t)}e^{-i\phi(0)}\rangle_\beta &= \frac{1}{Z_\beta}tr\{e^{\frac{iH_{\mathrm{Bath}}t}{\hbar}}e^{i\phi(0)}e^{-\frac{iH_{\mathrm{Bath}}t}{\hbar}}e^{-i\phi(0)}e^{-\beta H_{\mathrm{Bath}}}\} \\
&= \frac{1}{Z_\beta}tr\{e^{-i\phi(0)}e^{-\beta H_{\mathrm{Bath}}}e^{\frac{iH_{\mathrm{Bath}}t}{\hbar}}e^{i\phi(0)}e^{-\frac{iH_{\mathrm{Bath}}t}{\hbar}}e^{\beta H_{\mathrm{Bath}}}e^{-\beta H_{\mathrm{Bath}}}\} \\
&= \frac{1}{Z_\beta}tr\{e^{-i\phi(0)}e^{\frac{iH_{\mathrm{Bath}}}{\hbar}(t+i\beta\hbar)}e^{i\phi(0)}e^{-\frac{iH_{\mathrm{Bath}}}{\hbar}(t+i\beta\hbar)}e^{-\beta H_{\mathrm{Bath}}}\} \\
&= \langle e^{-i\phi(0)}e^{i\phi(t+i\beta\hbar)}\rangle_\beta
\end{aligned} \tag{C.5}$$

and similarly we can show the translation invariance of the correlation function

$$
\begin{aligned}
\langle e^{-i\phi(t)} e^{i\phi(t')} \rangle_\beta &= \frac{1}{Z_\beta} tr\{ e^{\frac{iH_{\rm Bath}t}{\hbar}} e^{-i\phi(0)} e^{-\frac{iH_{\rm Bath}t}{\hbar}} e^{\frac{iH_{\rm Bath}t'}{\hbar}} e^{i\phi(0)} e^{-\frac{iH_{\rm Bath}t'}{\hbar}} e^{-\beta H_{\rm Bath}} \} \\
&= \frac{1}{Z_\beta} tr\{ e^{\beta H_{\rm Bath}} e^{-\frac{iH_{\rm Bath}t'}{\hbar}} e^{-\beta H_{\rm Bath}} e^{\frac{iH_{\rm Bath}t}{\hbar}} e^{-i\phi(0)} e^{-\frac{iH_{\rm Bath}t}{\hbar}} e^{\frac{iH_{\rm Bath}t'}{\hbar}} e^{i\phi(0)} e^{-\beta H_{\rm Bath}} \} \\
&= \frac{1}{Z_\beta} tr\{ e^{\frac{iH_{\rm Bath}}{\hbar}(t-t')} e^{-i\phi(0)} e^{-\frac{iH_{\rm Bath}}{\hbar}(t-t')} e^{i\phi(0)} e^{-\beta H_{\rm Bath}} \} \\
&= \langle e^{-i\phi(t-t')} e^{i\phi(0)} \rangle_\beta \qquad \text{(C.6)}
\end{aligned}
$$

Bibliography

[1] D. J. Averin and V. Y. Aleshkin, Resonance tunneling of Cooper pairs in a system of two small Josephson junctions, Pis'ma Zh. Eksp. Teor. Fiz. **50**(7), 331 (October 1989).

[2] Y. Nakamura, P. Y. A., and J. S. Tsai, Coherent control of macroscopic quantum states in a single-Cooper-pair box, Nature **398**, 786 (1999).

[3] A. Käck, Private Communication.

[4] T. A. Fulton and G. J. Dolan, Observation of Single-Electron Charging Effects in Small Tunnel Junctions, Phys. Rev. Lett. **59**(1), 109 (1987).

[5] M. H. Devoret, D. Esteve, H. Grabert, G.-L. Ingold, H. Pothier, and C. Urbina, Effect of the Electromagnetic Environment on the Coulomb Blockade in Ultrasmall Tunnel Junctions, Phys. Rev. Lett. **64**(15), 1824 (1990).

[6] Y. Nakamura, C. D. Chen, and J. S. Tsai, Quantitative analysis of Josephson-quasiparticle current in superconducting single-electron tranmsistors, Phys. Rev. B **53**(13), 8234 (1996).

[7] A. M. van den Brink, G. Schoen, and L. J. Geerligs, Combined Single-Electron and Coherent-Cooper-Pair Tunneling in Voltage-Biased Josephson Junctions, Phys. Rev. Lett. **67**(21), 3030 (Nov. 1991).

[8] A. M. van den Brink, A. A. Odintsov, P. A. Bobbert, and G. Schoen, Coherent Cooper pair tunneling in systems of Josephson junctions: effects of quasiparticle tunneling and of the electromagnetic environment, Z. Phys. B Condensed Matter **85**, 459 (1991).

[9] W. Lu, K. D. Maranowski, and A. J. Rimberg, Charge transport processes in a superconducting single-electron transistor coupled to a microstrip transmission line, Phys. Rev. B **65**, 060501 (January 2002).

[10] H. Grabert and M. H. Devoret, editors, *Single Charge Tunneling*, volume B 294 of *NATO ASI Series*, Plenum, N.Y., 1992.

[11] G. Schön, Single-Electron Tunneling, in *Quantum Transport and Dissipation*, edited by R. Wengenmayr, chapter 3, page 149, Wiley-VCH Verlag GmbH, 1998.

[12] G.-L. Ingold, Ladungseffekte in ultrakleinen Tunnelkontakten, Habilitationsschrift, Januar 1993.

[13] A. O. Caldeira and A. J. Leggett, Path integral approach to quantum Brownian motion, Physica A **121**, 587 (1983).

[14] H. Kamerlingh Onnes, Leiden Comm. **120b, 122b, 124c** (1911).

[15] F. London and H. London, Proc. Roy. Soc. (London) **A 149**, 71 (1935).

[16] V. L. Ginzburg and L. D. Landau, Zh. Eksperim. i. Teor. Fiz. **20**, 1064 (1950).

[17] J. Bardeen, L. N. Cooper, and J. R. Schrieffer, Theory of Superconductivity, Phys. Rev. **108**, 1175 (1957).

[18] M. Tinkham, *Introduction to Superconductivity*, McGraw-Hill, Inc., second edition, 1996.

[19] K. Kopitzki, *Einfëhrung in die Festkörperphysik*, B. G. Teubner, Stuttgart, 3 edition, 1993.

[20] B. D. Josephson, Possible new effects in superconductive tunneling, Phys. Lett. **1**, 251 (1962).

[21] B. D. Josephson, Adv. Phys. **14**, 419 (1965).

[22] V. Ambegaokar and A. Baratoff, Tunneling between superconductors, Phys. Rev. Lett. **10**, 586 (1963).

[23] V. Ambegaokar and A. Baratoff, Tunneling between superconductors, erratum, Phys. Rev. Lett. **11**, 104 (1963).

[24] W. Lu, *Single Electron Transistor: Effects of the Environment and Detecting Electron Motion in Real Time*, PhD thesis, Rice University, 2003.

[25] A. B. Zorin, S. V. Lotkhov, H. Zangerle, and J. Niemeyer, Coulomb Blockade and Cotunneling in Single Electron Circuits with On-chip Resistors: Towards the Implementation of R-pump, J. Appl. Phys **88**, 2665 (2000).

[26] Y. A. Pashkin, Y. Nakamura, and J. S. Tsai, Room-temperature Al single-electron transistor made by electron-beam lithography, Appl. Phys. Lett. **76**(16), 2256 (April 2000).

[27] M. T. Tuominen, J. M. Hergenrother, T. S. Tighe, and M. Tinkham, Experimental Evidence for Partity-Based 2e Periodicity in a Superconducting Single-Electron Tunneling Transistor, Phys. Rev. Lett. **16**(13), 1997 (1992).

[28] J. S. Penttilë, U. Parts, P. J. Hakonen, M. A. Paalanen, and E. B. Sonin, "Superconductor-Insulator Transition" in a Single Josephson Junction, Phys. Rev. Lett. **82**, 1004 (1999).

[29] A. A. Clerk, S. M. Girvin, A. K. Nguyen, and A. D. Stone, Resonant Cooper-Pair Tunneling: Quantum Noise and Measurement Characteristics, Phys. Rev. Lett. **89**(17), 176804 (Oct. 2002).

[30] G. Johansson, Population inversion through charge measurement using a superconducting single-electron transistor biased in the subgap regime, cond-mat , 0210539 (Oct. 2002).

[31] J. B. Kycia, J. Chen, R. Therrien, C. Kurdak, K. L. Campman, A. C. Gossard, and J. Clarke, Effects of Dissipation on a Superconducting Single Electron Transistor, Phys. Rev. Lett. **87**(1), 017002 (2001).

[32] R. Kubo, The fluctuation-dissipation theorem, Rep. Prog. Phys. **29**, 255 (1966).

[33] U. Weiss, *Quantum Dissipative Systems*, volume 10 of *Series in Modern Condensed Matter Physics*, World Scientific, second edition, 2001.

[34] F. K. Wilhelm, G. Schön, and G. T. Zimanyi, Superconducting Single-Charge Transistor in a Tunable Dissipative Environment, Phys. Rev. Lett. **87**(13), 136802 (2001).

[35] F. K. Wilhelm, *Ladungstransport in supraleitenden Nanostrukturen*, PhD thesis, Universität Karlsruhe, 1999.

[36] I. S. Gradsteyn and I. M. Ryzhik, *Table of Integrals, Series, and Products*, Academic Press, ‘, 1980.

Acknowledgements

Finally, I would like to thank all the persons who made this thesis possible.

I wish to thank Prof. Dr. Jan von Delft for giving me the opportunity to work in his group and for some interesting discussions.

It is a pleasure to thank Dr. Frank K. Wilhelm, who constantly provided support and advice. Moreover I want to thank him for many enlightening physical discussions and his support during the time of writing this thesis up.

I wish to thank Dr. Jens Siewert for pointing out the proper assumptions to me. Of course, I want to thank all persons in the group for spending their time, if I approached them with any issue. In particular I would like to thank Dr. Alexander Khaetskii for his help with the evaluation of a complicated integral, Ralph Simmler for keeping the computers running, Udo Hartmann, Markus Storcz and Michael Sindel, Henryk Gutmann and Rolf Helmes for their help on technical problems with Mathematica, Maple, LaTeX and other technical questions and physical discussions. Furthermore I wish to thank Stephane Schoonover for organising the office environment.

I wish to thank Stefan Schwärzler who constantly makes my life wonderful for his support during the last weeks of writing this thesis.

Furthermore it is a pleasure to thank my parents Ute and Michael Jähne and my grandparents Bärbel and Werner Zwick for their support through all the years I have been studying.

Financial support by Studienstiftung des Deutschen Volkes is gratefully acknowledged.

Ich versichere, dass ich diese Arbeit selbständig verfasst und keine anderen als die angegebenen Quellen und Hilfsmittel benutzt, sowie die Zitate kenntlich gemacht habe.

München, den 01. Juni 2004

Referent:	Prof. Dr. Jan von Delft
Korreferent:	Prof. Dr. Hermann Wolter